ABSTRACT

Title of Document: DEVELOPING EARTH OBSERVATIONS REQUIREMENTS FOR GLOBAL AGRICULTURAL MONITORING: TOWARD A MULTI-MISSION DATA ACQUISITION STRATEGY

Alyssa K. Whitcraft, Doctor of Philosophy, 2014

Directed By: Professor Christopher O. Justice, Department of Geographical Sciences

Global food supply and our understanding of it have never been more important than in today's changing world. For several decades, Earth observations (EO) have been employed to monitor agriculture, including crop area, type, condition, and yield forecasting processes, at multiple scales. However, the EO data requirements to consistently derive these informational products had not been well defined. Responding to this dearth, I have articulated spatially explicit EO requirements with a focus on moderate resolution (10-70m) active and passive remote sensors, and evaluate current and near-term missions' capabilities to meet these EO requirements.

To accomplish this, periods requiring monitoring have been identified through the development of agricultural growing season calendars (GSCs) at 0.5˚ from MODIS surface reflectance. Second, a global analysis of cloud presence probability and extent using MOD09 daily cloud flags over 2000-2012 has shown that the early-

to-mid agricultural growing season (AGS) – an important period for monitoring – is more persistently and pervasively occluded by clouds than is the late and non-AGS. Third, spectral, spatial, and temporal resolution data requirements have been developed through collaboration with international agricultural monitoring experts. These requirements have been spatialized through the incorporation of the GSCs and cloud cover information, establishing the revisit frequency required to yield reasonably clear views within 8 or 16 days. A comparison of these requirements with hypothetical constellations formed from current/planned moderate resolution optical EO missions shows that to yield a scene at least 70% clear within 8 or 16 days, 46-55% or 10-32% of areas, respectively, need a revisit more frequent than Landsat 7 & 8 combined can deliver. Supplementing Landsat 7 & 8 with missions from different space agencies leads to an improved capacity to meet requirements, with Resourcesat-2 providing the largest incremental improvement in requirements met. No single mission/observatory can consistently meet requirements throughout the year, and the only way to meet a majority (77-94% for ≥70% clear; 47-73% for 100% clear) of 8 day requirements is through coordination of multiple missions. Still, gaps exist in persistently cloudy regions and periods, highlighting the need for data coordination and for consideration of active EO for agricultural monitoring.

DEVELOPING EARTH OBSERVATIONS REQUIREMENTS FOR GLOBAL AGRICULTURAL MONITORING: TOWARD A MULTI-MISSION DATA ACQUISITION STRATEGY

By

Alyssa K. Whitcraft

Dissertation submitted to the Faculty of the Graduate School of the
University of Maryland, College Park, in partial fulfillment
of the requirements for the degree of
Doctor of Philosophy
2014

Advisory Committee:
Dr. Christopher O. Justice, Chair
Dr. Samuel N. Goward
Dr. Inbal Becker-Reshef
Dr. Jeffrey G. Masek
Dr. Eric F. Vermote
Dr. Richard A. Weismiller

Preface

Chapter 2 is comprised of jointly authored and published work of which Alyssa K. Whitcraft is the primary author. Chapter 3 is in preparation for submission (Alyssa K. Whitcraft is again the primary author of that jointly authored work), and includes a dataset generated by Eric F. Vermote. Chapters 4-5 include datasets and inputs from members of the Group on Earth Observations Global Agricultural Monitoring (GEOGLAM) Community of Practice, as well as from the Committee on Earth Observation Satellites (CEOS) Ad Hoc Team for GEOGLAM. All external contributions are identified with citations, references, and/or footnotes. All other methods, analyses, and results were developed and/or executed by Alyssa K. Whitcraft, as is all text contained herein.

Dedication

For the survivors, everywhere.

"Go out and change the world you live in; it is the only world you have!"

– StaceyAnn Chin

Acknowledgements

I want to start by thanking my committee. I'd like to thank Chris Justice and Inbal Becker-Reshef, for their time, effort, and mentorship these past few years. I want to thank Eric Vermote for guidance and inputs into the cloud cover analyses, and also acknowledge Sam Goward and Jeff Masek for their feedback during and outside committee meetings that has helped shape this research. I'd also like to thank Richard Weismiller for serving as the Dean's representative.

I would like to acknowledge the National Aeronautics and Space Administration (NASA) Earth and Space Science Fellowship Program for supporting this dissertation research [NNX11AL56H]. I would like to acknowledge the CEOS Ad Hoc Team for GEOGLAM for their crucial role in developing the requirements table, as well as express my gratitude to the CEOS Systems Engineering Office (particularly Brian Killough, Paul Kessler, and Shaun Deacon) for creating the COVE tool and providing key inputs to the overpass analysis. I would also like to acknowledge members of the Group on Earth Observations Agricultural Monitoring Community of Practice, particularly for the vetting of the growing season calendars presented herein.

I would like to thank Louis Giglio, Luigi Boschetti, Judy Carney, Tom Gillespie, and Joe Sexton for technical guidance and kind encouragement over the years. I would also like to acknowledge Tatiana Loboda for her help in the early stages of this research.

I would also like to thank the GEOGLAM team here at UMD for being so enthusiastic about agriculture and solutions to pressing global concerns. I would like

to acknowledge other members of the Department of Geographical Sciences – fellow graduate students, faculty, and staff. They deserve many thanks for the camaraderie and support they have provided throughout this process.

And last, but absolutely not least, I would like to thank all of my family and friends near and far, those still with us and those sadly departed, for making this crazy, confusing, exciting, short spin on this little blue ball worthwhile. But especially: thank you, Mom, for your love, patience, and encouragement; thank you, Drake, for thinking I'm a big deal even when I feel small; and Jeremy, thank you so very much for your love, kindness, and just about everything else.

Table of Contents

List of Tables

List of Figures

Chapter 1: Introduction – Context, Research Goals, and Guiding Questions

1.1 Research Context, Questions, & Goals

With changes in climate, increasing instances of extreme weather events, a growing global population, and the associated pressures upon Earth's resources, issues of food security and agricultural production are becoming more relevant and urgent than ever (Justice & Becker-Reshef, 2007). Earth observations (EO) using satellite data have been used continuously for over forty years to provide timely and synoptic information on broad agricultural landscapes and processes, including crop area, type, and condition, as well as yield forecasting (Allen, Hanuschak, & Craig, 2002; Anderson & Kalcic, 1982; Bastiaanssen, Molden, & Makin, 2000; MacDonald, Hall, & Erb, 1975; MacDonald & Hall, 1980; Pinter et al., 2003; Steven, 1993; Wu et al., 2013a). Earth observing missions such as the National Oceanic and Atmospheric Administration (NOAA) Advanced Very High Resolution Radiometer (AVHRR) and National Aeronautics and Space Administration (NASA) Moderate Resolution Imaging Spectroradiometer (MODIS) Terra/Aqua, with the capacity to image the entire Earth's land surface daily, have proven useful in the generation of timely agricultural information, though they miss crucial information existing at the very fine to moderate (VFTM; <5-100m) level (Becker-Reshef et al., 2009; Lobell & Asner, 2004; Reed et al., 1994).

Agricultural monitoring, for the purpose of this proposed research, refers to the use of remotely sensed EO to provide either direct information on or indicators of

agricultural parameters such as yearly crop area, type, progress, and vigor to gather information toward the goal of accurately modeling and monitoring crop yield, and providing early warnings of crop failure (Justice & Becker-Reshef, 2007). The utility of satellite data for agricultural monitoring is contingent upon the EO being first acquired at appropriate spectral, spatial, temporal, and radiometric resolutions, and then made available and accessible to users in a timely manner. Therefore, EO requirements for agricultural monitoring are geographically-defined spatial, spectral, and temporal imaging resolution requirements which are necessary to derive, in a timely manner, the direct information on and/or indicators of those agricultural parameters listed previously for agricultural areas across the globe.

Due to onboard data storage limitations, as well as pixel size-to-swath ratio trade-offs, current systems that collect data finer than 100m have not yet had the capacity to image the entire cropped area of the Earth at every overpass opportunity (Arvidson, Gasch, & Goward, 2001; Hansen & Loveland, 2012; Wulder et al., 2008). However, in the near-term (2014-2015), the planned moderate spatial resolution missions Sentinel-2A and Sentinel-2B are purported to acquire moderate resolution data at every overpass opportunity with a combined revisit of 5 days (Drusch et al., 2012). Even with these systematic or near-systematic acquisitions in the optical moderate resolution domain, geographic and temporal variability in cloud cover contamination and obscuration means that these missions need to be harmonized in order to secure cloud free observations. The historical and current lack of coordinated image acquisition efforts with respect to agricultural monitoring means the capabilities of most of these VFTM systems have not been optimized for the purpose of gathering

crucial agricultural information throughout the growing season. As such, the amount of remotely sensed data and information available throughout the growing season is regionally and temporally inconsistent, leaving knowledge gaps in the satellite-based contribution regarding the food and agricultural situation in many parts of the world. Strategic monitoring of the Earth's surface under cultivation is needed in order to generate timely, synoptic, and accurate agricultural information at multiple scales (Arvidson et al., 2001; Becker-Reshef et al., 2010a; Duveiller, López-Lozano, Seguini, Bojanowski, & Baruth, 2013).

It is in the context of agricultural market price volatility, food insecurity, and non-harmonized national to regional monitoring efforts that the need for a coordinated international effort to monitor global agriculture has become clear (Atzberger, 2013; Naylor, 2011; Wu et al., 2013a). Indeed, the G20 agricultural ministers in 2011 mandated the creation of a global agricultural monitoring system of systems known as the Group on Earth Observations Global Agricultural Monitoring (GEOGLAM) initiative, a crucial component of which is the coordination of EO data for operational agricultural monitoring (Becker-Reshef et al., 2010a; Duveiller et al., 2013; Justice & Becker-Reshef, 2007; Singh Parihar et al., 2012). Since its formal inception in 2011, GEOGLAM has been actively engaged with the Committee on Earth Observations Satellites (CEOS) in order to translate imaging requirements for monitoring into an actionable acquisition strategy which leverages EO capabilities from space agencies around the world. Crucial to this task is the articulation of the temporal (*When? How frequently?),* spatial (*Where? At what spatial resolution?*), and spectral (*active vs. passive)* requirements for a suite of agricultural monitoring

applications. However, prior to this research, this articulation had not been attempted in a comprehensive and spatially explicit manner. From this point of departure, the dissertation research presented herein seeks to answer the following research questions:

1. When, where, and at what temporal and spatial resolutions should VFTM resolution remotely sensed imagery be acquired for monitoring of global croplands?

2. What is the impact of cloud cover on our ability to view croplands on the Earth's surface using passive optical plus thermal (O+TIR) data throughout the agricultural growing season?

3. Are our present and near-term moderate resolution O+TIR Earth observing missions' capabilities sufficient to meet our moderate resolution O+TIR EO requirements for global agricultural monitoring?

From these overarching research questions emerge several specific questions and related steps which are addressed through this dissertation's original research, contributions from members of the agricultural monitoring community, and/or extensive review of the literature (Table 1.1).

Table 1.1: Research Sub-Questions, Response Steps, & Sources

Ch.	**Questions**	**Steps**	**Sources**
2, 4	a. Where are the agricultural lands that are to be monitored?	a. Determination of the 'best available' satellite-derived cropland masks to identify agricultural regions of interest	Dissertation Research + existing cropland masks
2	b. When are the average start, peak, and end of season dates for major	b. The use of MODIS Terra surface reflectance converted to Normalized Difference	Dissertation Research + existing

	global croplands?	Vegetation Index (NDVI) data to extract vegetation phenological metrics and agricultural growing season (AGS) timing.	cropland masks
3, 4	c. What is the impact of cloud cover on obtaining clear views of the Earth's surface throughout the AGS, at different times of day (AM vs. PM), and in different regions of the world?	c. The analysis of 10-13 years of MODIS Aqua and Terra surface reflectance cloud flags over agricultural regions throughout the growing season to determine the probability of a cloud free clear view at 0.05˚, as well as the percentage of each 0.05˚ which is cloudy.	Dissertation research + daily cloud probability and daily cloud percent at 0.05˚ (Vermote)
4	d. Where are fine vs. moderate vs. coarse resolution imagery required in order to resolve fields?	d. Crowd-sourced field size dataset and determination of appropriate resolution for agricultural applications.	S. Fritz et al., (unpublished) + requirements table (Table 4.1)
4	e. Where, when, and at what temporal resolution do we need our VFTM spatial resolution satellite missions to acquire data for a suite of agricultural monitoring applications?	e. Synthesize location (a, d), timing of necessary imaging (b), and cloud cover impacts on required image frequency (c) to generate maps of monthly requirements;	All of the above
5	f. Which present and near-term planned moderate spatial resolution missions are candidates for meeting EO requirements and what are their combined overpass (temporal resolution) capabilities?	f. Development of scenarios combining different overpass swaths to illustrate what temporal resolution different mission combinations can generate.	CEOS COVE Tool (Killough et al., NASA Langley)
5	g. Can our present and near-term moderate spatial resolution O+TIR missions meet our EO requirements for monitoring? h. Which regions/times of the year are	g-h. Overlay the requirements (f) with different mission capabilities (g) to determine which/whether missions combinations can meet requirements; where requirements for O+TIR are not met, consider microwave	All of the above

	pervasively and persistently cloudy during the AGS, requiring the consideration of active microwave SAR data?		

While this research discusses EO requirements in the VFTM spatial resolution range, the primary focus is on moderate spatial resolution (10-70m) instruments in both the O+TIR and active microwave spectral ranges. Because O+TIR data at coarse spatial resolution (250-1000m) are already available on roughly a daily basis, no strategy beyond the maintenance and continuity of the related missions is required. In the case of fine (5-10m) and very fine (<5m) spatial resolution data, all requirements (Table 4.1) are to cover relatively small areas (either sample, or for a subset of croplands – medium and small, or only small), and due to the pointing capabilities of candidate sensors (e.g. RapidEye REIS, SPOT-6 HRG, IKONOS-2 OSA, and others) very frequent revisit rates across the globe are possible. However, as these data are from the private sector, they can be very costly. The priority growth area for regional to global scale analyses in the agricultural monitoring context is in the moderate spatial resolution range. A number of monitoring applications rely upon data at this resolution (Duveiller & Defourny, 2010), yet the lack of consistent cloud free acquisitions with sufficiently high temporal resolution has provided a boundary to full implementation in the agricultural monitoring context (Duveiller et al., 2013).

1.2 Background: Agricultural Monitoring using Remote Sensing

Remote sensing has its roots in agricultural research and applications. Some of the earliest applications of remote sensing were undertaken through the Large Area Crop Inventory Experiment (LACIE), initiated in 1974, the Agricultural Research Service (ARS) Wheat Yield Project, initiated in 1976, and the Agriculture and Resource Inventory Surveys Through Aerospace Remote Sensing (AgRISTARS) Program, initiated in 1980 (Pinter et al., 2003). LACIE, a collaboration between the United States Department of Agriculture (USDA), NASA, and NOAA, aimed to improve the U.S.'s domestic and international crop forecasting ability through the use of Landsat 1 (Earth Resources Technology Satellite-1) data. Following the success of LACIE, the ARS Wheat Yield Project began, where early methods for detecting deviations from normal crop condition originated, while expanding satellite-based agricultural monitoring to international sites (Wiegand et al., 1992). AgRISTARS furthered work from LACIE and ARS Wheat Yield Project, defining ideal conditions for agricultural observations, as well as experimenting with remote sensing as a tool for early warning, crop condition assessment, yield modeling, and measurements of soil moisture (Baker et al., 1985; Boatwright, Ravet, & Taylor, 1985; Jackson, 1986; Pinter et al., 2003).

Agricultural monitoring through remote sensing continued to evolve and expand throughout the 1980s, 1990s, and 2000s, bearing witness to substantial increases in satellite platforms in orbit and in understanding of the biophysical properties of crops and agricultural lands (Justice & Becker-Reshef, 2007; Wu et al., 2013a). The lingering dearth of a coordinated imaging strategy designed specifically

for agricultural monitoring is due at least in part to the fact that the task of agricultural monitoring is distributed amongst many different and disconnected international groups, with only the past few years demonstrating the beginning of coordinated EO activities (Justice & Becker-Reshef, 2007; Singh Parihar et al., 2012). Those acquisition strategies that do exist are sensor-specific, and managed by a single entity. In the early Landsat years, there was an effort to obtain complete global coverage at least once per year. With the privatization of Landsat, data were collected based largely on customer demand. For Landsat 7 ETM+, a Long-Term Acquisition Plan (LTAP) was developed to build a meaningful archive of Landsat data over a range of land covers, acquiring the approximately 400-450 (originally 250) best, cloud free scenes of the up to 630 daylit land-containing scenes that are observable every day (Arvidson, Gasch, & Goward, 1999; Arvidson et al., 2001; Arvidson, Goward, Gasch, & Williams, 2006). A similar strategy is being developed for Landsat 8 Operational Land Imager (OLI), although at present that instrument is already acquiring 550-600 scenes/day, thereby coming close to "acquiring every opportunity," which would be up to 630 scenes per day (Eugene Fosnight, personal communication, 5 February 2014). The original LTAP takes a seasonality approach, wherein acquisition dates are determined by AVHRR NDVI-based seasonal transition dates (green-up and senescence are the most dynamic periods of the year, so they get the most acquisitions). While not an acquisition plan designed exclusively with agricultural monitoring in mind, it does have an agricultural component, wherein agricultural scenes of interest have been identified by the USDA Foreign Agriculture Service (FAS). In 1996, the USDA FAS requested 2161 scenes, which was later negotiated

down to 237 scenes, and upped by 45 additional scenes over Argentina in the year 2000 (Terry Arvidson, personal communication, 7 May 2010.). LTAP directs Landsat 7 ETM+ to acquire imagery at every opportunity in the United States' agricultural areas, regardless of cloud cover, while for the 282 international agricultural scenes of interest only acquiring during the growing season (determined by general phenology, not cropland specific phenology) on overpasses for which cloud cover is predicted at less than 60% (Arvidson et al., 2001). However, because the combined satellite revisit rate for Landsat 7 and Landsat 8 is every eight days (with each individual sensor having a nominal revisit of 16 days), and cloud cover is a persistent problem in many regions of the world during the growing season, there have historically been very long gaps between clear Landsat images for many agricultural areas worldwide (Arvidson et al., 2001, 2006; Brisco & Brown, 1995; Roy et al., 2010; Roy, Lewis, Schaaf, Devadiga, & Boschetti, 2006). This issue has been compounded since the Landsat 7's scan-line corrector failure in 2003. In fact, because 22% of data in each Landsat 7 scene are now missing (Scaramuzza, Micijevic, & Chander, 2004), the United States Department of Agriculture National Agricultural Statistics Service (USDA-NASS) has stopped using Landsat 7 data in the production of its Cropland Data Layer (Johnson, 2008).

Due to the highly dynamic nature of agricultural processes at multiple scales, no single moderate resolution sensor is alone capable of securing a reasonably cloud free view of every actively cropped agricultural area of the world at a sufficiently frequent interval to resolve meaningful changes in crop vigor, crop stage, crop type, or crop yield, as these processes happen beneath the 16 day time step (Becker-Reshef,

Vermote, Lindeman, & Justice, 2010b; Duveiller et al., 2013; Johnson, 2014; Reed, Schwartz, & Xiao, 2009). Doing so would require leveraging multiple EO missions with different spectral and spatial resolutions, as different agricultural monitoring applications require acquisition at different spatial resolution in order to resolve crucial differences. For example, Duveiller and Defourny (2010) found that estimating crop area requires finer resolution pixels than does monitoring stages of crop growth, further corroborating the point that multiple resolutions of data are necessary for agricultural monitoring.

With these issues of cloud cover, rate of change in agricultural parameters, and necessary scale of detection in mind, the lack of an acquisition strategy for agriculture becomes especially apparent. In order to ensure that cloud free data at the appropriate spatial resolutions are acquired throughout the growing season, it is necessary to articulate the timing, frequency and spatial resolution requirements for VFTM resolution active and passive remote sensing Earth observations of global croplands. Such a coordination of imaging efforts would facilitate the agricultural monitoring community's opportunities to gain access to and effectively employ consistent, quality, appropriate data toward the production and application of timely agricultural information on a global basis.

1.3 Organization of Dissertation

At the time this research was proposed (2010), the Group on Earth Observations (GEO) had produced a diagram for its Task 07-03 ("improved international coordination on EO for global agriculture monitoring") which describes what it viewed as necessary temporal and spatial resolutions for a variety of

operational agricultural monitoring applications, regardless of whether or not a mission capable of fulfilling a requirement existed (Figure 1.1). This requirements diagram was the result of collaboration of several experts in the agricultural monitoring community, and provided the context and rationale for this dissertation work. Further, it paved the way for the generation of a requirements table (Table 4.1) which provides more precise information on spectral, temporal, and spatial resolution requirements for different landscapes (characterized by crop type and/or field size).

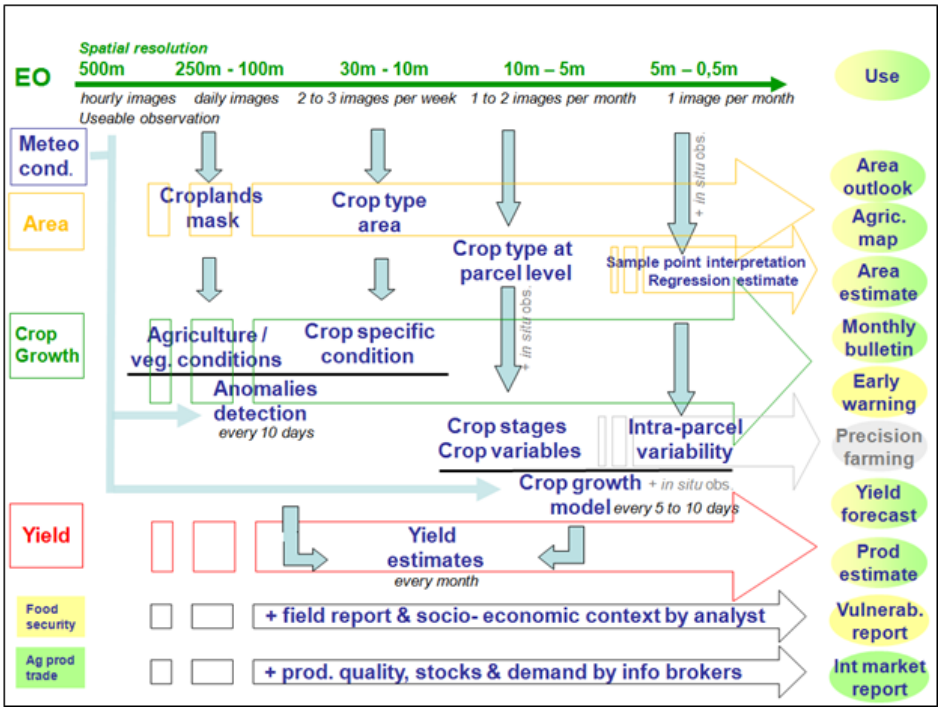

Figure 1.1: The GEO Requirements diagram for the necessary temporal and spatial resolutions of remotely sensed Earth observations for operational agricultural monitoring.

The research presented here takes the general requirements for monitoring detailed in these efforts, and roots them firmly in the spatial domain by considering spatially explicit agricultural growing season (AGS) timing, cropland locations, cloud cover constraints, and field size information (Figure 1.2).

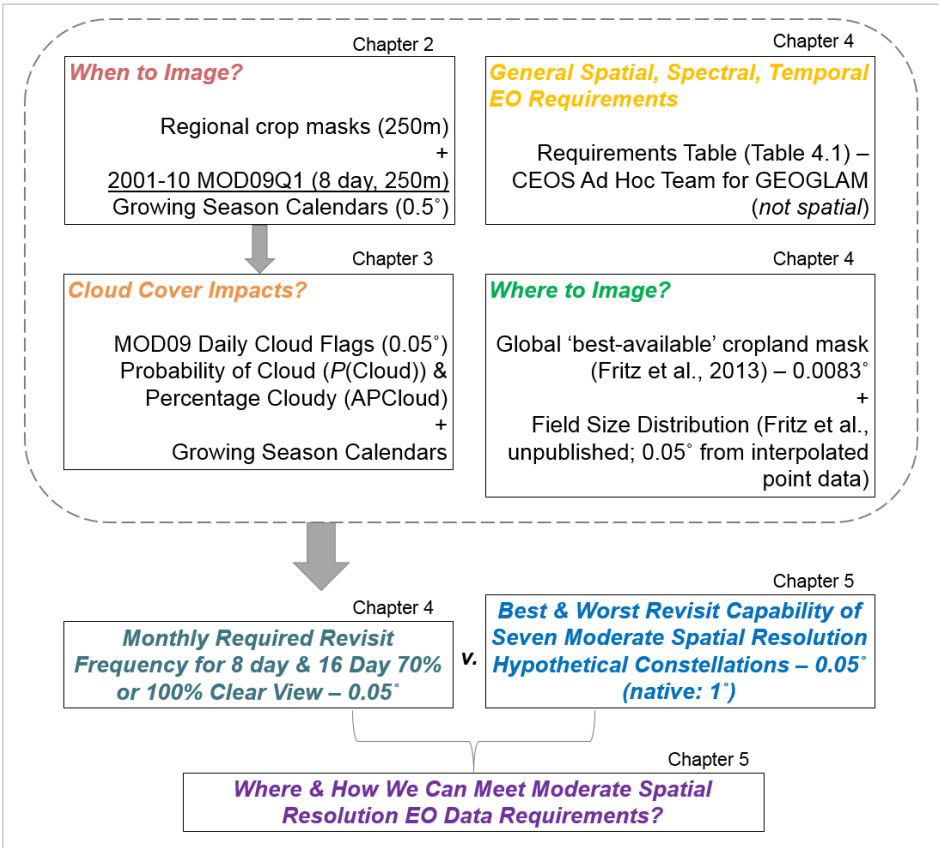

Figure 1.2: Schematic illustrating the organization, flow, and components of this dissertation research.

Timing of the agricultural growing season comes from the development of the first global, spatially-explicit, satellite-derived agricultural growing season calendars at 0.5˚ (Chapter 2). These GSCs are derived from ten years of 8 day MODIS surface reflectance, and include phenological transitions dates (PTDs) for start of season, peak period of season, and end of season. Previously, global information on the timing of the agricultural growing season was restricted to ground based crop calendars which often lacked regional or sub-national phenological characterization, rendering them inappropriate for identifying in a spatially explicit manner the EO requirements for agricultural monitoring.

Information on how cloud cover impacts optical imaging over agricultural areas, throughout the growing season, and at different times of day is discussed in Chapter 3. This is accomplished through the use of 10-13 years of MODIS Terra and Aqua surface reflectance cloud flags compiled in such a way that provides perspective both on the extent and frequency of cloud cover.

Chapter 4 introduces the aforementioned requirements table (Table 4.1), which is a collection of spatial, spectral, and temporal requirements derived from "best-practices" for a variety of different agricultural monitoring applications. In this chapter, supplementary datasets are introduced and then combined with the GSCs from Chapter 2 and cloud cover information from Chapter 3 to place the EO requirements in a spatial context. It provides insight on the revisit frequency required to probabilistically yield reasonably clear views of actively cropped 0.05˚ cells every 8 or 16 days around the world throughout the agricultural growing season.

Finally, Chapter 5 relates these spatialized EO requirements to current and planned near-term polar orbiting moderate spatial resolution O+TIR missions, detailing where and when those data requirements can be met and where and when alternative data sources (primarily microwave SAR, but also geostationary optical) must be considered. Chapter 6 concludes the dissertation work and provides insights into future research directions. This dissertation research provides key inputs and baseline results from which to construct an image acquisition strategy for global agricultural monitoring.

Chapter 2: Spatially Explicit Timing of the Agricultural Growing Season

2.1 Introduction

In order to articulate EO requirements and in turn develop an acquisition strategy designed particularly for agriculture monitoring, one must identify at a meaningful spatial scale using repeatable methods both *where and when crops are growing* (Becker-Reshef et al., 2010a; Singh Parihar et al., 2012) – conditions which can be satisfied using satellite remote sensing (Lobell & Asner, 2004; Pan et al., 2012; Zhang et al., 2003). From this point of departure, this chapter seeks to identify the start, peak period, and end of agricultural growing season phenological transition dates (PTDs) for global cropped areas using ten years (2001-2010) of 8 day 250m MODIS surface reflectance (MOD09Q1) data converted to NDVI and aggregated to 0.5°, providing guidance for as to when imagery are required for monitoring. While for certain monitoring applications (such as crop progress and condition), information is crucial throughout the agricultural growing season (AGS), for others (such as early within-season crop area estimates), the most important information is derived from data acquired during the start of season (SOS) and peak period (Becker-Reshef et al., 2010b; Boken & Shaykewich, 2002).Breaking the season down by the PTDs SOS, peak period (the period during which the true NDVI maximum will likely exist), and end of season (EOS) provides information that will help determine when and how frequently (Chapter 3) data are required for these different applications.

The use of remote sensing data for the production of global agricultural phenology provides the unique benefits of a finer spatial resolution than existing

ground-based information on agricultural phenology and of information on interannual variability in PTDs. Ground-based crop calendars have been the primary source of information about the timing and duration of the AGS to-date. They are crop-specific, only representing one cropping cycle as opposed to the two or three per year (or five every two years) that can exist in multicropping systems (Biradar & Xiao, 2011), and typically involve a large amount of spatial interpolation from survey-based dates to provide regional- or national-level coverage (Sacks, Deryng, Foley, & Ramankutty, 2010), thereby missing within-region variations in growing season periods. For the conterminous United States (CONUS), the United States Department of Agriculture National Agricultural Statistics Service (USDA-NASS) has developed good quality crop calendar information at the state-level, detailing the ranges of planting and harvesting dates for a variety of field crops commonly cultivated (USDA-NASS, 1997; 2010). However, these data still rely considerably on spatial interpolation of census-based data, and while they provide perhaps the best available comparison dataset, they should not be considered completely correct in all cases as they miss sub-regional variation (Stehfest, Heistermann, Priess, Ojima, & Alcamo, 2007).

Outside of the CONUS, information on crop timing is limited and often unreliable, as existing crop calendars have unclear/unknown data sources, are often out of date, are poorly documented, generally lack subnational growing season characterization, and are not spatially explicit (Portmann, Siebert, & Döll, 2010; Sacks et al., 2010; Stehfest et al., 2007). In an attempt to generate a global product that also considers geographical variations in climate, Stehfest et al. (2007) modelled

planting dates at 30 arc minutes (0.5°) for several major crops by choosing the highest modelled yield's associated planting month. However, such an approach made no attempt to identify the peak or the harvesting periods. Additionally, due to the lack of existing observed planting dates at a sufficiently fine resolution, they were unable to evaluate the reliability of this modelled approach. Lack of data for comparison or validation is an issue common to phenological studies (Sakamoto et al., 2005, 2010; Wardlow, Kastens, & Egbert, 2006; Wu et al., 2013b).

With these limitations of crop calendars for the purpose of defining the necessary period of image acquisition in mind, this chapter introduces a set of global, spatially explicit growing season calendars (GSCs). This approach is a fundamental departure from past investigations into general land surface phenology, which consider all vegetation types or crop-specific phenology (Reed et al., 2009; Sakamoto et al., 2005, 2010; Xiao et al., 2005). Rather than defining planting and harvest dates for a single crop, these GSCs seek to identify the SOS, peak period, and EOS dates for all crops in a geographical area appropriate for both moderate resolution sensors' imaging swaths and regional agricultural variations. For this purpose, the selected resolution is 0.5°, roughly 56 km at the Equator, which falls beneath the swath widths of moderate resolution sensors (e.g. Landsat at 185 km or AWIFS at 720 km), and roughly equivalent to the USDA Foreign Agriculture Service's (USDA-FAS) IJ units, their smallest aggregations of international agricultural information (Becker-Reshef et al., 2010a).

Data acquired during a vegetation index's peak (maximum) period, such as that of the normalized difference vegetation index (NDVI), provide particularly

important inputs to yield models as well as planted area mapping (Becker-Reshef et al., 2010b; Boken & Shaykewich, 2002; Ozdogan, 2010; Wardlow & Egbert, 2008). However, as NDVI data are known to saturate in areas with high leaf area index (Huete et al., 2002), and as the mixing of multiple crop signals together can change apparent timing of the NDVI maximum, the approach taken here is to identify a broader time period in which the maximum is likely to occur. This period is herein referred to as the "peak period," and is presented with a discussion of caveats associated with detecting the peak period in areas with multiple cropping cycles. Concise definitions of these phenological parameters can be found in Table 2.1.

Table 2.1: Phenological Transitions Dates Parameter Descriptions

PTD Parameter Name	**PTD Parameter Definition and Algorithm Specification**
Start of Season (SOS)	Greenness onset; emergence of above ground biomass; first point at which an upward trending NDVI which precedes the NDVI maximum (peak) surpasses a given threshold
Peak Period Start (PPS)	Onset of green leaf area maximum; start of the period during which the NDVI maximum is likely to occur; first point above 75% of annual range in NDVI which precedes the NDVI maximum (peak)
NDVI Maximum (Peak)	The NDVI maximum observed within a given growing season
Peak Period End (PPE)	Onset of senescence; end of the period during which the NDVI maximum is likely to occur; last point above 75% of annual range in NDVI which follows the NDVI maximum (peak)
End of Season (EOS)	End of senescence; termination of photosynthetic activity; last point at which a downward trending NDVI which follows the NDVI maximum (peak) dips below a given threshold

In reality, in nearly every landscape, the 0.5° grid cell is comprised of more than one single crop type often with different phenologies, particularly if there is a

mix of winter and spring/summer crops (Ozdogan, 2010; Pan et al., 2012). The problem of subpixel heterogeneity in cultivated areas is frequently encountered in crop type mapping and monitoring (Duveiller & Defourny, 2010; Lobell & Asner, 2004; Ozdogan & Woodcock, 2006; Pax-Lenney & Woodcock, 1997), and it is expected that the mixing of these signals will similarly impact the apparent timing of these different PTDs, with the extent to which these signals are mixed changing the extent to which the PTDs deviate from a given crop's calendar. That is, a 0.5° cell for which the majority of the 250m cropped pixels' crop type is corn will yield PTDs closer to that of corn's crop calendar than will an area that is equal parts corn and winter wheat (Pan et al., 2012). A test of the effects of mixing known winter and spring crops' signals (individual cropped pixels extracted from USDA-NASS Cropland Data Layer from 2006 and 2007 (Boryan, Yang, Mueller, & Craig, 2011; Han, Yang, Di, & Mueller, 2012; Johnson, 2010) in different proportions on PTD determination has been performed for a few sites in Kansas and Missouri to give preliminary insight into this complex topic (see Section 2.3.4).

Due to reliability issues as well as thematic differences in types of existing studies of land surface phenology, no appropriate global comparison data exist for these growing season calendars. Vegetation phenology is too general, and the disagreement/agreement between the GSCs and any set of compiled crop calendars would only be meaningful in areas of homogeneous crop-type cover (e.g. the US Corn Belt). Further, the degree of agreement between the GSCs and the comparison data would vary with the latter's compilation approach (i.e. for areas with multiple crops, which crop's calendar dates should be used for comparison?). As such, a

quantitative validation between these existing crop calendars and finer resolution GSCs would be negatively impacted by the lack of within-region variation in the crop calendars (Sakamoto et al., 2010; Wardlow et al., 2006), something that will be discussed and addressed in Section 2.3.1.1. For this reason, a quantitative comparison will only be provided for the CONUS where Sacks et al. (2010) have digitized USDA-NASS (1997) usual planting and harvest dates.

To illustrate the sensitivity of GSCs to interannual variability as well as to within-region heterogeneity in phenology, correlations with USDA-NASS Quick Stats (USDA-NASS, 2013) yearly crop progress are presented and discussed. To address this lack of validation outside of the United States, the global calendar dates which are presented in this chapter were reviewed and refined by agricultural experts from around the world.

2.2 Methods

2.2.1 Data pre-processing and preparation

The processing steps and the general logic behind the phenological transition dates extraction algorithm are outlined in Figure 2.1. Ten years (2001-2010) of global, 250m 8 day surface reflectance data (MOD09Q1) were converted to NDVI (Rouse, Haas, Schell, Deering, & Harlan, 1974), and then were adjusted through the application of strict quality assessment (QA) bits from the state QA layer for MOD09A1 (Vermote, El Saleous, & Justice, 2002) which had been resampled from 500m to 250m. The data were not, however, adjusted for the effects of bidirectional reflectance. Data converted to NDVI have been shown to be less impacted by variable

view and azimuth angles throughout the growing season than the Enhanced Vegetation Index (EVI), or red and near-infrared channel data alone, at least partially justifying the lack of BRDF adjustment (Bréon & Vermote, 2012; Sims, Rahman, Vermote, & Jiang, 2011).

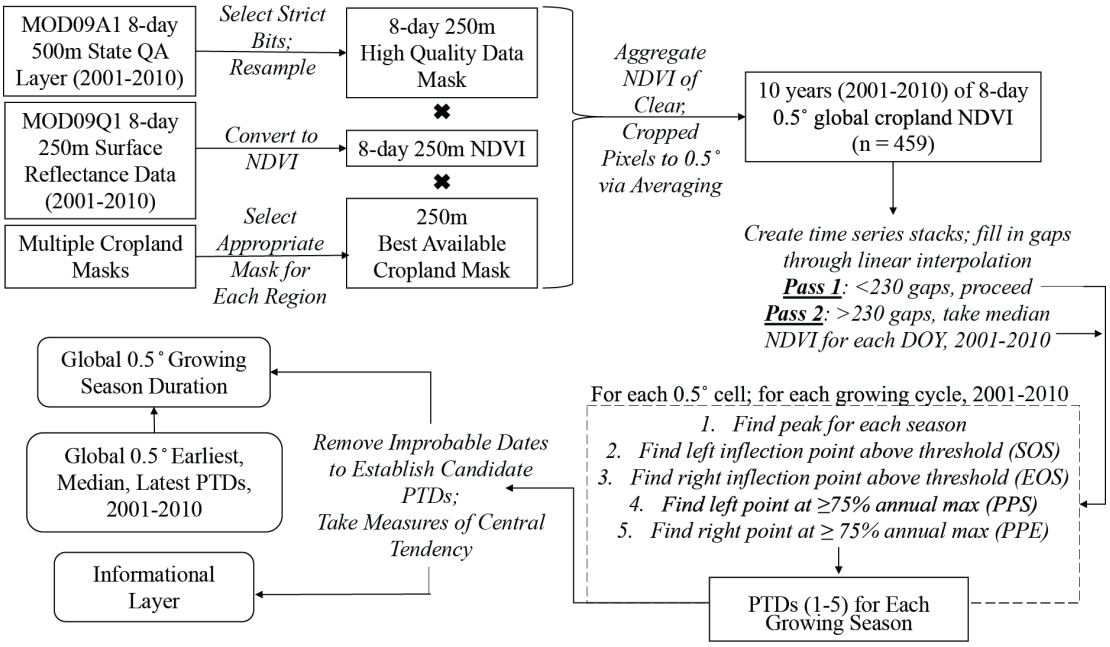

Figure 2.1: A flowchart depicting the pre-processing and data preparation steps, the basic logic of the PTD extraction algorithm, as well as the steps leading to the generation of the final data products. Intermediate data products and steps are in solid rectangles, actions are connecting arrows accompanied by italicized text, and final data products are in soft-cornered rectangles.

Before aggregating from 250m to 0.5° to create a general cropland NDVI, cropland pixels needed to be identified. Several cropland masks and land cover products were used to do so, all produced in 2001 or more recently, with preference given to those products which were percentage or probability products (Table 2.2). For example, in the CONUS, the cropland layer from the 2001 National Land Cover Database (Homer et al., 2007) was used by resampling from crop/non-crop values at

30m to 250m, with only those 250m pixels which were ≥80% cropped being aggregated to 0.5° through averaging. Due to some spatial gaps left after the analysis using NLCD-2001, an additional "background" layer was generated from Pittman et al.'s (2010) discrete cropland mask to generate more complete coverage. The cropland mask used for each 0.5˚ grid cell is identified in a supplementary informational layer.

Table 2.2: Crop Masks Used

Name	**Notes & Specifications**	**Associated Citation**
NLCD 2001[1]	Pass 1, ≥80%	(Homer et al., 2007)
Global Cropland Extent (Discrete)	Pass 1; Pass 2	(Pittman, Hansen, Becker-Reshef, Potapov, & Justice, 2010)
Geocover 2000	Pass 1; ≥90%	(Tucker, Grant, & Dykstra, 2004)
Global Cropland Extent (Probability)	Pass 1; ≥90%	(Pittman et al., 2010)
MOD12 2004	Pass 1; Pass 2	(Friedl et al., 2002)
CORINE 2000	Pass 1; Pass 2	(Bossard, Feranec, & Otahel, 2000)

Each resulting time series of these 0.5˚ 8 day QA-adjusted cropland NDVI images had a number of temporal gaps due to the stringent QA requirements. These gaps as well as those values which dropped below the mean annual minimum NDVI (2001-2010) for that grid cell (perhaps due to errors in cloud screening; Huete et al., 2002) were replaced using linear interpolation, so as not to distort the annual ranges of NDVI. This gap-filled time series of 0.5˚ cropland NDVI was run through the PTD extraction algorithm during Pass 1. Those 0.5˚ grid cells for which >50% (n=230) of the 10-year time series was missing (largely due to chronic cloud cover) were initially

[1] Originally at 30m, the masks for NLCD 2001 and Geocover 2000 were aggregated to 250m and placed in the MODIS gridding scheme by Inbal Becker-Reshef.

not processed for PTDs in Pass 1. A subsequent pass (Pass 2 in Figure 2.1) at processing was carried out for these areas in which a single year-long time series was constructed out of the median NDVI value for each compiling day of the year (DOY) over 10 years and then processed for PTDs. This latter pass yielded useable dates for many areas, but still left some persistently cloudy areas (e.g. central Africa, parts of southeast Asia) without PTDs.

2.2.2 Extracting Phenological Transition Dates from Time Series NDVI

NDVI is a metric which has long been used as an indicator of above ground green biomass (AGB), vigor, stress, photosynthetic capacity, and leaf area index (LAI), and as a proxy for vegetation health (Baret & Guyot, 1991; Jackson, 1986; Rouse et al., 1974; Sellers, 1985; Tucker, Holben, Elgin, & McMurtrey, 1981; Tucker, 1979; Wiegand & Richardson, 1990). The Moderate Imaging Spectroradiaometer (MODIS), with improved radiometric and geometric properties and atmospheric correction, has provided higher quality data which have proven useful for land biophysical applications (Justice et al., 1998; Vermote et al., 2002; Wardlow et al., 2006). The NDVI was chosen because it has been shown to be suitable for studying phenology in the CONUS (Goward, Tucker, & Dye, 1985), and involves only the two MODIS bands which have 250m (231.65635m, precisely) resolution, whereas the Enhanced Vegetation Index (EVI) would require the incorporation of coarser 500m data (Huete et al., 2002) in addition to being less resistant to BRDF effects (Sims et al., 2011). In areas where croplands are small and fragmented and the agricultural landscape is heterogeneous, the use of finer resolution data can potentially reduce the inclusion of non-cropped surfaces (Duveiller, Baret, &

Defourny, 2011; Duveiller & Defourny, 2010; Pittman et al., 2010; Townshend & Justice, 1988; Wardlow, Egbert, & Kastens, 2007), justifying the choice of 250m over 500m observations.

Planting and harvest are processes which are not easily detected by moderate-to-coarse sensors such as the MODIS instruments, as planting does not result in instantaneous crop-specific above ground biomass (AGB) generation, and harvesting often leaves a large volume of AGB present, continuing to influence reflectance for some time after the end of the cropping season (Reed et al., 1994; Wardlow et al., 2006). Furthermore, soil background and in some cases non-crop vegetation can influence the signal in advance of and immediately after planting (Galford et al., 2008; Wardlow et al., 2006). For these reasons, this analysis identifies a series of PTDs (Table 2.1) that can be related to cropping practices: first, the start of growing season (SOS) has been identified as the point when an up-sloping NDVI surpasses a certain threshold (for background vegetation) in a period preceding an annual maximum (peak) NDVI. This point describes the onset of photosynthetic activity, also known as "the greenup" (Zhang et al., 2003), and marks the beginning of a crucial time for monitoring crop development (Becker-Reshef et al. 2010a). Second, the end of growing season (EOS) is considered the point at which a down-sloping NDVI drops below a certain threshold in the period following the annual peak, marking the end of senescence and the termination of photosynthetic activity for the crops (Zhang et al., 2003). The thresholds used in detection of SOS and EOS were determined through an iterative process and were instituted largely to avoid the detection of volunteer weeds which precede the green-up of actual crops and would

bias the SOS earlier, an issue which is likely to be more impactful in areas with high precipitation where tilling is not used (Galford et al., 2008; Wardlow et al., 2006). Finally, the peak timing and duration have been identified as the period during which NDVI is ≥75% of its annual range falling around the apparent NDVI maximum. This "peak" metric is unique to satellite data, with Zhang et al. (2003) having described a conceptually similar period (for all vegetated surfaces, not just crops) as representative of the period between the onset of green leaf maximum for a vegetated surface (peak period start; PPS), and the onset of senescence and subsequent rapid decline of photosynthetic activity (peak period end; PPE). Therefore, SOS and EOS dates span the entire active growing season, and are rough estimators of planting and harvest, with SOS theoretically occurring after the actual planting, while the peak period bounds the portion of the growing season during which the LAI maximum will likely occur (Zhang et al., 2003).

Multiple methods have been established in the literature for extracting phenological information from temporal curves of NDVI, primarily using thresholds, inflection points, largest increases/decreases, and divergence from an established trend (Jönsson & Eklundh, 2004; Reed et al., 2009). Several studies have used NDVI thresholding approaches to detect seasonal changes in vegetation, wherein a certain NDVI value is assumed as indicative of a change in vegetation stage (Fischer, 1994; Lloyd, 1990; White, Thornton, & Running, 1997), while others identified as beginning, peak, and end of season the sign changes (inflection points) of the first derivative of the NDVI curve (Moulin, Kergoat, Viovy, & Dedieu, 1997). The

methodology adopted for this study can be described as a combination of the application of thresholds with detection of inflection points.

2.2.3 Growing Season Calendar Compilation

For each 0.5˚ grid cell, the PTD detection algorithm yielded up to ten viable SOS and EOS dates as well as ten viable PPS and PPE dates (Figures 2.2a-b). When defining the agricultural growing season for the purpose of satellite imagery acquisition, cost and operational constraints are critically important and as such the exclusion of even potentially spurious dates is crucial from a strategic standpoint. Outlier removal is challenging and problematic in very dynamic cropping systems with high interannual variability, but is justifiable in the context of developing an image acquisition strategy, where imaging resource and cost constraints must be considered. Accordingly, measures of central tendency were taken to identify and remove dates which fell more than one median absolute deviation from the median. From this "cleaned-up" set of PTD candidates, the earliest, median, and latest SOS, and EOS dates were extracted for each 0.5˚ grid cell. Two separate growing season duration metrics were calculated: first, the median observed growing season duration from a single season was taken (i.e. each season's detections were analysed separately); and secondly, the number of days between the earliest SOS and the latest EOS date was taken, regardless of whether those observations were from the same season, in order to give an idea of the maximum possible period of time for which observations would be necessary. Meanwhile, the median peak period duration within a single season was extracted, and the corresponding PPS and PPE dates were preserved.

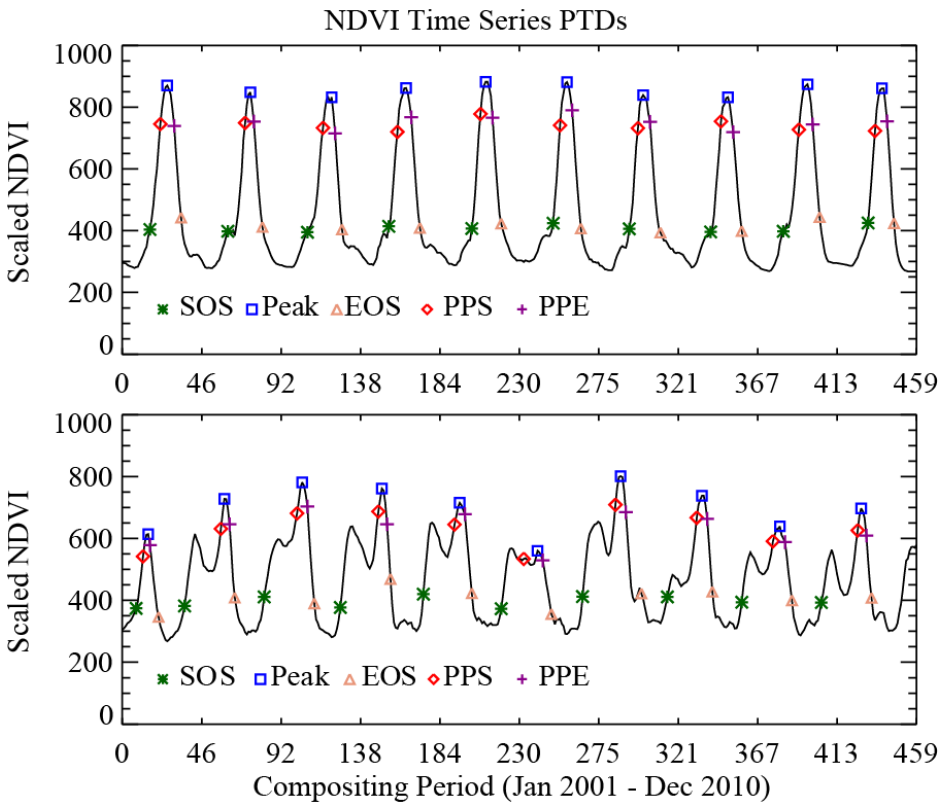

Figures 2.2a-b: Plots of the gap-filled time series of 8-day composites of scaled NDVI (x 1000), 2001-2010 (46 per year x 10 years = 460 values), from which PTDs were detected. a) Top, NDVI time series from a location in southern Kansas, providing an example of a winter wheat dominated landscape, with the SOS being detected in the October-November time period, and the EOS being detected in the June-July time period. The algorithm selects the post-dormancy resumption of growth (Miller, 1999) of the crop as the peak period, and in 2001 places the SOS in March (contemporaneous with this post-dormancy re-emergence) due to the true SOS taking place in 2000, before the initiation of the time series. b) Bottom, NDVI time series from a location in central Indiana, providing an example of a corn/soy mix, with the SOS being detected in April-May, and the EOS being detected in October.

To accompany these GSCs, an informational map layer was stored which tracks for each 0.5˚ grid cell the use of quality assessment bits, the impacts of cloud cover, the crop mask used, the degree of interpolation ("gap-filling") necessary, as well as measures of central tendency for the dates detected for each cell. This information can be used as a sort of "confidence layer" in future exercises.

2.3 Results

Broadly speaking, the agricultural growing season spans the spring to fall period for Northern and Southern Hemispheres, with notable exceptions for areas of known winter crop (e.g. wheat, barley) cultivation in Australia, the southern Plains/Pacific Northwest of the US, China, and in areas of southern Europe (Figures 2.3a-b). For summer/spring crop cultivating areas, the PTDs follow broad patterns of climate limitation, with later SOS and earlier EOS for areas which are further inland (continental climate), more arid (dryer), and/or further from the Equator (lower winter temperatures). Other factors, such as ability to irrigate, selection of seed varieties, and farmer decision making are likely implicated in these regional variations, but analysis of these factors is beyond the scope of this analysis.

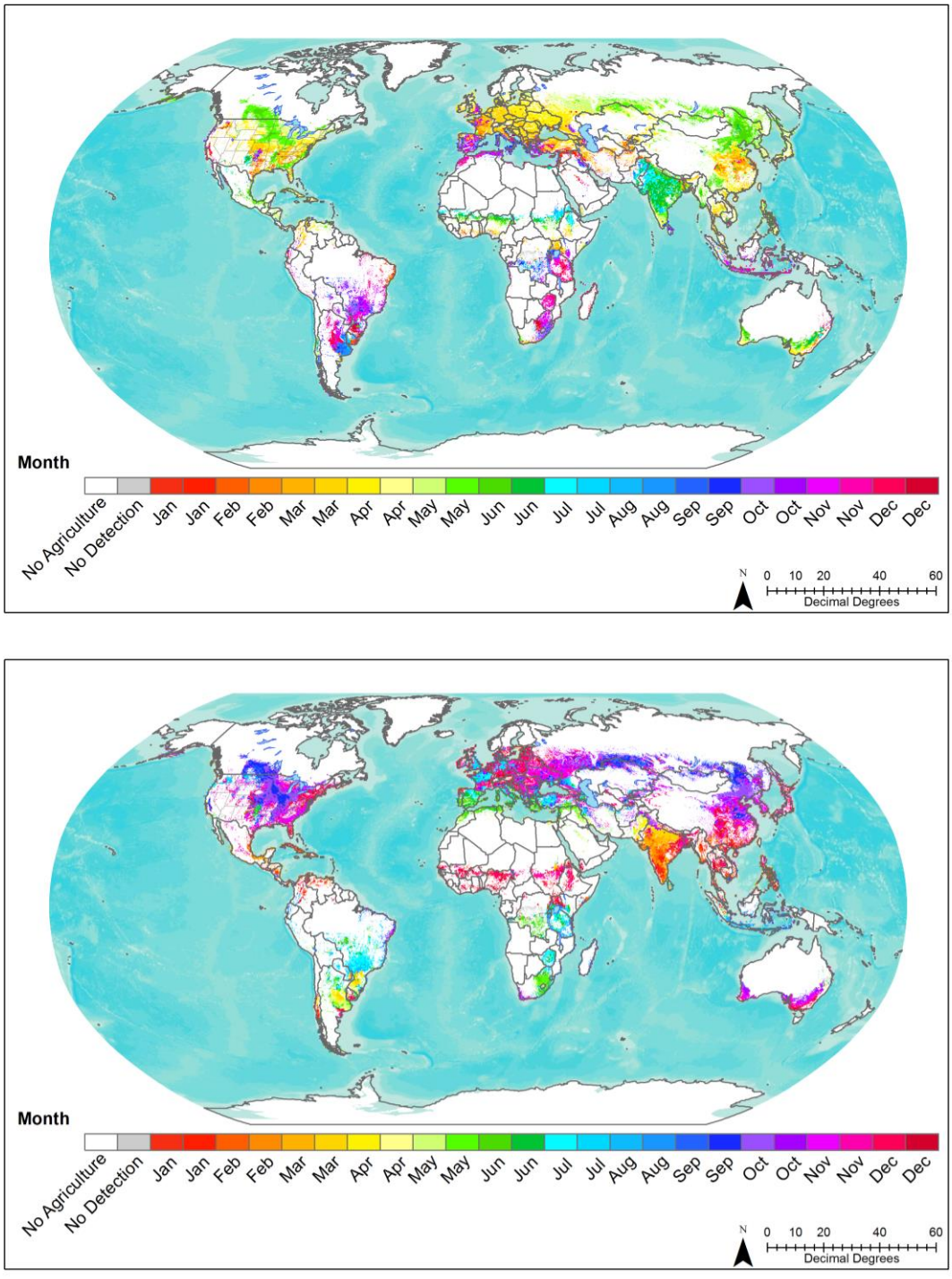

Figures 2.3a-b: The global median, a) Top, SOS date, and b) Bottom, EOS date, as observed between 2001 and 2010. The PTDs are natively at 0.5˚, but the inclusion of even a single 250m cropped pixel in any of those half-degree grid cells would lead to a large overestimation of cropland extent. In this global view, a cropland indicator mask (GLAM-UMD, unpublished raw data) at 0.05˚ has been overlaid to provide a more realistic extent of cropland area. Some grid cells (shown in grey) had no detection over 2001-2010 (due to cloud cover or low quality observations), despite having at least some cropland present.

As discussed previously, there are no reliable data against which the global product can be compared. For this reason, these GSCs were vetted by regional and national experts within the GEO Agricultural Monitoring Community of Practice, whose evaluations of the product's accuracy and suggested changes were ingested into the final product. Preliminary discussion with experts in areas of Australia, Canada, Argentina, Uruguay, Ukraine, Spain, and Russia show that the time periods encapsulated by these GSCs are indeed representative of the periods during which satellite imagery are necessary for their respective areas. For the CONUS, however, this paper presents a comparison of GSC dates against crop calendar dates for a few states in the corn and soy cultivating areas of the CONUS from Sacks et al. (2010) digitization of USDA-NASS (1997) Usual Planting and Harvest Dates. Additionally, state-level crop progress data (each state's crop's planting, emergence, and harvesting progress) from USDA-NASS from 2001-2010 are compared with each individual year's PTDs to illustrate the GSCs sensitivity to interannual variability.

2.3.1 Geographical Patterns of PTDs Observed in the CONUS

Including small contributions from Alaska and Hawaii, an average of 98.9 million hectares were harvested in the USA each year between 2001-2010, including those areas for which there were multiple crop rotations and for which each harvest's area was counted. More than 80% of total area harvested is accounted for by three crops: maize (30.9%), soybeans (29.8%), and wheat (both winter & spring varieties, 20.4%), the remainder being largely composed of seed cotton (4.7%), sorghum (2.7%), barley (1.5%), and rice (1.3%) (FAOSTAT, 2012). A majority of the cultivation is spring and summer crops, although winter wheat and barley are

commonly cultivated in the southern half of the CONUS, with much of the west coast states cultivating specialty crops throughout the year (USDA-NASS, 1997; 2010). The GSCs model these known phenomena, with clear winter crop dominated cultivation in the southern Plains states (Texas, Oklahoma, Kansas) as well as in some portions of the Pacific States, where SOS dates come between August and December (Figures 2.4a-b). The major corn and soybean producing states are well-characterized with the earliest SOS dates falling generally in April to May and the median SOS dates falling predominately in late May. Meanwhile, the median EOS dates fall in late-September and the latest EOS season dates fall from October to November, aligning well with planting ranges (April-May) and harvest ranges (September-November) articulated by USDA-NASS (1997; 2010).

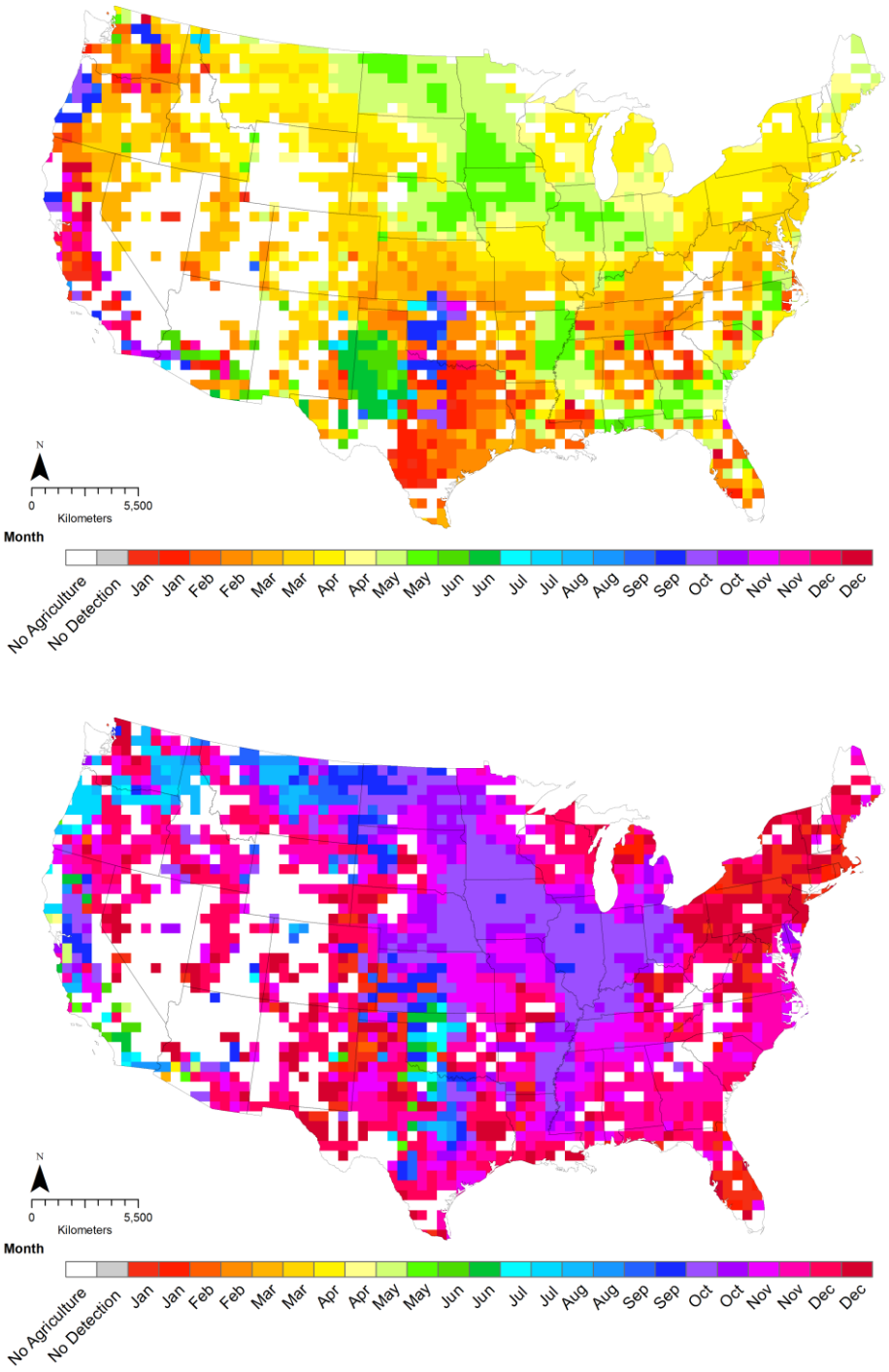

Figure 2.4a-b: For the CONUS, the median a) Top, SOS date, and (b) Bottom, EOS date, as observed between 2001 and 2010. The GSCs are shown at their native resolution (0.5˚) without any post-processing application of a finer scale cropland mask to account for true cropland extent estimation (as in Figures 2.3a-b).

In Illinois, Iowa, and Indiana, corn is planted 2-3 weeks before and harvested 1-2 weeks after soybeans. It is expected, then, that SOS dates – which by accounting for multiple crops on the landscape and by approximating emergence are expected to come a few weeks after planting – will fall after corn planting and right around soy planting. Meanwhile, EOS is a rough approximation of harvest without a specified direction of disagreement, and thus EOS should fall sometime around soybean harvest and just before corn harvest. Both of these expectations are represented in the GSCs, as shown through comparison with USDA-NASS's (1997) average planting and harvest dates for corn (Figure 2.5a-b) and soybean (Figures 2.5d-c), respectively, for Illinois, Indiana and Iowa (n=161, 0.5˚ cells). Each of these states produces large quantities of corn and soybean relative to other crops, meaning that their relative homogeneity makes them an appropriate area for comparing single crop calendars with the GSCs.

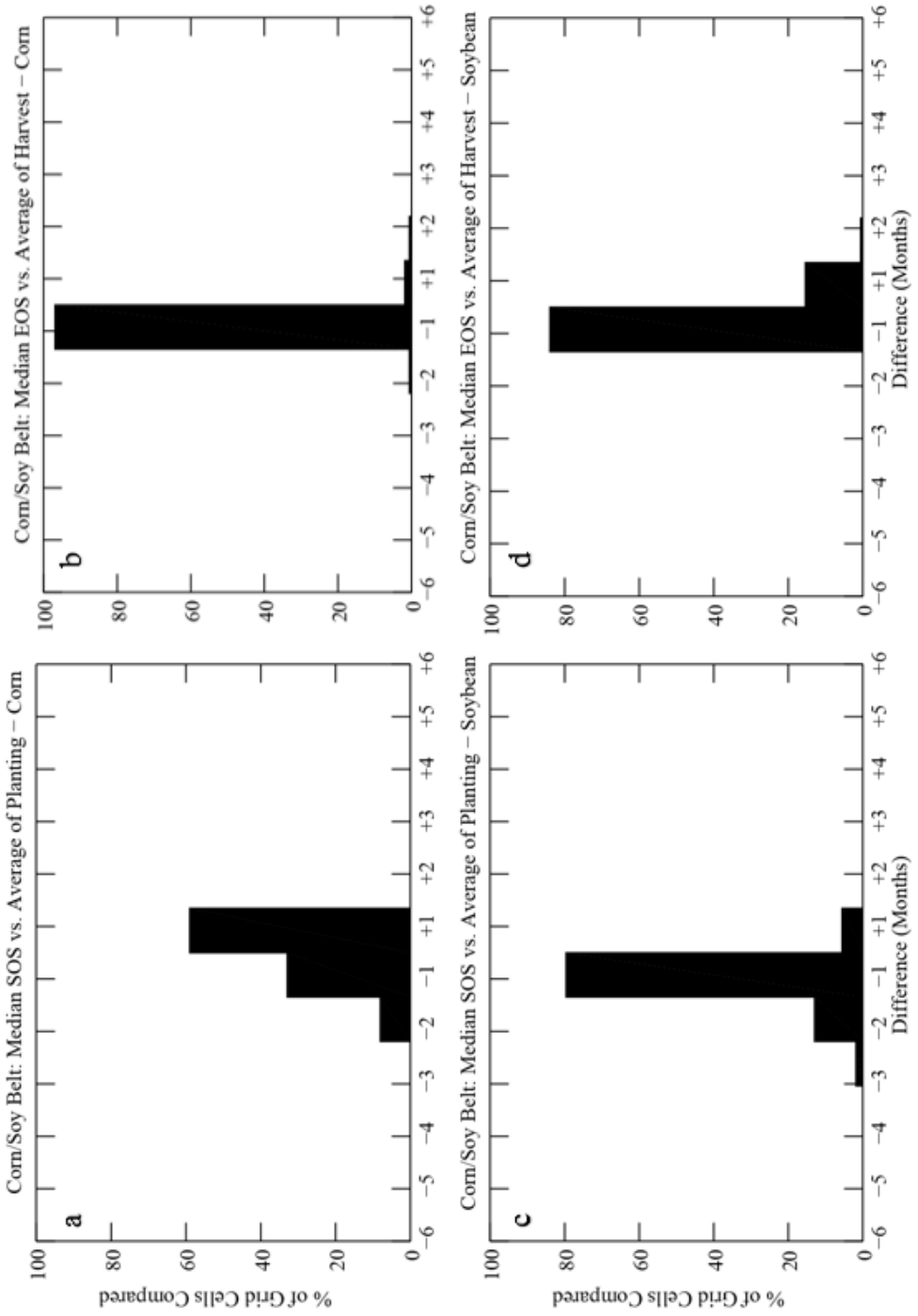

Figures 2.5a-d: Histograms of GSCs minus Sacks et al. (2010)/USDA (1997) planting or harvest dates for corn/soybean cultivating states Illinois, Indiana, and Iowa. A negative value indicates an earlier GSC and a positive value indicates a later GSC relative to planting or harvest dates. Very few 0.5˚ grid cells agreed perfectly, and so were placed in the +1 month category if they existed. Clockwise from top left: a) median SOS date minus average corn planting date; b) median EOS minus average corn harvesting date; c) median SOS date minus average soybean planting date; d) median EOS minus average soybean harvesting date.

Beyond the major corn and soy producing states of the CONUS, there also exist three major areas of cotton cultivation – western Texas (TX), along the Mississippi River (Louisiana, Arkansas, and Mississippi), and in the southeast (southern Georgia and eastern Carolinas). In TX, the most active planting takes place in May-June, with the most active harvest period taking place during November, while in both the southeast and the states along the Mississippi River, planting takes place during April-May with harvest occurring in October-November in the former case, and primarily October in the latter case (USDA-NASS, 1997). All of these dates are accurately represented by the GSCs.

In California (CA), the existence of a climate that is amenable to year-round cultivation leads to a more variable suite of suitable crops, including a wide variety of specialty crops. According to USDA-NASS (1997), in CA planting spans the entire year, while harvesting spans from April 1st (sugarbeets) until December 10th (sugarbeets), and this is not to mention specialty crops (e.g. grapes, tomatoes, berries) growing in the state. The GSCs reflect these dynamics, even detecting rice cultivation in the Sacramento River Valley, spanning from May until October (consistent with those dates in USDA-NASS, 1997). With respect to the northeast, the majority of cultivation in that area is actually alfalfa hay (year round cultivation) with a small area of corn production in New York, for which the corresponding USDA-NASS (1997; 2010) crop calendar dates (April/May to October/November) are closely approximated in the GSCs, April/May to November/December. This area is not a high priority for agricultural monitoring due to its low production of food crops, and therefore does not merit further investigation for the purpose of this analysis.

2.3.1.1 Sensitivity of GSCs to Interannual and Regional Phenological Variations

The USDA-NASS's Usual Planting and Harvesting Dates for US Field Crops (1997; 2010) referenced in this chapter give ranges of observed planting and harvest dates for entire states for a given crop, aggregating information from multiple geographic locations and multiple years. These roughly decadal releases are based off of yearly crop progress data on state-wide percentage of crop type that have been planted, emerged, and harvested. Meanwhile, for a given year, a single set of progress information exists for an entire state despite the percentage planted/emerged/harvested values themselves essentially being aggregations of geographic variations in planting, emergence, and harvest timing across a state (that is to say, the progress data indicates on a certain day of the year, 20% of the state has been planted, but there is no spatial information on *which* areas that 20% occupies). In contrast, the GSCs are at a finer resolution (0.5˚), meaning that they avoid this geographic aggregation and provide insight into within-state variations in phenological transitions.

For Illinois, Indiana, and Iowa, the days of year which correspond with five thresholds (0-20%, 20-40%, 40-60%, 60-80%, and 80-100%) of area planted and area emerged corn progress data for each year 2001-2010 have been extracted from the USDA-NASS Quick Stats Database (USDA-NASS, 2013). These threshold dates have been correlated with SOS dates to try to determine whether the GSC PTDs are sensitive to interannual variability in cropping dynamics. The same approach has been taken with area harvested thresholds and EOS dates. Because of the geographic aggregation present in the state-level corn progress data, it is expected that certain

percent planted/emerged/harvested thresholds will produce better correlations with SOS/EOS dates for certain grid cells. Figures 2.6a-c show the maximum correlation value (0-1) as well as that maximum value's corresponding crop progress threshold. Keeping in mind that this is a correlation for only corn, and not soybeans or winter wheat or any other crop that may exist in these states, the GSC PTD algorithm is fairly sensitive to interannual variability in cropping dynamics, particularly with SOS/percent emerged and EOS/percent harvested. This not only demonstrates that the GSC PTD algorithm is sensitive to interannual variability in cropping dynamics, but also clearly illustrates the utility of this type of finer scale analysis of cropland phenology over previous articulations, particularly in the context of planning fine resolution/small swath satellite image acquisitions.

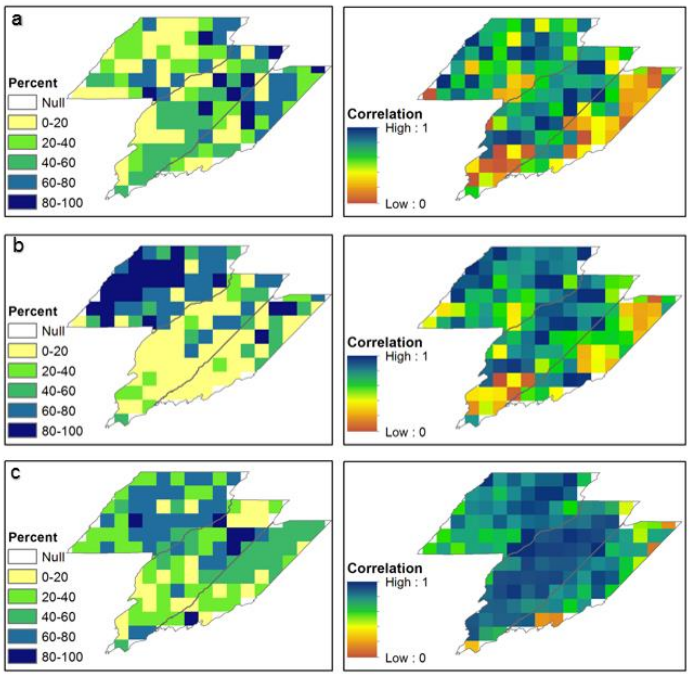

Figure 2.6a-c: Maps of yearly GSC 0.5˚ grid cells correlated with different crop progress percentages from state-level USDA-NASS yearly crop progress data, both sets from 2001-2010. On the right is the maximum correlation value from the five crop progress percentage thresholds, and on the left is the crop progress threshold for which that maximum correlation value exists. a) Yearly percent planted correlated with yearly SOS; b) yearly percent emerged with yearly SOS; c) yearly percent harvested with yearly EOS.

2.3.2 Duration of the Agricultural Growing Season

There are several ways to define the duration of the agricultural growing season when there are several years of SOS and EOS PTDs. For example, the maximum possible number of days for which imagery would be required could be taken as the number of days between the earliest SOS and the latest EOS date observed between 2001-2010, regardless of whether those dates are from the same growing season or not. This, however, might yield an artificially long growing season due to interannual variability in cultivation practices. Instead, presented here is median growing season duration observed in a single season between 2001 and 2010 (Figure 2.7).

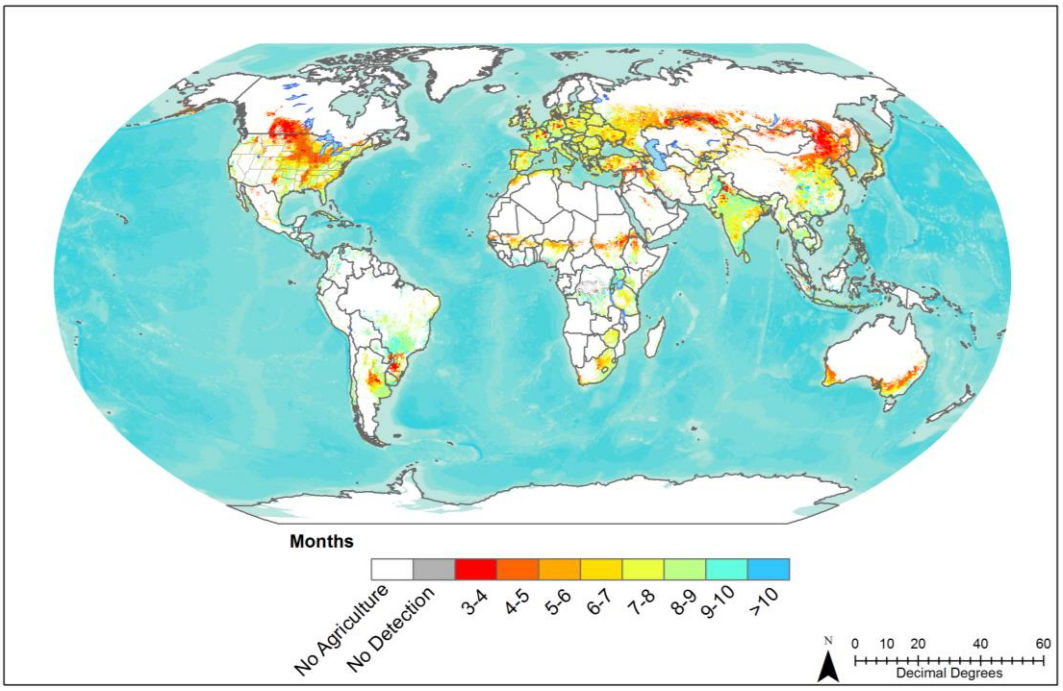

Figure 2.7: The median duration of the agricultural growing season (SOS to EOS from the same growing season), 2001-2010. As in Figures 2.3a-b, the GLAM-UMD cropland indicator mask at 0.05˚ is overlaid the native 0.5˚ GSCs to more accurately represent cropland extent.

While the agricultural growing seasons range from 96 to 352 days in duration, the mean growing season length for the entire world is 216 days (median = 224 days), which is just over seven months. Generally speaking, areas with cooler winters (e.g. higher latitudes, areas of higher elevation) and/or less precipitation (e.g. the Sahel) have shorter growing season durations while areas which are characterized by a warmer and wetter climate have longer growing seasons. The shortest growing seasons are found in the Peace River Valley in Canada as well as in eastern Russia, north of China. While certain winter crop cultivating areas have apparently shortened growing season durations due to the post-dormancy resumption of growth (Miller, 1999) being tagged as the SOS (Section 2.3.4), this at least highlights the most active period of the AGS for monitoring and is important and new information.

These relationships hold in the CONUS, where growing season durations follow a geographic pattern largely dictated by regional climate, ranging from 96-304 days. The mean growing season length for the CONUS is ~205 days, or just shy of seven months, with 3.0% of the 0.5° grid cells having growing seasons lasting 3-4 months, 12.9% of grid cells lasting 4-5 months, 15.7% lasting 5-6 months, 19.2% lasting 6-7 months, 26.8% lasting 7-8 months, 15.2% lasting 8-9 months, and 7.3% lasting 9-10 months. For Midwestern states characterized by a continental climate and limited by very cold winters, the growing season tends to be shorter (3-6 months), while those areas characterized by a warmer or less variable year-round climate (West Coast and Southern states) tend to have longer growing seasons (up to 10 months). Exceptions to these rules are found in western Texas and the Arkansas/Mississippi/Louisiana border, each of which are heavy cotton cultivating

areas with 4-5 month growing periods (USDA-NASS, 1997). Somewhat surprisingly, longer growing seasons are found in the north eastern CONUS where a distinct seasonality and cold winter would suggest a shorter, climate-limited growing season. In fact, as stated in Section 2.3.1, the cultivation of alfalfa hay along with some corn is responsible for this seemingly unusual growing season duration (USDA-NASS, 1997).

2.3.3 Peak Period Timing and Duration

The period during which green leaf area is highest is contemporaneous with the NDVI maximum (Zhang et al., 2003). For reasons identified previously, it is important to determine the period during which this NDVI maximum is most likely to occur. However, at 0.5˚ resolution, an area over which many 250m pixels potentially representing a variety of crop types have been averaged, the relationship between apparent NDVI maximum and individual crop's LAI maximum is perhaps more tenuous as out-of-sync pixel-level NDVI maxima are blended to form a flatter and broader peak period. To allow for this flattening and broadening effect and encompass a wider period during which the maximum NDVI is likely to occur, the peak period was defined as the period for which NDVI is ≥75% of the annual NDVI range (between the peak period start (PPS) and the peak period end (PPE); Figures 2.8a-c). This value – 3/4 maximum – was selected through an iterative process, so as simply to define a period of time just broad enough to likely bound the NDVI maximum. Ten years of PPS and PPE dates were detected (Figures 2.2a-b), and compiled similarly to the SOS/EOS dates (see Section 2.2.3).

Figures 2.8a-c: The median, a) peak period start date and, b) peak period end date as observed between 2001 and 2010, as well as, c) the median peak period duration for that period, which is the number of days between (a) and (b). As in Figures 2.3a-b and 8, the GLAM-UMD cropland indicator mask at 0.05˚ is overlaid the native 0.5˚ GSCs to more accurately represent cropland extent.

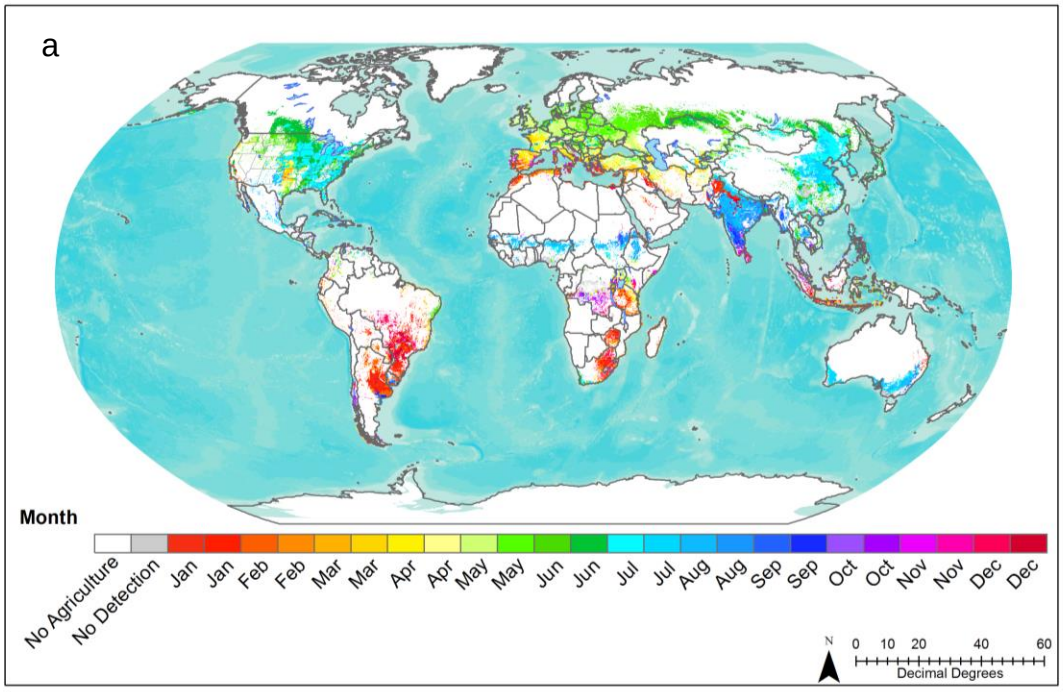

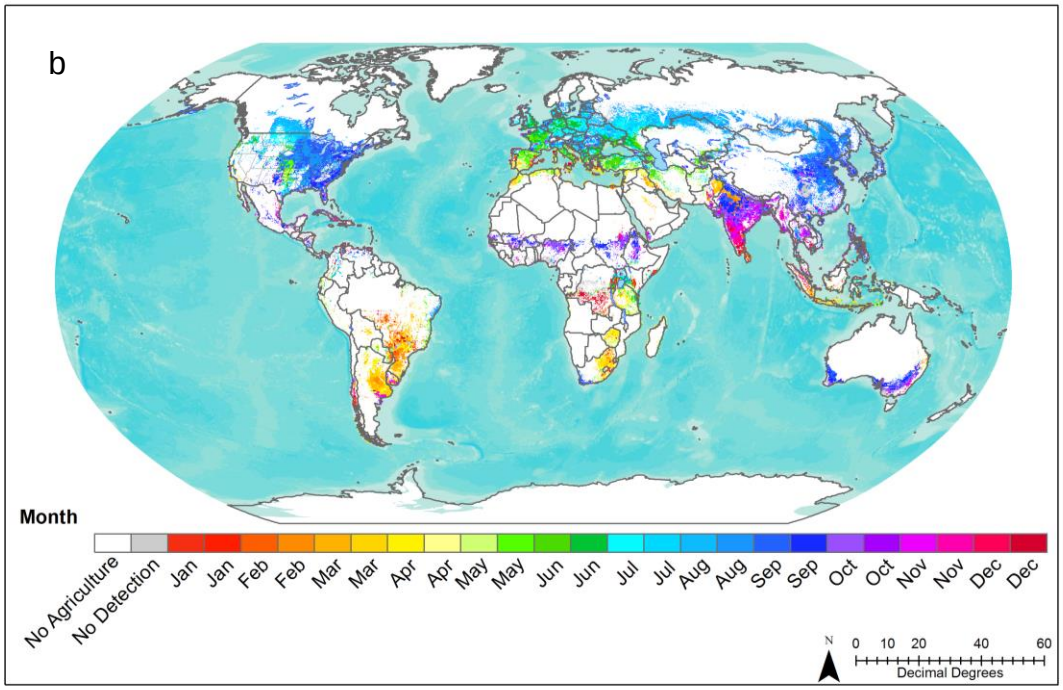

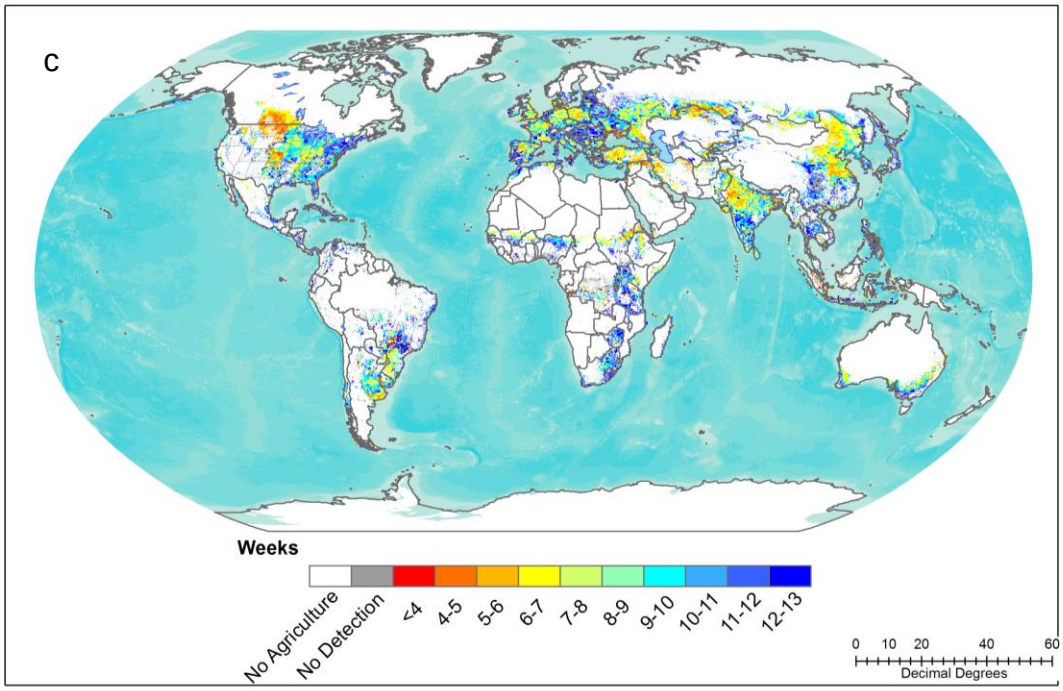

For most agricultural regions, the peak period lasts between 4 and 12 weeks, with longer peak periods typically occurring in the same areas that have longer growing season durations and/or that are known to have multiple crops present on the

landscape. Within the CONUS, there are two areas with distinctly shorter peak period durations: 1) the major winter wheat cultivation area in Kansas/Oklahoma (KS/OK), and, 2) the Montana (MT) and western North/South Dakotas (ND/SD). In the former case, the shortened peak period corresponds with the steeper, shorter (duration) peak associated with the winter wheat's post-dormancy resumption of growth. In the latter case, MT and western ND cultivate almost solely spring wheat and spring barley, which have nearly identical calendars (USDA-NASS, 1997). In contrast, eastern ND/SD have large areas of sugar beet, corn, and soybean cultivation in addition to wheat (spring in ND, winter and spring in SD) and barley (mostly ND), and accordingly have longer peak period durations, illustrating how multiple crops' signals, even when somewhat similarly timed, can combine to create a broader, longer apparent peak NDVI period.

In areas for which multiple, distinct cropping cycles and therefore distinct peaks exist, the peak period approach weakens as the algorithm considers only the dates that surround the annual maximum NDVI rather than allowing for multiple peaks in a year. In the KS/OK area dominated by winter wheat production, the peak period is capturing the winter wheat cultivation's peak; however, there is considerable corn and soy cultivation there as well, and, as discussed in the following Section 2.3.4, the extent to which the increases in corn/soy NDVI impact the apparent timing of the winter wheat NDVI peak is contingent upon the relative proportions of winter vs. spring crops.

2.3.4 Winter Wheat Presence and Impacts on PTD Detection

Figure 2.9 shows a comparison of a corn & soybean only compilation of Sacks et al.'s (2010) digitization of USDA-NASS (1997) usual planting and harvest dates with the GSC SOS dates. Moving toward areas with a larger winter wheat presence, such as Kansas, eastern Colorado, western Nebraska, South Dakota, and southern Illinois, the GSC SOS dates begin to come *before* the start of planting dates for corn and soy, which illustrates that winter crop presence causes an earlier SOS detection, although the extent of this impact is contingent upon the ratio of winter to spring/summer crops in an area.

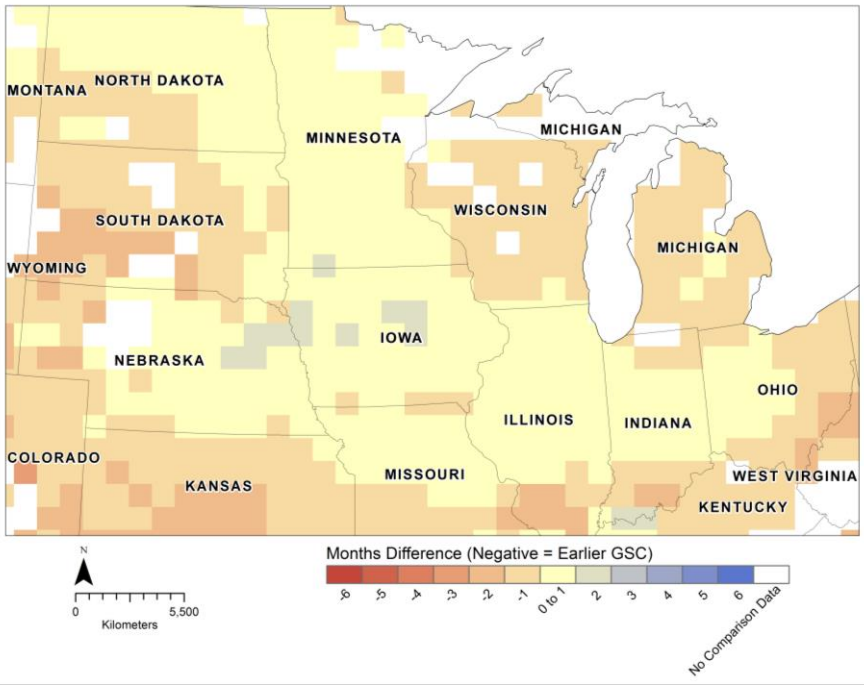

Figure 2.9: The earliest SOS date (2001-2010) minus a corn & soybean-only compilation of the Start of Planting period (based on maximum harvested area fraction (Monfreda, Ramankutty, & Foley, 2008)) for the CONUS' Corn Belt. A negative number indicates an earlier GSC SOS date relative to the start of the planting period, while a positive number indicates a later GSC SOS date versus the start of the planting period**.**

In fact, it is not until southern Kansas, central Oklahoma, and the Texas/Oklahoma border – where winter wheat becomes the dominant crop – that the GSC PTDs begin to correspond more strongly with known winter wheat calendar dates (September planting, June/July harvesting; USDA-NASS, 1997). After planting and an initial emergence, winter wheat enters a period of dormancy during the winter and resumes growth in the early spring (Miller, 1999). It is not uncommon that this initial emergence does not produce a sufficiently large increase in NDVI to be detected and classified as a start of season, particularly if within the same 0.5˚ grid cell there is a large spring/summer crop presence, as the spring/summer crop's contemporaneous NDVI decrease from end of season senescence and harvesting further mutes any NDVI increase. Due to these factors, the GSC's often detect an SOS date for an area with a considerable winter crop presence as late as the end of March, which in reality is the point in time when the crop resumes growth after dormancy. This phenomenon is present in Ukraine and parts of Russia (Figure 2.3a) as well as in certain areas of Kansas, Oklahoma, Colorado, and Missouri, where winter wheat is grown alongside a large quantity of spring/summer crops (primarily corn and soy, though in some cases also sorghum). This phenomenon lends itself to a high level of disagreement between a typical winter wheat planting date in September or October and its associated emergence (SOS) date. While the majority of agricultural monitoring applications only require imagery during the most active part of the growing season (from post-dormancy resumption of growing until end of season), biophysical growth models rely on crop biophysical information throughout the growing season including initial emergence/SOS (Brisson et al., 1998; Jones et

al., 2003), and crop type identification applications rely on observations during the SOS, meaning delayed SOS detections are impactful and require attention.

As a preliminary investigation into the impacts of mixed signals on PTD detection, I have used the USDA-NASS Cropland Data Layers from 2006 & 2007 for the Kansas and Missouri areas, extracting 250m time series for a handful of adjacent corn, soy, and winter wheat cultivating areas (Boryan et al., 2011; Han et al., 2012; Johnson, 2010), and processing these "pure" pixel signals for crop-specific PTDs using the same algorithm as for the general agricultural GSCs. So as to better understand how grid cells of varying winter wheat proportion diverge from "pure" wheat pixel's PTDs, these corn, soy, and wheat NDVI values have been added together in different ratios and processed for PTDs to create simulations of the various mixed pixels that can exist. Preliminary results show that the proportions of winter wheat required to result in the detection of a PTD equivalent to that of a "pure" wheat pixel varies for SOS, peak of season (NDVI maximum; POS), as well as EOS. For SOS, the required winter wheat proportion is 33-75%, for POS of season is 33-50%, and for EOS is 67-85%. Meanwhile, even a small proportion of wheat was capable of changing apparent PTDs by one compositing period (8 days) for corn (SOS: 25-50%; POS: 5-17%; EOS: 7-33%) or soy (SOS: 9-25%; POS: 5-20%; EOS: 5-50%). These findings are from only a small sample of sites and are very preliminary, but serve to suggest that in the context of deriving PTDs, the proportions of crops that make up the unit of analysis do matter and merit further investigation.

2.4 Discussion, Known Issues, & Future Research

This chapter has introduced a suite of results that improve our understanding of the agricultural growing season worldwide. First and foremost, it provides a set of GSCs at 0.5˚, providing SOS and EOS PTDs detected between 2001 and 2010 from MODIS surface reflectance data. This information enables the identification of the period during which different scales and resolutions of Earth observations for agriculture monitoring are required. For the purpose of developing an image acquisition strategy for agriculture monitoring, this study has articulated the timing of necessary image acquisitions for the global agricultural regions, providing the foundation for a continued investigation into the frequency of necessary observations, as well as the necessary spatial and spectral (optical vs. active/microwave) resolutions as inputs to a global agriculture monitoring imaging constellation system (Chapter 4).

There remain a few areas for which no viable detection was possible, usually due to persistent cloud cover creating too many gaps in the time series. Tandem efforts exist at the International Rice Research Institute (IRRI) for the production of rice crop calendars. As many of the areas lacking dates are rice cultivating – for example, coastal West Africa and Southeast Asia – this provides a remedy.

As discussed previously and demonstrated by a preliminary analysis (Section 2.3.4), the impacts of multiple cropping's mixed signals on PTD detection are present but their magnitude is not well understood. In the future, a more in depth analysis of these impacts for a larger sample of sites would provide insight into the limitations of coarser spatial resolution analyses of croplands in general and phenology in particular.

In addition to farmer decision making and farming systems, climatic variables such as temperature and precipitation are known to impact observed SOS and EOS dates both across regions and between years. An analysis of the relationships between climatic variables and PTDs merits further research, but is beyond the scope of this analysis.

While the emphasis of this research is on defining the growing season from the perspective of developing Earth observations requirements as inputs to an image acquisition strategy for agriculture monitoring in the context of GEOGLAM, the growing season calendar and its associated methodology could be useful as inputs for other applications. This is particularly true if attempts are made to separate out the major crops and move back into the realm of crop-specific growing season calendars, research that would be facilitated by crop-specific masks which currently do not exist globally at a sufficiently fine resolution, although efforts to develop them are underway. The present resolution (0.5˚) was chosen to fall within the swath widths of moderate resolution sensors, but the PTD detection algorithm is suitable for use at any resolution. As the algorithm has been shown to reasonably model known cropland phenology and to account for regional and interannual variability in cropping practices (at least in the Corn Belt of the CONUS), it can be applied to crop-specific time series in order to generate fine resolution, spatially explicit crop-specific crop calendars to accompany the general agricultural GSCs presented herein.

Chapter 3: Cloud Cover throughout the Agricultural Growing Season

3.1 Introduction & Background

Cloud cover impedes optical plus thermal (O+TIR) instruments from obtaining clear views of the Earth's surface. This occlusion has been a persistent barrier to operational monitoring of croplands for many regions of the world. In order to improve the quality of agricultural monitoring information in the context of GEOGLAM, the adequate provision of satellite data through the development of an acquisition strategy designed to meet a suite of agricultural monitoring data needs must be ensured (Singh Parihar et al., 2012). This is partially enabled through the articulation of revisit frequency (temporal resolution) requirements for monitoring that take into account the degree to which cloud cover obscures data acquired over agricultural areas throughout the agricultural growing season.

Cloud cover varies throughout the day, over geographic space, and throughout the year, following broad brush patterns (Cairns, 1995; Mercury et al., 2012; Minnis & Harrison, 1984; Roy et al., 2006; Wylie, Jackson, Menzel, & Bates, 2005; Wylie & Menzel, 1999). Very broadly speaking, the afternoon is cloudier than the morning (Cairns, 1995; Minnis et al., 2008), the Equatorial zone and very high-latitudes are cloudier than mid-latitudes, and clouds vary seasonally – all important considerations both in incorporating existing missions into an acquisition strategy as well as in planning for future missions. However, in the context of articulating EO requirements specifically for agricultural monitoring, and translating them into an implementable

acquisition strategy that will utilize multiple missions, it is necessary to determine with greater spatial precision how cloud cover varies throughout the agricultural growing season and in turn impacts optical data acquisitions of the cropped land surface. To this end, this present analysis draws upon the growing season calendars' phenological transitions dates (Table 2.1) described in Chapter 2, and aims to characterize usual cloud cover over agricultural areas of the Earth between these different PTDs, as well as its impact upon obtaining clear views of the Earth's surface when collecting data in the visible, reflected infrared, and thermal infrared portions of the Electromagnetic Spectrum.

There have been multiple studies of cloud cover as it varies diurnally (Cairns, 1995; Kaufman et al., 2005; Minnis & Harrison, 1984), seasonally or intra-annually (Gunderson & Chodas, 2011; Ju & Roy, 2008; Wylie et al., 2005; Wylie & Menzel, 1999), and between different sensors (Chernokulsky & Mokhov, 2009; Minnis et al., 2008, 2011; Stubenrauch et al., 2013). Meanwhile, a handful of studies have looked specifically at cloud cover's impacts on a missions' ability to meet their science objectives (Gunderson & Chodas, 2011; Ju & Roy, 2008; Mercury et al., 2012; Roy et al., 2006) including the Landsat program's Long-term Acquisition Plan (LTAP), which compares usual cloud cover information with near-term daily predictions of cloud cover for an area for real-time acquisition scheduling (Arvidson, Gasch, and Goward 2001; Arvidson et al. 2006; Irish et al. 2006). Ju and Roy (2008) found that monitoring applications that required more than one Landsat ETM+ image per year would be severely limited due to cloud cover coupled with on-board data storage limitations. Considering that all agricultural monitoring applications require more

than one image during the agricultural growing season, with many of them requiring bi-weekly, weekly temporal sampling of an area to monitor crop condition, forecast crop yield, and provide early warning of crop failure, cloud contamination of optical imagery presents a major limitation and supports the perspective that an imaging constellation of sensors with multiple overpass times is necessary for agricultural monitoring (Gao, Masek, Schwaller, & Hall, 2006; Goward et al., 2012; Goward, Arvidson, Williams, Irish, & Irons, 2009; Goward, Williams, Arvidson, & Irons, 2011; Ju & Roy, 2008; Roy et al., 2006; Singh Parihar et al., 2012). However, to date no studies have approached the issue of cloud obscuration of optical imagery at the global scale specifically from the perspective of agricultural regions, agricultural growing seasons, and agricultural monitoring.

In the context of articulating temporal EO requirements for a multi-mission acquisition strategy geared specifically toward agricultural monitoring, a number of factors must be considered. The first is the resolution of analysis – the information must be at a sufficiently fine resolution to be scalable to the multiple swath widths which exist on current and near-term VFTM spatial resolution missions (approximately 11 km [Ikonos] to 740 km [AWIFS]). For this reason, 0.05˚ (~5.6 km at the Equator) has been chosen. The second factor which merits consideration is the acceptable threshold of cloud amount for each monitoring application. To indicate how frequently a completely clear view can probabilistically be obtained, I analyze the probability of a cloud free clear view over 0.05˚ throughout different portions of the agricultural growing season as well as for each month of the year (herein denoted as "*P*(clear)", shorthand for "probability of cloud free clear view"). This effectively

provides the upper boundary of required image frequency (the "worst case scenario") by accepting only completely clear 0.05˚ cells. However, multi-date image compositing is a common approach for studies which do not rely on very fine temporal resolution analyses of phenological progress to separate characteristics (Becker-Reshef et al., 2010b; Roy et al., 2010; Hansen et al., 2008), and thus I perform an additional analysis of the portions of scenes which are clear and can be used to create a cloud free, multi-date image composite. Accordingly, the average percentage of each 0.05˚ which is clear (cloud free) throughout the agricultural growing season is investigated as well (herein denoted as "APClear," shorthand for "average percentage clear"). While at the local level cloudiness in agricultural areas is well-understood, this study presents the global perspective, providing information which is suitable and necessary for incorporation into an image acquisition strategy for global agricultural monitoring.

3.2 Methods

Both MODIS Terra and Aqua cloud cover detections have been shown to compare well with existing cloud cover datasets such as International Satellite Cloud Climatology Project (Rossow & Schiffer, 1999) and High-resolution Infrared Radiation Sounder (Wylie et al., 2005), with the primary differences in cloud coverage occurring in high latitudes or during winter due to high zenith angles (Chernokulsky & Mokhov, 2009; Mercury et al., 2012). As the majority of croplands fall between 60˚ N and 60˚ S, and those that lie in cold climates are typically dormant/not actively cropped with food crops that impact global food supply during the winter months, these dissimilarities relative to HIRS and ISCCP are not impactful.

For consistency, the baseline dataset for both analyses was 1 km surface reflectance cloud flags from the state QA layer (Vermote et al., 2002) from MODIS Aqua (MYD09) for the afternoon analysis (overpass = 1:30 pm local solar time), and from MODIS Terra (MOD09) for the morning analysis (overpass = 10:30 am local solar time)[2].

3.2.1 Generation of Probability of Cloud Free Clear View at 0.05˚

Twelve years (2000-2011) of daily 1 km MODIS Terra (MOD09 - AM) and ten years (2002-2011) MODIS Aqua (MYD09 - PM) surface reflectance quality assessment (QA) cloud presence flags were each separately analyzed and aggregated to 0.05˚ wherein even a single cloudy 1 km pixel would return a cloudy 0.05˚ value for cell for that year. Then, for each DOY for all years, the number of cloudy observations was divided by the total number of observations over that period (10 for Aqua, 12 for Terra). This *P*(cloud) value was inverted to show *P*(clear), yielding two sets of 365 maps of probability of a cloud free clear view in a 0.05˚ grid cell, one for each day for each time of day (morning and afternoon). A schematic using dummy data that shows this aggregation process and the calculation of *P*(cloud) as well as *P*(clear) is shown Figure 3.1. This analysis answers the question, "*what is the probability of a completely cloud free clear view over this 0.05˚ cell for a given day of year (DOY) or a given portion of the year?*" These data can be converted arithmetically to show the days until cloud free clear view (*DUC)* for a given revisit frequency (*f*):

[2] This baseline dataset (daily cloud presence probability and cloud cover percentage) was developed and compiled by Eric Vermote et al. I performed all subsequent analyses.

1. ***DUC = f ÷ P*(clear)**

As this analysis only accepts spatial units (herein, 0.05˚) which are completely clear, this provides insight into the "worst case scenario" for the frequency of clear views to be expected from a sensor or constellation of sensors with (combined) revisit capability *f*.

3.2.2 Generation of Average Clear Percentage of Each 0.05˚ Cell

The same input data as used in the generation of the clear view probability dataset were used to generate the average clear percentage of each 0.05˚, however there exist two key differences. First, due to the point in time at which the datasets were produced, the analysis was extended through 2012, meaning there are thirteen years (2000-2012) of daily 1 km MODIS Terra (MOD09 - AM) and eleven years (2002-2012) of daily 1 km MODIS Aqua (MYD09 - PM) used in this analysis. Second, while in the probability analysis, a pixel was flagged as "not clear" if it contained cloud, was adjacent to cloud, or contained cloud shadow, in this latter analysis, only those pixels which contained cloud were flagged as "not clear." Because the purpose of the *P*(clear) analysis was to essentially establish the "worst case scenario" boundary for clear view frequency, this broader definition of unusable data was appropriate. This percentage clear analysis is, in a sense, establishing the "best case scenario" for the capability of compositing a reasonably, partially clear view, and as such has used a less inclusive definition of what is "not clear."

For each DOY in each year, the percentage of each 0.05˚ grid cell which was cloudy was calculated as the number of cloud containing 1 km pixels divided by the

total number of pixels within that grid cell (Figure 3.1). Next, all years' percent cloud values were averaged for each DOY, yielding average daily percentage cloud (APCloud) and its inverse, APClear, for all 365 days of the year, for both morning and afternoon observations, at 0.05˚.

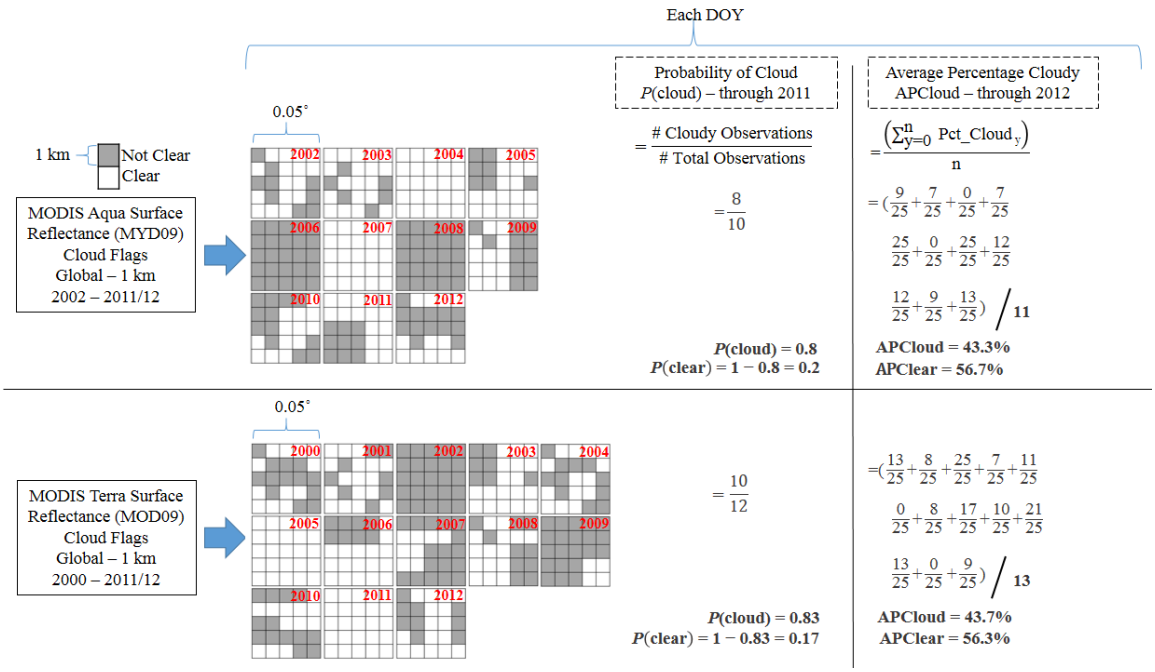

Figure 3.1: Schematic showing the method by which both APClear and *P*(clear) were compiled from 1 km single pixel surface reflectance cloud flags into indicators of cloud cover extent and cloud presence frequency, respectively.

Roy et al. (2006) analyzed the probability of generating cloud free composites from multi-date MODIS imagery by using a similar baseline dataset as APCloud/APClear. Within a spatial unit that is only 0.05˚, it can be assumed that the percentage of the cell which is cloudy is the same as the probability that any given pixel/portion within that cell is cloudy (below denoted as $P(\text{cloud}_{\text{portion}})$, not to be confused with *P*(cloud) previously introduced, which refers to the probability that any cloud exists within a 0.05˚ cell). Following Roy et al. (2006), this analysis assumes that there is no spatial or temporal correlation of cloud occurrence probability, and

that the probability that a given pixel within a spatial unit (here, 0.05˚) is cloudy on consecutive looks is equal to the product of each of those looks' probabilities of cloud ($P(\text{cloud}_{\text{portion}})$). Therefore, the final percentage of a spatial unit that is clear (FPC) after a certain number of looks (revisit frequency, *f*) within a certain compositing period (*c*) beginning on day *d* is given by:

2. $$\textbf{FPC} = 1 - [P(\text{cloud}_{\text{portion}})_{d} * P(\text{cloud}_{\text{portion}})_{d+f} \ldots * P(\text{cloud}_{\text{portion}})_{[d + (c \div f)]}]$$

This analysis gives the "best case scenario" in terms of the frequency of partially clear views to be expected from a sensor or constellation of sensors with (combined) revisit capability *f*, thereby complementing the "worst case scenario" perspective described in Section 2.2.1 and effectively bounding the problem of identifying the impacts of cloud cover on securing usable data of the Earth's cropped surface during the AGS.

3.3 Results

Different agricultural monitoring applications span different portions of the growing season. For example, early within-season planted area estimates require data principally from the early-to-mid growing season while harvested area estimates require data from the late season as well, and some yield forecasting applications require very frequent data during the peak period (Becker-Reshef et al., 2010b; Boken & Shaykewich, 2002), and crop progress and crop condition require data sampled continuously throughout the growing season. Long term studies of changes in agricultural land cover and land use require data sampled from throughout the entire year, including the period during which crops are not actively growing (non-AGS), so

as to detect deviations from previously established phenology. Accordingly, the AGS has been broken down into periods between different phenological transition dates in order to understand how cloud cover can probabilistically impact optical observations of agricultural areas on the Earth's surface. Each of these two cloud datasets were averaged over different portions of the agricultural growing season (resampled to 0.05˚ from the 0.5˚ growing season calendars described in Chapter 2) for each 0.05˚ grid cell:

- Start of season (SOS) to peak period start (PPS)
- PPS to peak period end (PPE)
- PPE to end of season (EOS)
- EOS to SOS, the non-AGS

Additionally, in order to summarize geographic and diurnal differences in cloud cover, each of the datasets have been aggregated into 1˚ increments of latitude for both the Eastern and Western Hemispheres for different portions of the AGS, extracting multiple measures of central tendency (mean, median, maximum, minimum, and standard deviation), although the focus will be the mean cloud presence frequency and mean cloud amount.

3.3.1 Global Patterns in Cloud Cover Frequency and Amount

Equatorial zones (between roughly 15˚ N and 15˚ S) and higher mid-latitudes (above 40˚ N and below 40˚ S) have higher cloud frequency and cloud cover amount (illustrated by APClear; Figure 3.2a-b) than do the lower mid-latitudes (15˚ to 40˚ N and S, roughly). For continental (non-coastal) land mass areas, afternoons are generally cloudier than mornings (a consideration in the design of MODIS Terra

(Minnis et al., 2008) particularly in the southern lower mid-latitudes of both the Eastern and Western Hemispheres (Figure 3.3a-b). This holds with findings from the ISSCP project that the global average maximum in low level cloud amount occurs at 1:30 pm local time (Cairns, 1995), consistent with MODIS Aqua's overpass. Further, *P*(clear) and APClear (divided by 100) consistently disagree by approximately 0.2 at all latitudes, indicating that for most parts of the world regardless of the portion of the year, where there is frequent cloud cover, cloud amount is high, and where there is infrequent cloud cover, clouds amount is low. Stated differently, this shows the spatially auto-correlated character of clouds, and suggests that in chronically and expansively cloudy areas, whether the requirement is for partially or completely clear views, the requirement will be difficult to meet with optical observations (further discussed in Chapters 4 and 5).

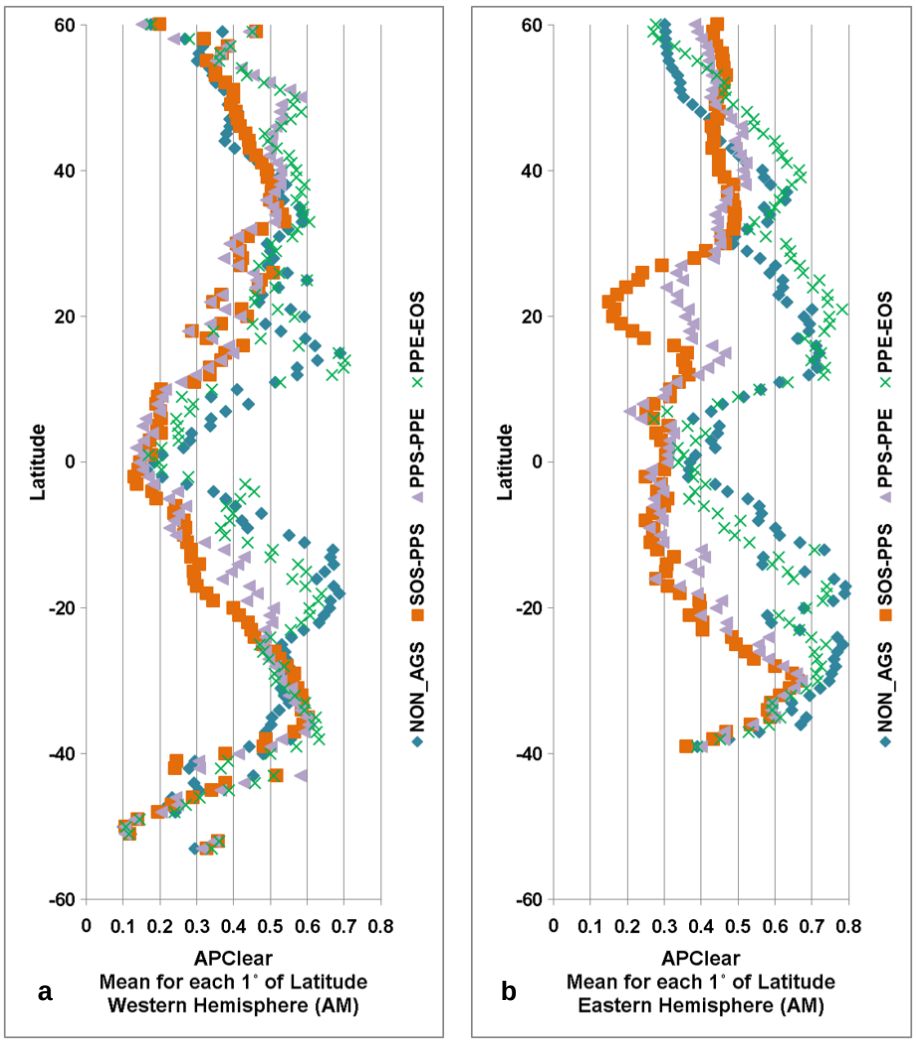

Figure 3.2a-b: For each 1˚ of latitude in the Western Hemisphere (a, left) and Eastern Hemisphere (b, right), the mean percentage of each 0.05˚ cell which is clear over different portions of the agricultural growing season (SOS to PPS; PPS to PPE; PPE to EOS) and non-agricultural growing season (EOS to SOS). The patterns observed are very similar for the probability of cloud absence (*P*(clear)), as well, but are not shown herein.

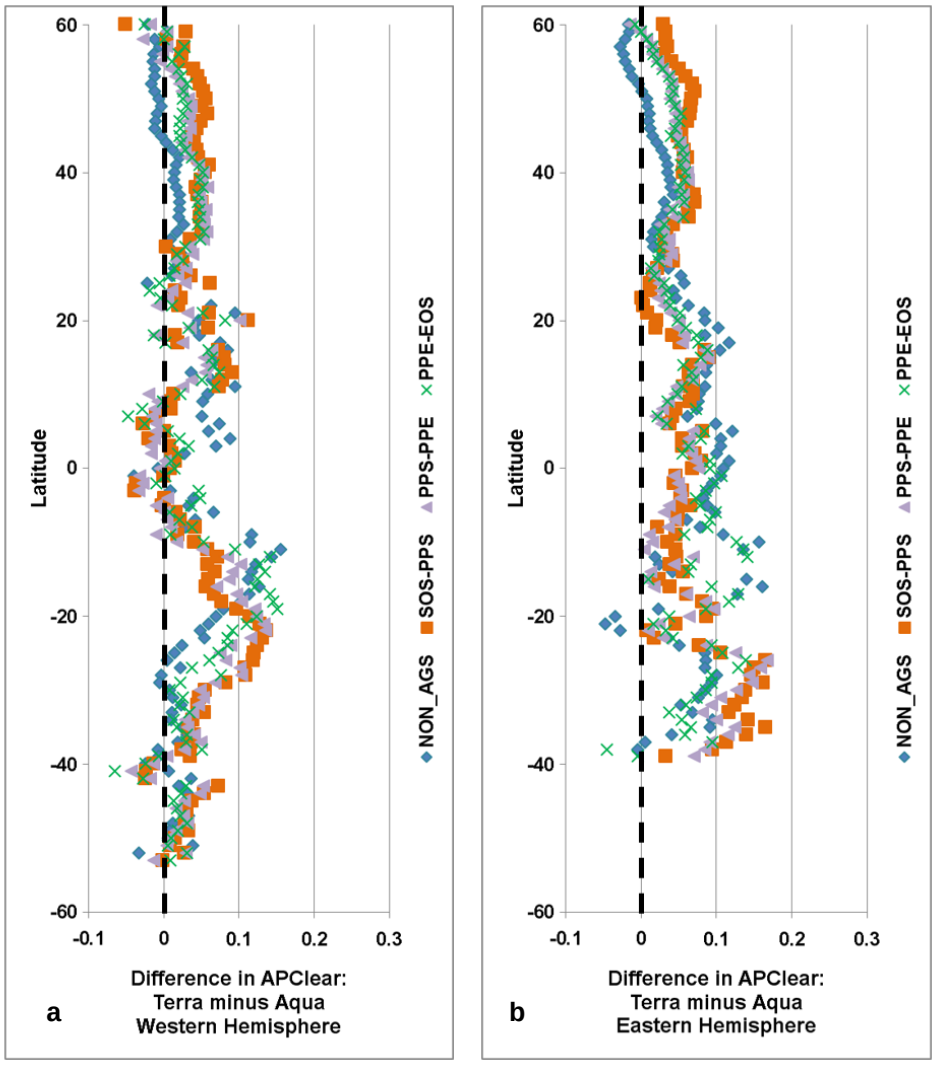

Figure 3.3a-b: For each 1˚ of latitude in the Western Hemisphere (a, left) and Eastern Hemisphere (b, right), the difference (Terra minus Aqua) in mean percentage of each 0.05˚ cell which is clear over different portions of the agricultural growing season (SOS to PPS; PPS to PPE; PPE to EOS) and non-agricultural growing season (EOS to SOS). The dotted vertical line in each graph shows where the morning and afternoon have, on average, equal amounts of cloud cover for that degree of latitude. The markers on the right of the dotted line indicate for which degrees of latitude the morning is, on average, clearer for that portion of the AGS/non-AGS, while the markers to the left of the dotted line indicate where the afternoon is, on average, clearer.

The most interesting patterns, however, emerge when breaking down cloud presence frequency and cloud cover amount by different portions of the agricultural growing season (Figures 3.2a-b, 3.4a-f). At nearly every latitude, the early AGS

(between the start of season and peak period start (SOS-PPS)) is as cloudy if not considerably cloudier than later portions of the growing season and the non-AGS. This is particularly pronounced around 20˚ N in the Eastern Hemisphere due to the Indian summer monsoon, coinciding with an area of expansive agricultural activity (Figure 3.2b). Similarly, the mid-AGS (peak period start to peak period end (PPS-PPE)), is also generally cloudier than the late or non-AGS, both in frequency and amount. As farmers tend to plant in expectation of rains, it is not surprising that the early and mid-AGS are the cloudiest portions of the year. Unfortunately, these periods are also the most important periods for agricultural monitoring, because they allow the generation of early within season estimates of area, yield, and also because crop stress during this period is particularly impactful in terms of yield (Becker-Reshef et al., 2010b; Boken & Shaykewich, 2002; Johnson, 2014; Sakamoto, Gitelson, & Arkebauer, 2013). The high cloud cover presence frequency and cloud amount indicate, therefore, that more frequent optical observations and/or microwave data will be required for agricultural monitoring in these areas during these periods. For example, for an area with $P(\text{clear}) = 0.2$, one in five revisits would probabilistically yield a cloud free clear view. With the combined revisit frequencies of Landsat 7 and Landsat 8 standing at 8 days, this could mean 40 days between clear observations of the surface, well below that which is necessary to monitor meaningful changes in cropland phenology (Becker-Reshef et al., 2010a, 2010b; Duveiller et al., 2013; Justice & Becker-Reshef, 2007; Singh Parihar et al., 2012).

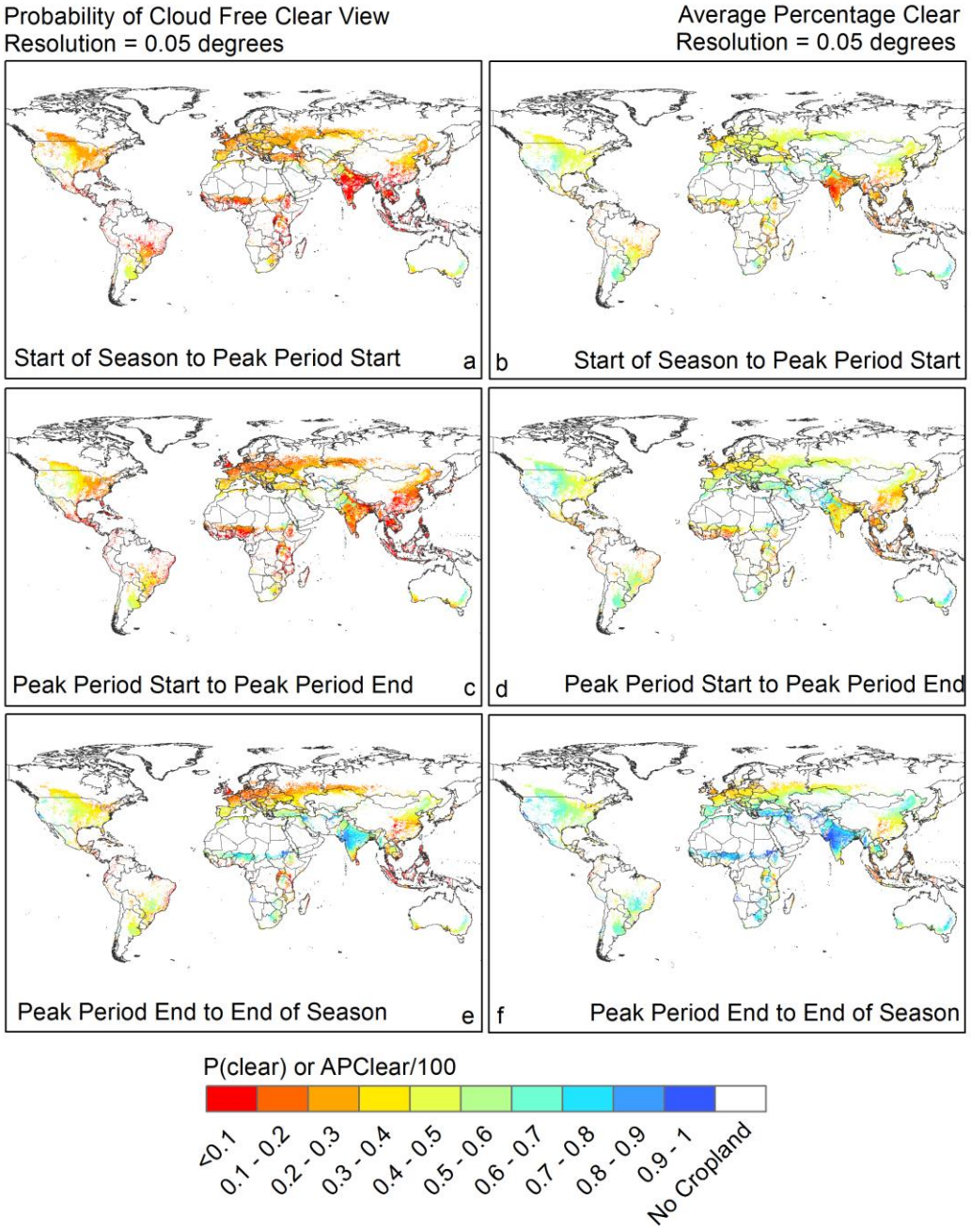

Figures 3.4a-f: The probability of a cloud free clear view (left; a, c, e) and the average percentage clear (right; b, d, f), averaged over different portions of the agricultural growing seasons.

The most expansively cropped latitudes in the Western Hemisphere are between 30˚ N and 50˚ N, with a peak around 40˚ N (Figure 3.5), which coincides,

fortunately, with low to moderate cloud cover frequency and amount throughout the AGS and non-AGS alike (Figure 3.2a). Meanwhile, in the Eastern Hemisphere, which has an overall greater amount of land mass and cropped area, agriculture is expansively cultivated between 10˚ N and 60˚ N, with a very large peak in cropping activity around 55˚ N. This peak, in particular, also coincides with low to moderate cloud cover frequency and amount (Figure 3.2b).While there is not as much agricultural land in the Southern Hemisphere as there is in the Northern Hemisphere due to the lower quantity of both general and arable land mass, several regions here are important areas for agricultural production, both in terms of global food supply and food security. The general patterns of cloud frequency and cloud amount are symmetrical about the Equator, which makes sense in the context of broad brush climatological patterns. A large exception to this symmetry is the seasonal divergence in cloudiness in the Indian Monsoon areas, where the early and mid-AGS show cloud cover probabilities and percentages inverted relative to those seen at the same latitudes in the Southern Hemisphere.

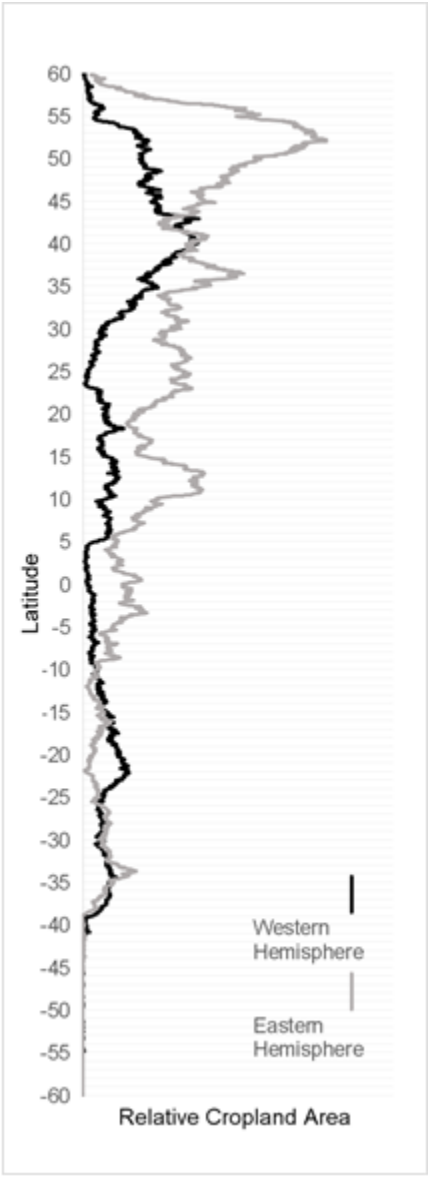

Figure 3.5: Latitudinal plot of relative cropland area for the Western Hemisphere (black) and Eastern Hemisphere (gray), based on Fritz et al. (2013) cropland mask.

3.3.2 Multi-Date Image Compositing throughout the Agricultural Growing Season

Due to the rapid rate of change in crop biophysics, clear views over contiguous land areas are preferred to multi-date image composites, particularly for crop condition monitoring and crop yield estimation applications (Becker-Reshef et al., 2010b). However, composites containing data from eight days apart are

acceptable for many cropland monitoring applications (Bolton & Friedl, 2013; Johnson, 2014; Sakamoto et al., 2013). While 16 day composites are commonly used for agricultural applications (Chen, Fedosejevs, Tiscareño-LóPez, & Arnold, 2006; Li, Liang, Wang, & Qin, 2007; Sakamoto et al., 2005; Wardlow et al., 2006; Zhang et al., 2003), the true temporal resolution when using consecutive 16 day composites has been shown to be greater than 16 days (as much as 30 days) roughly half of the time, (Guindin-Garcia, Gitelson, Arkebauer, Shanahan, & Weiss, 2012), a temporal resolution that is coarser than the rate of change in crop biophysical variables. Due to this fact, that many important crop processes happen on the roughly weekly time step, and that monitoring applications rely on high temporal resolution (historically at the expense of high spatial resolution), cloud cover impacts upon the production of 8 day composites are evaluated herein.

The final percentage of a 0.05˚ cell that will probabilistically be clear (FPC) for each 8 day compositing period throughout the AGS based on two modeled revisit frequencies (f = 2, 4) has been analyzed. From this, the percentage of these 8 day composites, based on morning acquisitions, during the AGS which will yield an FPC of at least 70%, 80%, or 90% clear for each 0.05˚ cell have been derived (Figures 3.6a-f). With the two day revisit frequency, there are four opportunities to acquire data within eight days, while with the four day revisit frequency, there are only two opportunities to acquire data, meaning that a two day revisit will probabilistically meet a given FPC requirement more often throughout the agricultural growing season than will the four day revisit. This relationship is particularly pronounced in North America where increasing the FPC requirement leads to a decrease the percentage of

eight day composites during the AGS for which the FPC requirement is met, as well as in northern Europe and Eurasia, where the increased FPC requirement coupled with a decrease in revisit capability leads to a complete lapse in ability to meet this established FPC requirement. Interestingly, over India, which has such strong seasonal cloudiness (i.e. during the Monsoon it is nearly completely cloudy and the rest of the year it is very clear, as discussed in Section 2.3.1), changing the frequency of acquisition or the FPC requirement has little impact on the percentage of eight day composites which meet their FPC requirement within the context of the entire AGS. For areas or portions of the AGS which cannot consistently (or at all) have their FPC requirement met, alternatives to polar-orbiting optical instruments, such as geostationary instruments with sub-daily revisit capability or active microwave SAR instruments, ought to be considered.

As previously noted, the assumption that there is no temporal or spatial correlation in cloud cover may lead to an underestimation of the impact of clouds on optical acquisitions and therefore an overestimation of the FPC (Roy et al., 2006). To accompany this "best case scenario" is the "worst case scenario" for days until cloud free clear view (DUC) with f = 2, 4 days based on the P(clear) analysis. Figures 3.7a-b show the percentage of 8 day periods throughout the AGS which would probabilistically have a cloud free clear view within them based on a 2 day and 4 day revisit frequency in the morning, respectively. Notably, due to the linear relationship between probability of a clear view and revisit frequency (Equation 1), the same percentages of 8 day periods yielding a clear view would result for a 16 day period with a 4 day revisit (Figure 3.7a) and an 8 day revisit (Figure 3.7b), respectively.

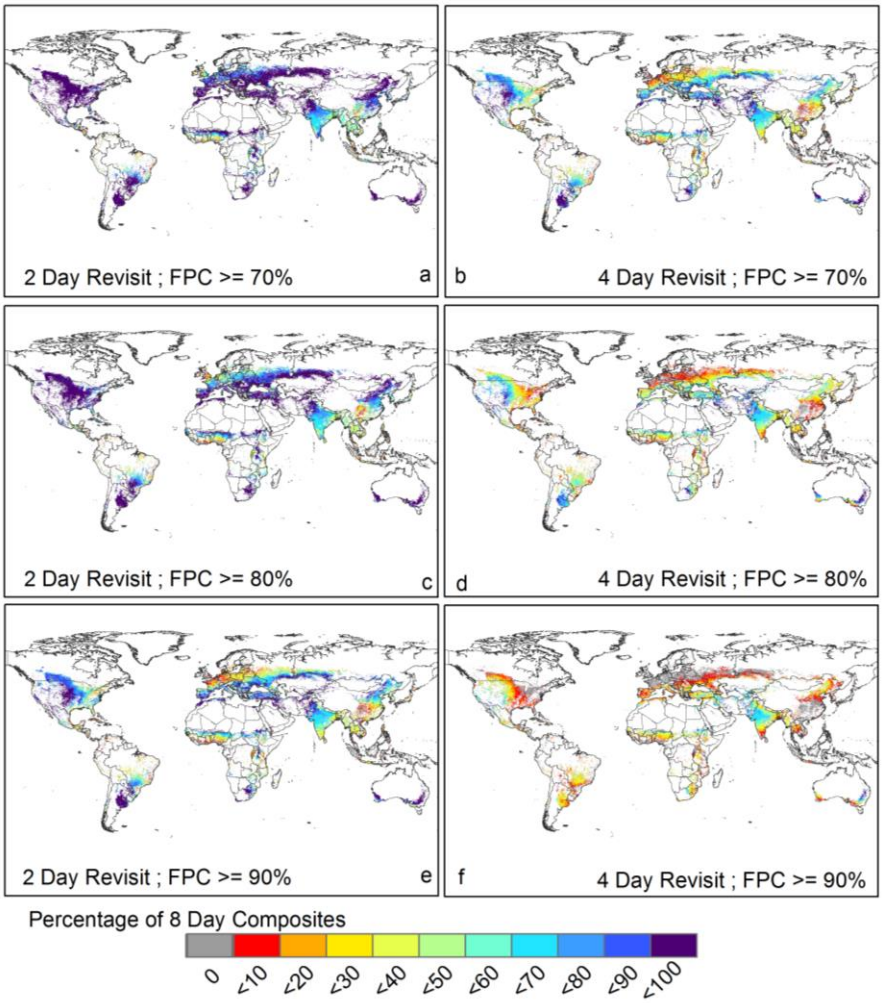

Figure 3.6a-f: The percentage of 8 day composites during the AGS yielding an FPC of at least 70% (a, b), 80% (c d), or 90% (e, f), based on a modeled revisit of 2 days (left) and 4 days (right). This analysis draws on APClear.

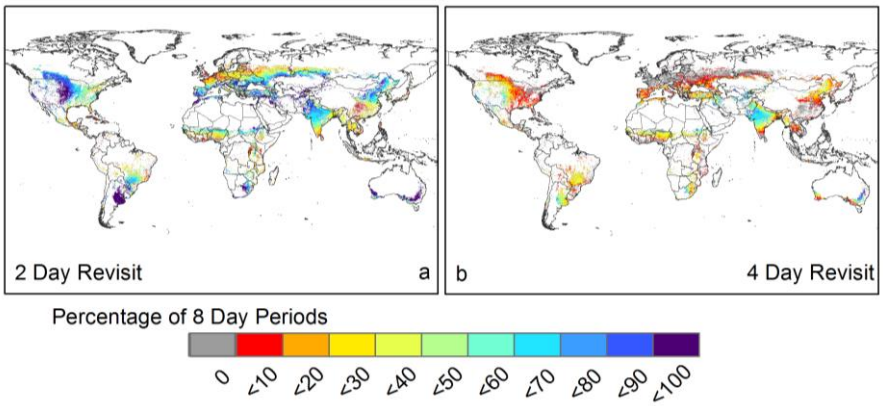

Figure 3.7a-b: The percentage of 8 day composites during the AGS yielding a completely clear view based on a modeled revisit of a) 2 days, and b) 4 days. This analysis is based on *P*(clear).

It is important to note, however, that it matters during which portion of the AGS the 8 day composites would probabilistically not reach their FPC requirement. Gaps in coverage during the early and especially the mid-AGS will be more negatively impactful than will gaps toward in the end of the AGS, as changes in crop condition leading up to and around the peak of season are generally more consequential in terms of yield and production than are those changes in condition that may occur once the crops are closer to harvest (Becker-Reshef et al., 2010b; Boken & Shaykewich, 2002; Johnson, 2014; Meng & Wu, 2008; Sakamoto et al., 2013). For this reason, Figures 3.8a-f show the areas for which each portion of the AGS (early [SOS-PPS], mid [PPS-PPE], and late [PPE-EOS]) has a given FPC (70%, 80%, or 90%) requirement met for at least 50% of 8 day periods, based on a 2 or 4 day modeled revisit frequency. All areas and portions of the AGS which meet any of the established FPCs are shown in green, yellow, or red, while those areas shown in gray are not able to meet a minimum FPC for at least half of that portion of the AGS. Areas shown in green return composites with an FPC of at least 90% at least 50% of the time, areas in yellow return composites with an FPC of at least 80% at least 50% of the time, and areas in red return composites with an FPC of at least 70% at least 50% of the time. The areas shown in gray, found more commonly during the early to mid AGS than during the late AGS, as well as in south/southeast Asia, northern Europe, west Africa, and in parts of both North America and South America (particularly during the early AGS), are areas/portions of the AGS which are frequently and pervasively occluded by cloud cover. A further discussion of whether

these areas/times of year may be poorly suited for monitoring by passive optical instruments is found in Chapter 5.

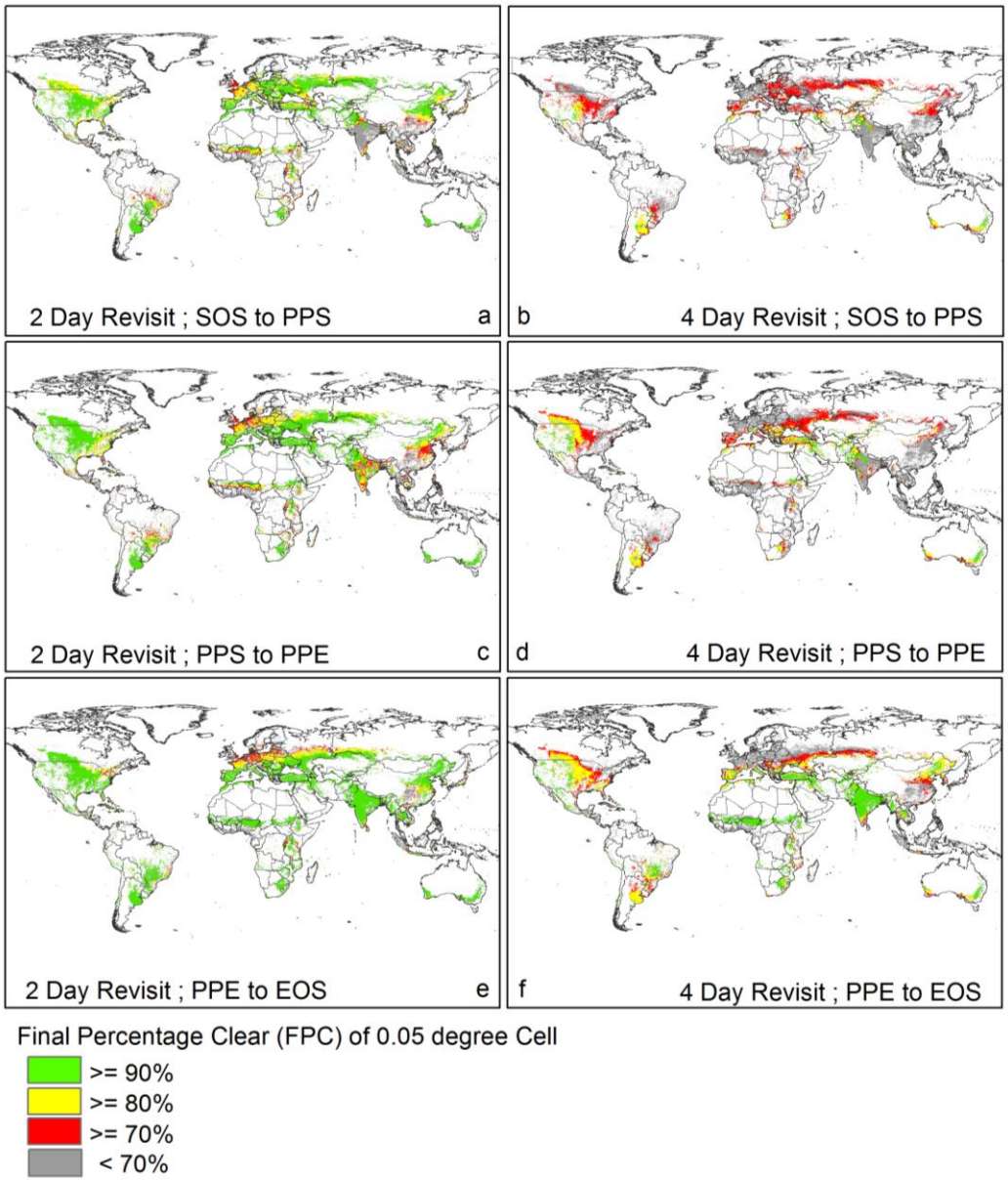

Figure 3.8a-f: Based on two modeled revisit frequencies (2 days: a, c, e; and 4 days: b, d, and f), the areas for which the FPC is <70% (gray), 70-80% (red), 80-90% (yellow), and 90-100% (green) for *at least half* of 8 day periods during different portions of the AGS (early, a-b; mid, c-d; and late, e-f).

3.4 Discussion, Future Research, and Caveats

This analysis has derived the percentage of each 0.05˚ cell that is clear at the end of an 8 day compositing period based on two hypothetical revisit frequencies (f = 2, 4 days), and from that shown the percentage of these 8 day compositing periods throughout the AGS for which we meet a given FPC requirement. Also presented is the percentage of 8 day periods throughout the AGS which would probabilistically have a completely cloud free clear view within them based on a 2 day and 4 day revisit frequency.

The impact of clouds on obtaining (reasonably) clear views of the land surface depends on the time of day, the time of year, the spatiotemporal dynamics of clouds, and the frequency with which (reasonably) clear views are required (Roy et al., 2006). In the context of agricultural monitoring, this research shows that these seasonal dynamics are particularly impactful as some of the most important monitoring activities rely on imagery during the early and mid-agricultural growing season, which are characterized by both frequent cloud cover and pervasive cloud extent. Some areas during certain portions of the year are so persistently and pervasively occluded by clouds that optical, polar-orbiting imaging is not likely to be a viable option for operational monitoring, and microwave imaging must be considered in its stead or as a complementary activity through a constellation approach. Geo-stationary optical imaging with multiple observations throughout the day could provide an increased opportunity for cloud free observation, but for moderate resolution imaging would require a significant increase in spatial resolution as compared to current geostationary systems (Duveiller et al., 2013). Additionally, this analysis has shown

that for most agricultural areas of the world during all portions of the AGS as well as the non-AGS, morning acquisitions are more likely to return clear views and are more likely to have a lower cloud amount, which is something to consider in the planning of future polar-orbiting Earth observing missions. Coastal areas, western and northern Europe, and southeastern China are the exceptions to this rule, although the degree to which afternoon observations are less impacted by clouds is very small (less than 5% clearer/more likely to be clear).

3.4.1 Future Research

The degree to which cloud cover impacts our ability to meet our requirements for clear views over cropped areas of the Earth throughout the AGS additionally depends upon the revisit frequency of available mission(s). This concern is addressed from a hypothetical standpoint by the analysis in which revisit frequencies (f) are modeled to show the DUC or the FPC after a given compositing period. Beyond this general evaluation, this analysis of modeled revisit frequency (f) could be expanded to reflect more precise orbital overpasses of current and near term Earth observing missions. In Chapter 4, the cloud cover data analysis is expanded to analyze the revisit frequency required (f_r) to probabilistically return a clear view within an established requirement period dictated by best practices for a suite of specific agricultural monitoring applications.

3.4.2 Caveats

Two perspectives on cloud cover have been presented: the probability of a cloud free clear view (P(clear)) within a 0.05˚ cell, and the average percentage of each 0.05˚ clear (APClear), both analyzed for specific days of the year as well as

throughout the AGS. Neither of these perspectives are perfect, with the latter likely underestimating the time to reach a given FPC and overestimating the FPC for a given compositing period with a certain revisit frequency (*f*) due to the assumption of no spatial and temporal correlation of clouds (Roy et al., 2006). The former is likely overestimating the time to a reasonably clear view by accepting only completely clear 0.05˚ cells. Further, within both analyses, there may be resolution errors as the percentage of cloud cover is overestimated where the resolution of the instrument(s) in use (here, 1 km MODIS Terra/Aqua) is larger than the most frequent cloud element size (Minnis, 1989; Rossow & Schiffer, 1999). Although extensively validated (Kotchenova, Vermote, Matarrese, & Klemm Jr, 2006; Kotchenova & Vermote, 2007; Vermote & Kotchenova, 2008), the MOD09 cloud flags may themselves include errors in cloud detection as a result in variable sensitivities to different cloud properties. This and the time it takes for a scan to be completed across swath (clouds move, as well) may introduce bias into the analysis (Kaufman et al., 2005; Mercury et al., 2012; Roy et al., 2006).

3.5 Conclusions

The two perspectives on cloud cover as it impacts the ability to obtain clear views of the Earth's cropped surface throughout the AGS described herein complement one another by bounding the problem, with the APClear analysis providing important information on the utility of multi-date compositing for global agricultural monitoring applications. Further, the *P*(clear) analysis' "overestimation" of cloud cover's effects on obtaining usable data of the Earth's surface is valuable in that it provides input into acquisition planning that is not at risk of being overly

optimistic (Gunderson & Chodas, 2011; Mercury et al., 2012). This research provides important insight into the seasonal, geographical, and diurnal variations in cloud cover over global agricultural areas and is an important contribution in the articulation of Earth observations requirements toward operational global agricultural monitoring.

Chapter 4: Earth Observations for Global Agricultural Monitoring: Requirements for Visible, Reflected, and Thermal Infrared Data

4.1 Introduction

The coordination of Earth observations (EO) data necessitates first the articulation of spatially explicit EO requirements for monitoring, namely what (spectral range), where, when, how frequently, and at what spatial resolution these data are needed. In 2007, there was an attempt by those in the Group on Earth Observations Agricultural Monitoring Community of Practice (GEO Ag CoP) to describe the data necessary for operational agricultural monitoring (Figure 1.1; Justice & Becker-Reshef, 2007), and a related effort was made to define the requirements specifically for Europe (Duveiller et al., 2013). While these efforts provided a sketch of the multiple spatial and temporal scales of required data inputs for a variety of monitoring applications and illustrated the inherent complexity of such an undertaking, they needed refinement and a higher degree of specificity in order to be translatable into data acquisition requests. In 2012, members of the newly formed Committee on Earth Observations Satellites (CEOS) Ad Hoc Team for GEOGLAM held a focused meeting with the goal of articulating the spatial (Table 4.1, Column B), spectral (Table 4.1, Column C), and cloud free temporal resolution (Table 4.1, Column D) requirements for meeting the data needs for a variety of agricultural monitoring applications or "target products" (Table 4.1, Columns G-M)[3].

[3] The development of this requirements table was a collaborative group effort, pulling on the expertise of a number of agricultural remote sensing scientists around the world, previous efforts to identify necessary EO (e.g. Figure 1.1), as well as relevant literature. I was present for and actively engaged in

These agricultural monitoring applications include mapping cropped area (crop mask) and crop type area, identifying the crop calendar, monitoring crop condition, forecasting crop yield, retrieving crop biophysical variables (such as leaf area index (LAI), green area index (GAI), and fraction of absorbed photosynthetically active radiation (fAPAR)), deriving environmental variables (such as evapotranspiration), and identifying agricultural practices and cropping systems (including burning, tillage, transplantation, and cropping intensity). In addition to the framework this provided, the table additionally referenced *where* the imagery were required (Table 4.1, Columns E & F) – extent of coverage varies as does the field sizes for which a given spatial/spectral resolution combination are required – as well as *when* the imagery were required (Table 4.1, Column D), with most of the requirements being for imagery during the agricultural growing season (AGS) but a few requesting data to be acquired during the non-AGS.

---

the development of this requirements table, and since its initial drafting in July 2012, I have been one of the primary people working to refine and update it.

Table 4.1: The requirements table developed by the CEOS Ad Hoc Team for GEOGLAM

A	B	C	D	E	F	G	H	I	J	K	L	M
						Target Products						
Req#	Spatial Resolution	Spectral Range	Effective observ. frequency (cloud free)	Extent	Field Size	Crop Mask	Crop Type Area and Growing Calendar	Crop Condition Indicators	Crop Yield	Crop Biophysical Variables	Environ. Variables	Ag Practices / Cropping Systems
	Coarse Resolution Sampling (>100m)											
1	500 - 2000m	optical + TIR	Daily	Wall-to-Wall	All			X		L		
2	100-500m	optical + TIR	2 to 5 per week	Cropland extent	All	X	X	X	L	L		L
3	5-50 km	microwave	Daily	Cropland extent	All						X	
	Moderate Resolution Sampling (10 to 100m)											
4	10-70m	optical + TIR	Monthly (min 3 in season + 2 out of season); Required every 1-3 years	Cropland extent (if #5 = sample, else skip)	All	X	L/M					X
5	10-70m	optical + TIR	Weekly (8 days; min. 1 per 16 days)	Sample (pref. Cropland extent)	All	X	X	X	X	X	X	X
6	10-100m	SAR	Weekly (8 days; min. 1 per 2 weeks)	Cropland extent of persistantly cloudy and rice areas	All	X	X	X	X	X	X	X
	Fine Resolution Sampling (5 to 10m)											
7	5-10m	optical	Monthly (min. 3 in season)	Cropland extent	M/S	M/S	M/S					
8	5-10m	optical	Weekly (8 days; min. 5 per season)	Sample	All		M/S	X		X	X	X
9	5-10m	SAR	Monthly	Cropland extent of persistantly cloudy and rice areas	M/S	M/S	M/S					M/S
	Very Fine Resolution Sampling (<5m)											
10	< 5m	optical	3 per year (2 in season + 1 out of season); Required every 3 years	Cropland extent of small fields	S	S	S					
11	< 5m	VISNIR	1 to 2 per month	Refined Sample (Demo)	All		X		X			X

Due to the rapid rate of change in crop phenology and progress – beneath the weekly time step (Duveiller et al., 2013; USDA-NASS, 2013) – cloud free imagery are generally required with greater frequency for agricultural monitoring than they are for applications which monitor more static phenomena or processes. For crop yield and crop condition, for example, clear views are needed weekly or at least biweekly, although even more frequent data are valuable (Becker-Reshef et al., 2010b; Boken & Shaykewich, 2002; Johnson, 2014; Sakamoto et al., 2013). To date, global scale

cropland monitoring has been predominately undertaken with coarse spatial resolution data, with MODIS at 250-500m with broad spectral coverage providing the primary data source over the past decade (Biradar & Xiao, 2011; Duveiller et al., 2011; Galford et al., 2008; Guindin-Garcia et al., 2012; Justice et al., 1998; Pan et al., 2012; Pittman et al., 2010; Sakamoto et al., 2005, 2010; Wardlow et al., 2007; Wardlow & Egbert, 2008; Xiao et al., 2005). An issue with coarse resolution analyses of cropland dynamics is subpixel heterogeneity (Duveiller & Defourny, 2010; Ozdogan, 2010; Pax-Lenney & Woodcock, 1997) with many small fields or highly heterogeneous landscapes having variability beneath the spatial resolution of the sensing instrument in use. While moderate spatial resolution has been used extensively in national scale analyses of land cover, including cropped area and crop type mapping efforts (Doraiswamy et al., 2004; Homer et al., 2007; Kauth & Thomas, 1976; Liu et al., 2005; Lobell & Asner, 2004; MacDonald et al., 1975; MacDonald & Hall, 1980; Odenweller & Johnson, 1984; Vogelmann et al., 2001; Wulder et al., 2008; Chang, Hansen, Pittman, Carroll, & DiMiceli, 2007; Mueller & Seffrin, 2006), their limited revisit frequency and/or limitations in on-board storage capacity have meant that these data have been too sparsely collected in time and often also in extent in order to be used for crop condition or crop yield monitoring (Johnson, 2014). Further, the persistence of cloud cover in certain agricultural regions and during certain portions of the AGS exacerbates the sparseness of usable data. The requirements established by the CEOS Ad Hoc Team for GEOGLAM builds upon the experiences of agricultural monitoring experts from around the world, who stand in agreement that more frequent moderate spatial resolution imagery are required for

operational cropland monitoring (beyond cropped area and crop type) than are presently freely available to and accessible by the public, particularly if more broad scale monitoring is to be undertaken.

With these requirements conceptualized, there remained the task of placing them in the geographical context with respect to target cropland locations, growing season calendar, and cloud cover considerations, showing precisely how frequently and to what spatial extent data are required throughout the calendar year. The focus herein will be on Requirement #5 (10-70m, O+TIR, 8-16 days), detailing the average revisit frequency required (f_r) to meet each associated cloud free clear view requirement during each month of the calendar year (Table 4.1, Column D). It should be noted that while the requirement is explicitly for "cloud free" data, in reality there are many cases where data which are *reasonably* cloud free are sufficient, and the revisit frequency required to meet these looser criteria (herein, 70% of a 0.05˚ cell being cloud free is considered reasonable) will be shown as well. While requirements have been established for O+TIR coarse resolution instruments as well (Table 4.1, Req. 1-2), these requirements are met in nearly every area through systematic acquisitions by systems such as MODIS, SPOT-5, VIIRS, and AVHRR, and therefore nothing more than the maintenance of quality and quantity of such a set of observations is required at this time.

4.2 Datasets & Methods

4.2.1 Input Datasets: Where to Image?

The first step in defining EO requirements for global agricultural monitoring is identifying the areas which require monitoring, namely the locations of global

croplands. To this end, Fritz et al. (2013) have developed a “best-available” cropland mask which provides the probability that any 0.0083˚ (~1 km at the Equator) cell contains cropland based on a suite of existing land cover and cropland masks (Figure 4.1). This harmonizing and synthesizing effort was undertaken in the context of GEOGLAM, and as such has been chosen as the cropland mask for this effort. Due to the resolution of other input datasets (namely, cloud cover, Section 4.2.3), and balancing data volume considerations with the need for a resolution sufficiently fine to be scalable to VFTM spatial resolution missions’ swath widths (approximately 11 km [Ikonos] to 740 km [AWIFS]), this cropland mask has been degraded to 0.05˚ (~5.6 km at the Equator). While different cropland probabilities are ideally suited for different areas of the globe, a threshold has been set at 20% as it aligns well with understood cropland distributions.

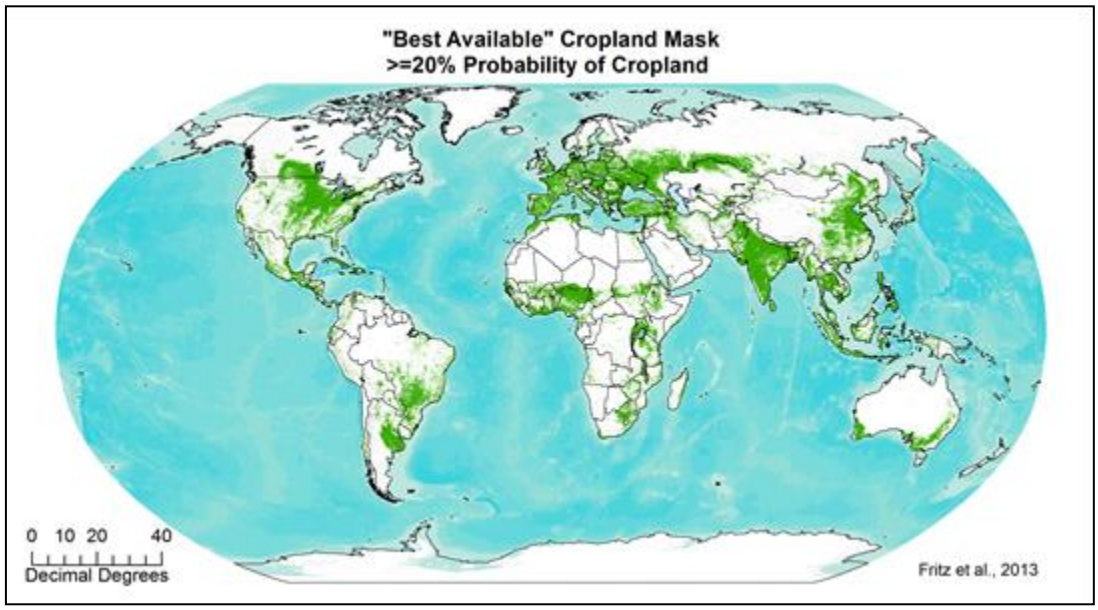

Figure 4.1: The “best-available” cropland mask used in this analysis, derived from Fritz et al. (2013). A threshold of ≥20% probability of cloud cover has been selected to produce the mask.

The requirements are also broken down by the field sizes for which they are prescribed. Generally speaking, larger fields require coarser spatial resolution data, medium fields require moderate spatial resolution data, and smaller fields require finer spatial resolution data. These relationships are further contingent upon shape, arrangement, fragmentation, and crop type heterogeneity of the fields as well as the imaging bandwidths (Duveiller, Defourny, & Gérard, 2008; Duveiller & Defourny, 2010), and future articulations of the requirements can be refined by the inclusion of this additional information. However, at present such datasets do not exist at the global level, and the broad relationship between field size and necessary spatial resolution is sufficient to allocate fine, moderate, and coarse spatial resolution data acquisitions. A research group at the International Institute for Applied Systems Analysis (S. Fritz et al., unpublished raw data[4]) have deployed an online collaborative tool called "GEO-WIKI" (Fritz et al., 2009, 2012) to gather "crowd sourced" information on field size. Volunteers from around the world visually interpret high resolution imagery on GEO-WIKI's Google Earth platform and use visual interpretation to estimate field size. As of 2013, over 50,000 individual fields had been identified, and this point information has been extrapolated to neighboring locations to create a global indicator layer for field size (Figure 4.2). The requirements table identifies fields as "small," "medium," or "large," corresponding with fields smaller than 1.5 ha, between 1.5 and 15 ha, and larger than 15 ha, respectively. This field size classification system was designed to align with very fine/fine (<5-10 m), moderate (10-70 m), and coarse resolution (100-1100 m) sensor

[4] Fritz, S. (2013). [Field Size Data Distribution from http://agriculture.geo-wiki.org]. Unpublished raw data.

spatial resolutions, respectively, and the ability to have at least the possibility of a few "pure" pixels of each class of sensors' systems fall within each field (Duveiller, Baret, & Defourny, 2012; Duveiller et al., 2013) .

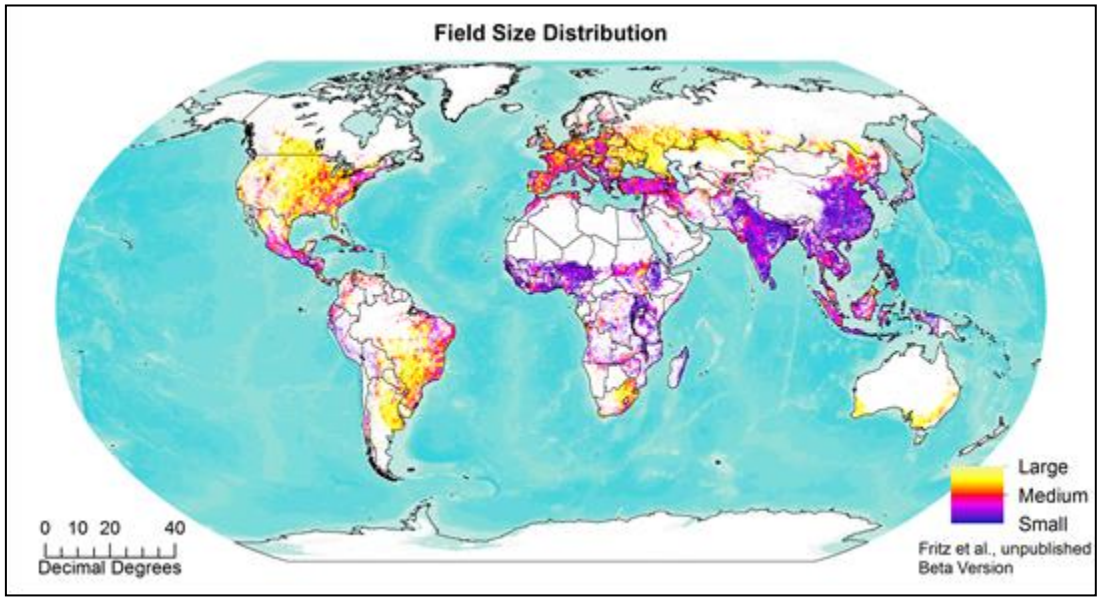

Figure 4.2: A map of field size distribution at 0.05˚, interpolated from more than 50,000 crowd-sourced points collected via the GEO-WIKI platform (S. Fritz et al., unpublished raw data). Large fields are >15 ha, medium fields are 1.5-15 ha, and small fields are <1.5 ha. This is a beta version generated in early 2013, with points constantly having been collected by the tool since then.

4.2.2 Input Datasets: When to Image?

Many agricultural monitoring applications including crop yield, crop condition, and crop type mapping rely on data acquired only during the period when crops are actually growing. By contrast, cropland area mapping efforts ("crop mask"), particularly in light of dynamics in year-to-year cropping practices and associated changes in land use, require data throughout the calendar year although the frequency with which imagery are required is reduced during the non-AGS as the goal is to detect long-term rather than short-term (as in, phenological) changes. This seasonal breakdown of the agricultural growing season is provided by the agricultural growing

season calendars detailed in Chapter 2, with the AGS spanning the period between the median start of season (SOS) and the median end of season (EOS) as observed over 2001-2010, and the non-AGS spanning the period between the median EOS and the median SOS.

4.2.3 Input Datasets: How frequently to Image for (Reasonably) Clear Views

As stated in the requirements table (Table 4.1, Column D), the temporal resolution requirement is for "cloud free" clear views of the Earth's surface. Whether the requirement is for a completely clear view of every pixel within a scene, or a mostly clear scene, is contingent upon the application and the expert opinion of the user, although increasingly scientists are moving toward per pixel analyses as opposed to per scene analyses (Hansen & Loveland, 2012; Hansen et al., 2013; Roy et al., 2010). For this reason, cloud cover has been analyzed from two perspectives – the probability of a cloud free clear view over a 0.05˚ cell (P(clear)) and the average percentage of a 0.05˚ cell that is clear (APClear), both based on MODIS surface reflectance cloud flags (Bréon & Vermote, 2012; Vermote et al., 2002). As detailed in Chapter 3, cloud cover varies seasonally, geographically, and diurnally, and as such the revisit frequency required (f_r) in order to satisfy a given clear view requirement (referred to as the "Effective Temporal Resolution" in Table 4.1) within a certain period varies throughout the year, with location, and also with the acceptable cloud threshold. As the great majority of VFTM EO satellites have morning overpasses, the revisit frequency required herein will be presented assuming a morning (10:30 am local solar time) overpass.

The revisit frequency required to yield a cloud free clear view within a 0.05˚ cell within a certain number of days (CVR) is given by the following equation:

3. $\boldsymbol{f_r = P(\text{clear}) * \text{CVR}}$

This, by accepting only clear views provides the "worst case scenario" for required revisit frequency. In contrast, some scientists/applications may accept 0.05˚ cells which are partially clear. The revisit frequency required to yield a cell with a given FPC after a certain number of days is given by the following equation:

4. $\boldsymbol{f_r = c \div [\ln(1 - \text{FPC})/\ln(P(\text{cloud}_{\text{portion}})]}$

Where *c* is the number of days within which reasonably clear data are required (or, the length of compositing period) and $P(\text{cloud}_{\text{portion}})$ is the probability that any given portion of a cell is cloudy during a given observation. This probability is the same as APCloud – the inverse of APClear – and is based on the assumption that the percentage of any cell that is cloudy is the same as the probability that any given portion of a cell is cloudy, following (Roy et al., 2006). As described in Chapter 3, it may underestimate the impact of clouds, and as such, it provides the "best case scenario" for revisit frequency required to meet a reasonable FPC requirement with a certain period (*c*).

4.2.4 Generation of Requirements Maps

For the establishment of a baseline of requirements and the subsequent analysis of our capacity to meet them with current and near-term remote sensing instruments (Chapter 5), it is necessary to analyze the year in segments mindful of agricultural growing seasons and cloud cover dynamics. For simplicity of analysis, the year has been divided into its calendar months, and acquisitions are considered

necessary during any month for which even one day is actively cropped (based on median SOS and median EOS). This may lead to overestimation of the period for which imagery are required, but variability in year-to-year cropping practices and climatological factors may justify the expanded period of acquisition. Additionally, APClear (in Equation 4, $P(\text{cloud}_{\text{portion}})$) and $P(\text{clear})$, while natively at daily temporal resolution, have been averaged over each calendar month to show the usual cloud condition (in terms of presence and amount) for that period.

With all of the components of the EO requirements established, what remains is an assemblage of these individual layers to provide spatially explicit monthly estimates of revisit frequency required to yield a completely clear view or one with a FPC of at least 70% within a certain time period, only for the extent of crops which are actively growing (or, in the case of those requirements for imagery during the non-AGS, for all croplands which are out of season) for that month. This present analysis focuses on moderate spatial resolution requirements, as coarse resolution missions already have systematic daily acquisitions, and the requirements for very fine and fine resolution data are for small samples or subsets of the cropland extent and can be managed by the capabilities of pointing satellites in that resolution class. This focus on moderate resolution will be further discussed in Chapter 5.

4.3 Results

For each individual requirement in Table 4.1, Column D, there is at least a minimum and a maximum days until clear view requirement during the AGS, and in Requirements #4 and #10 a tertiary requirement for imagery outside of the AGS. The

focus herein will be on Requirement #5, both its preferred revisit frequency (8 days[5]) as well as its minimum requirement (16 days) for all field sizes.

The resultant revisit frequency required (f_r) is often a non-integer. A non-integer revisit is an impossibility with polar-orbiting, sun-synchronous imaging systems, and when translating into data requests will have to rounded or otherwise altered. However, data coordination at this level is beyond the scope of this research, and as such herein the non-integer computational output has been maintained.

4.3.1 Requirement #5: 8 Day Reasonably Clear View Requirement

The requirements table establishes that moderate resolution data spanning the visible, reflected infrared, and thermal infrared portions of the electromagnetic spectrum are required for croplands of all sizes at least every 16 days throughout the AGS, however the precision and accuracy of satellite-based estimates, particularly regarding yield and condition, would be improved by having clear views every 8 days (Figures 4.3-4.14a-b). The data are preferred for the full cropland extent, but in the early phases of GEOGLAM's implementation, data acquired on a sampled basis will still yield important results. The location and extent of the statistical sampling frame will vary over time and with target crop, and thus the full extent of actively growing large, medium, and small fields have been analyzed, and can be later refined geographically to represent sample sites.

What is immediately noticeable, as with the analyses in Chapter 3, is the impact of the Indian summer monsoon on revisit frequency required. In India in

[5] Note that the requirements table says "Weekly" but puts "8 days" beside it in parenthesis. This is in acknowledgement that the two Landsat satellites together typically have a combined revisit of ~8 days (see Chapter 5), and that the different between 7 and 8 days is not significant enough to warrant the exclusion of these satellites from consideration for fulfillment of this requirement.

particular, the revisit frequency requirement for much of the country is up around 5-8 days in both scenarios (FPC of at least 70%, and for a completely clear view) during the months outside of the monsoon for which crops are in season (October-March), but during the monsoon, it is almost universally less than 1 day. Only southern Brazil comes close to having a similar magnitude of seasonal divergence in revisit frequency required.

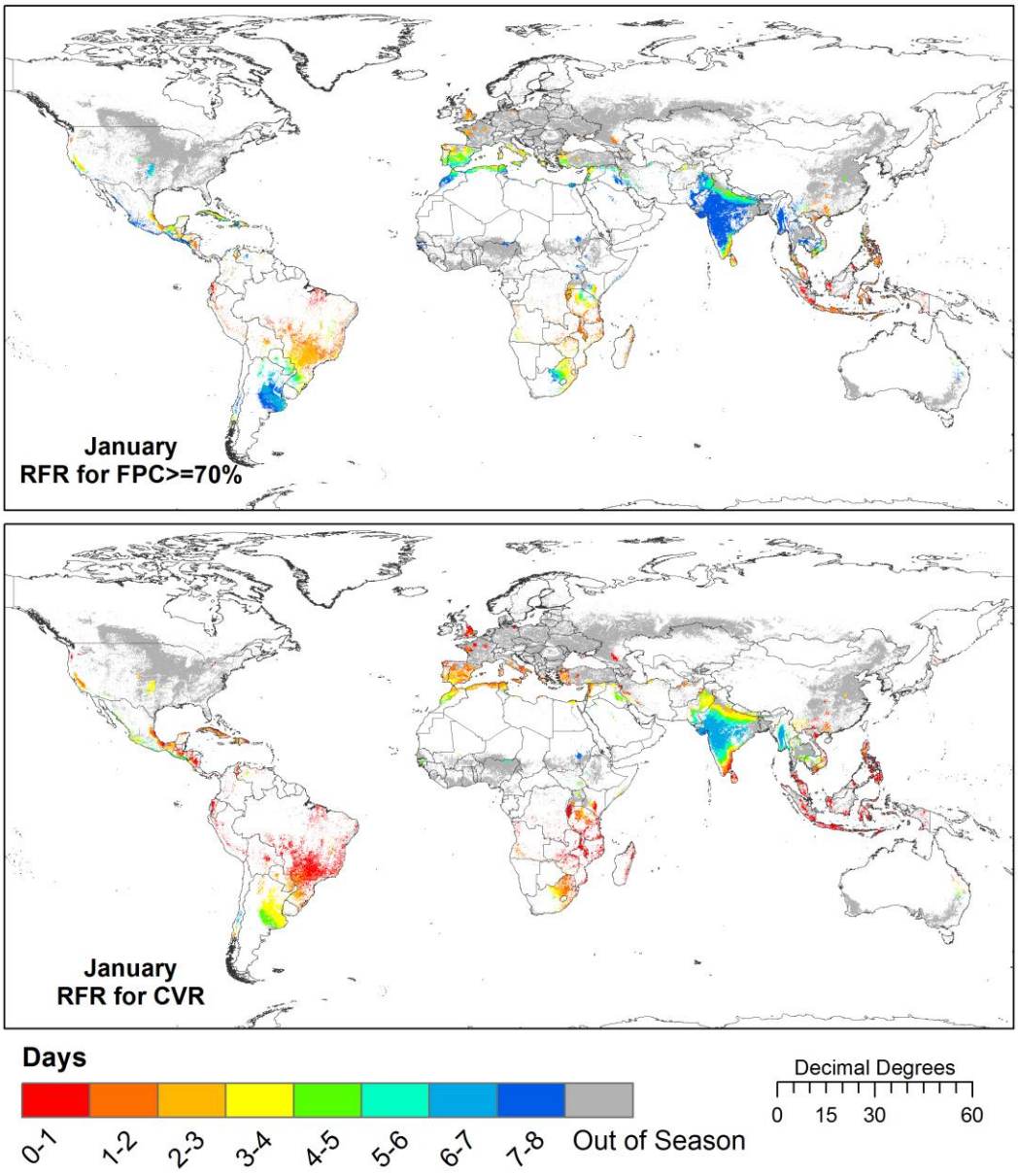

Figures 4.3a-b: The revisit frequency required to probabilistically yield, a) Top, a view at least 70%; or b) Bottom, a completely clear view (CVR), every 8 days during the month of January. Areas containing cropland out of season are shown in gray. Resolution is 0.05˚.

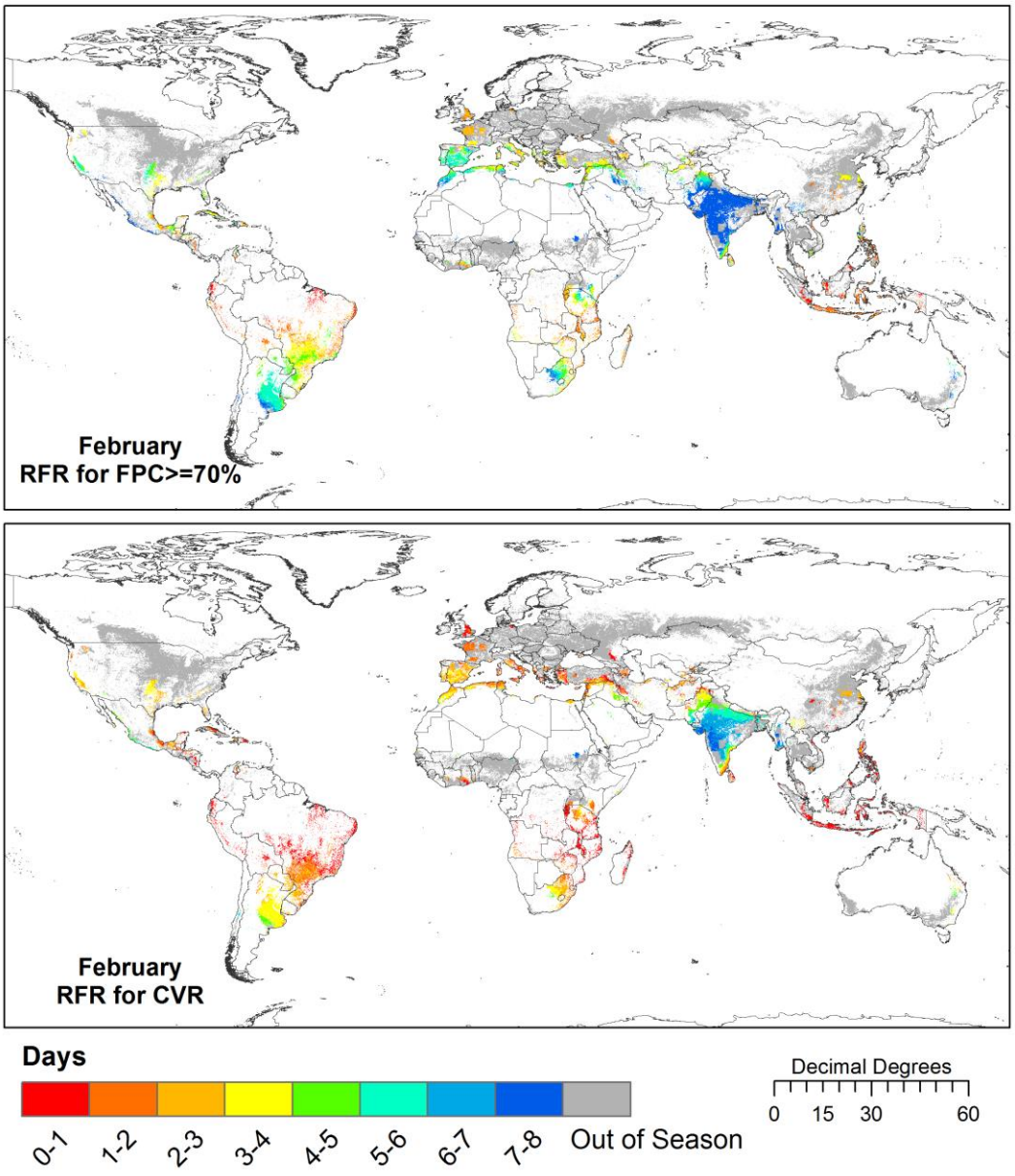

Figures 4.4a-b: The revisit frequency required to probabilistically yield, a) Top, a view at least 70%; or b) Bottom, a completely clear view (CVR), every 8 days during the month of February. Areas containing cropland out of season are shown in gray. Resolution is 0.05˚.

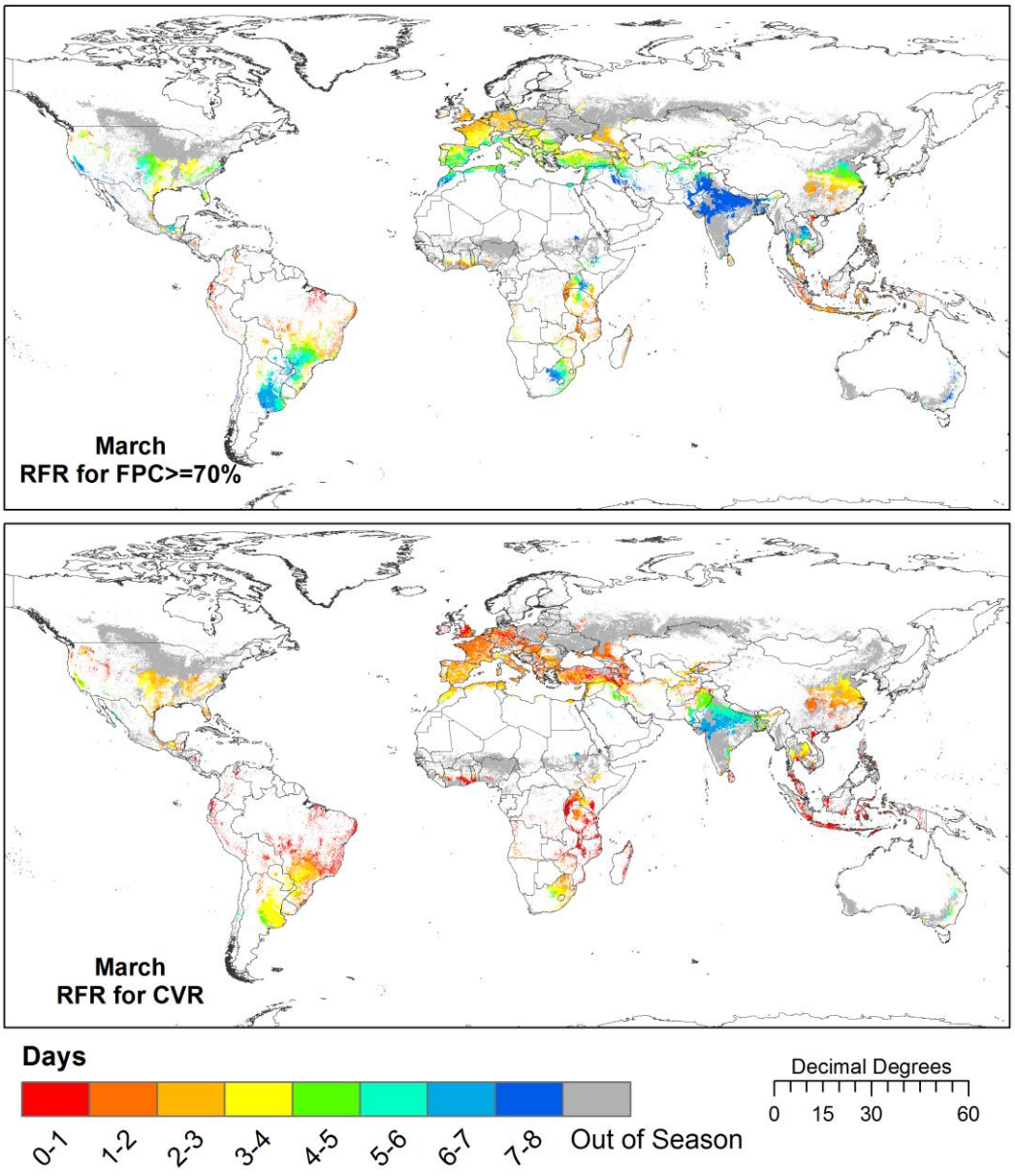

Figures 4.5a-b: The revisit frequency required to probabilistically yield, a) Top, a view at least 70%; or b) Bottom, a completely clear view (CVR), every 8 days during the month of March. Areas containing cropland out of season are shown in gray. Resolution is 0.05˚.

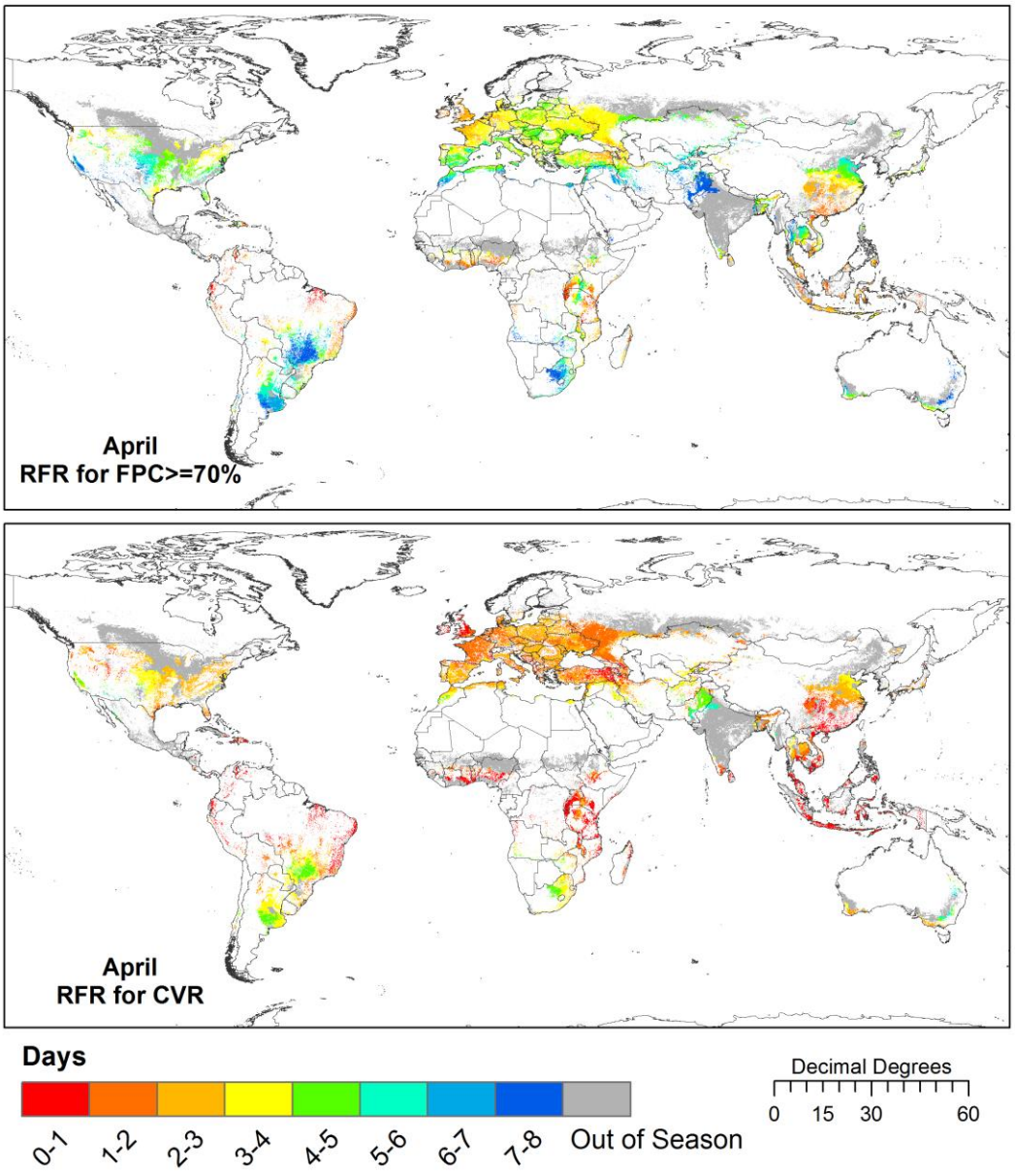

Figures 4.6a-b: The revisit frequency required to probabilistically yield, a) Top, a view at least 70%; or b) Bottom, a completely clear view (CVR), every 8 days during the month of April. Areas containing cropland out of season are shown in gray. Resolution is 0.05˚.

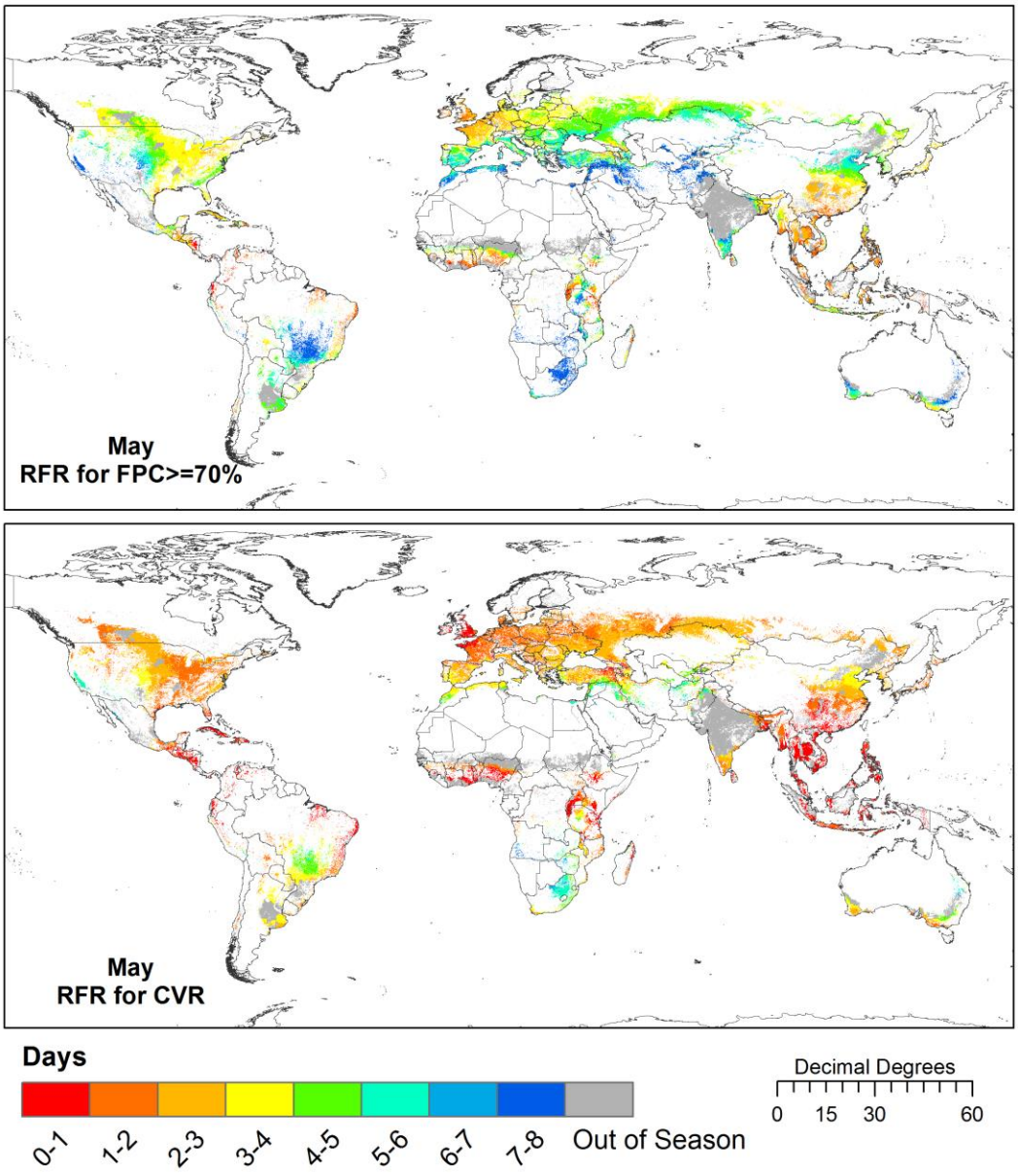

Figures 4.7a-b: The revisit frequency required to probabilistically yield, a) Top, a view at least 70%; or b) Bottom, a completely clear view (CVR), every 8 days during the month of May. Areas containing cropland out of season are shown in gray. Resolution is 0.05˚.

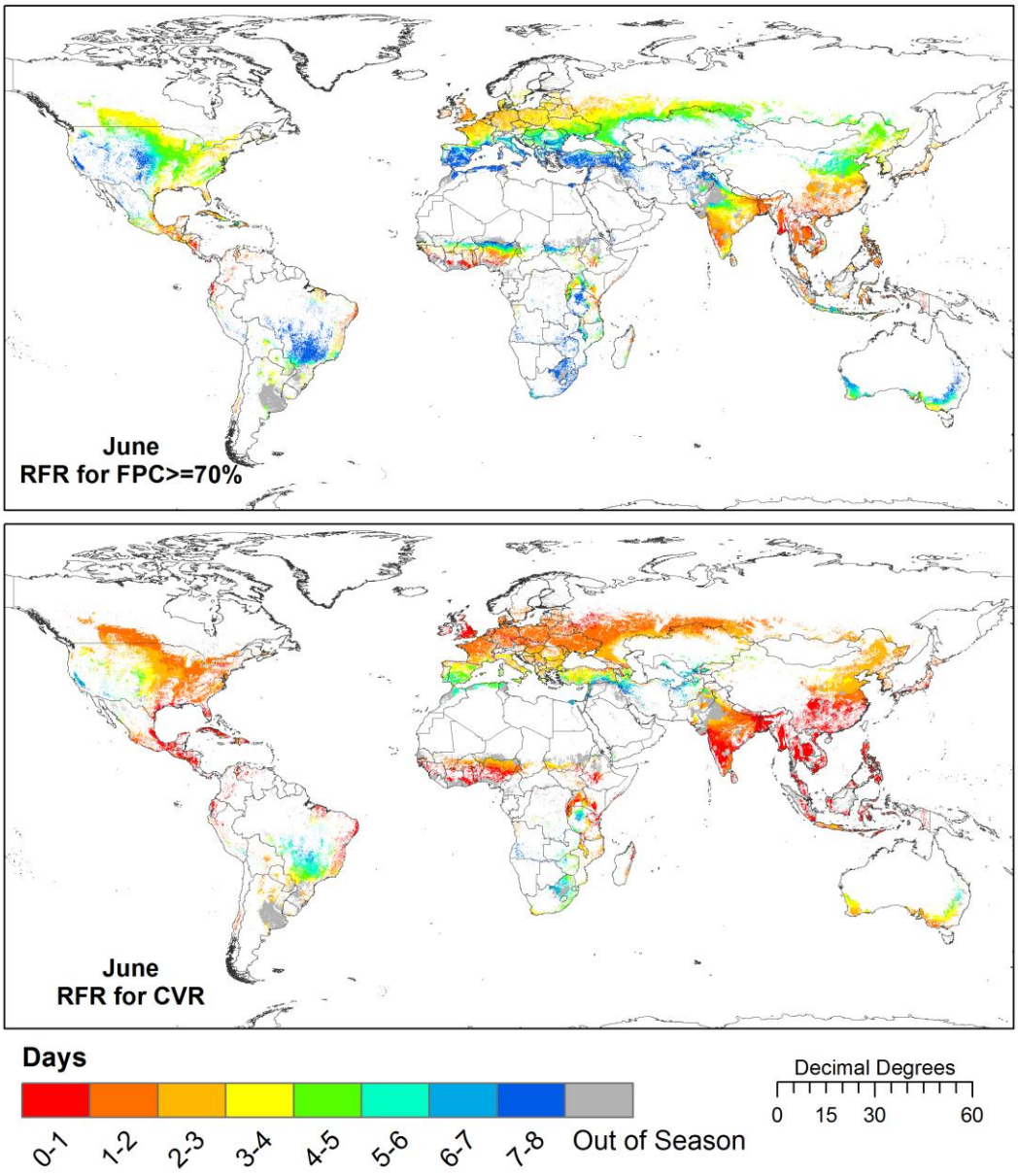

Figures 4.8a-b: The revisit frequency required to probabilistically yield, a) Top, a view at least 70%; or b) Bottom, a completely clear view (CVR), every 8 days during the month of June. Areas containing cropland out of season are shown in gray. Resolution is 0.05˚.

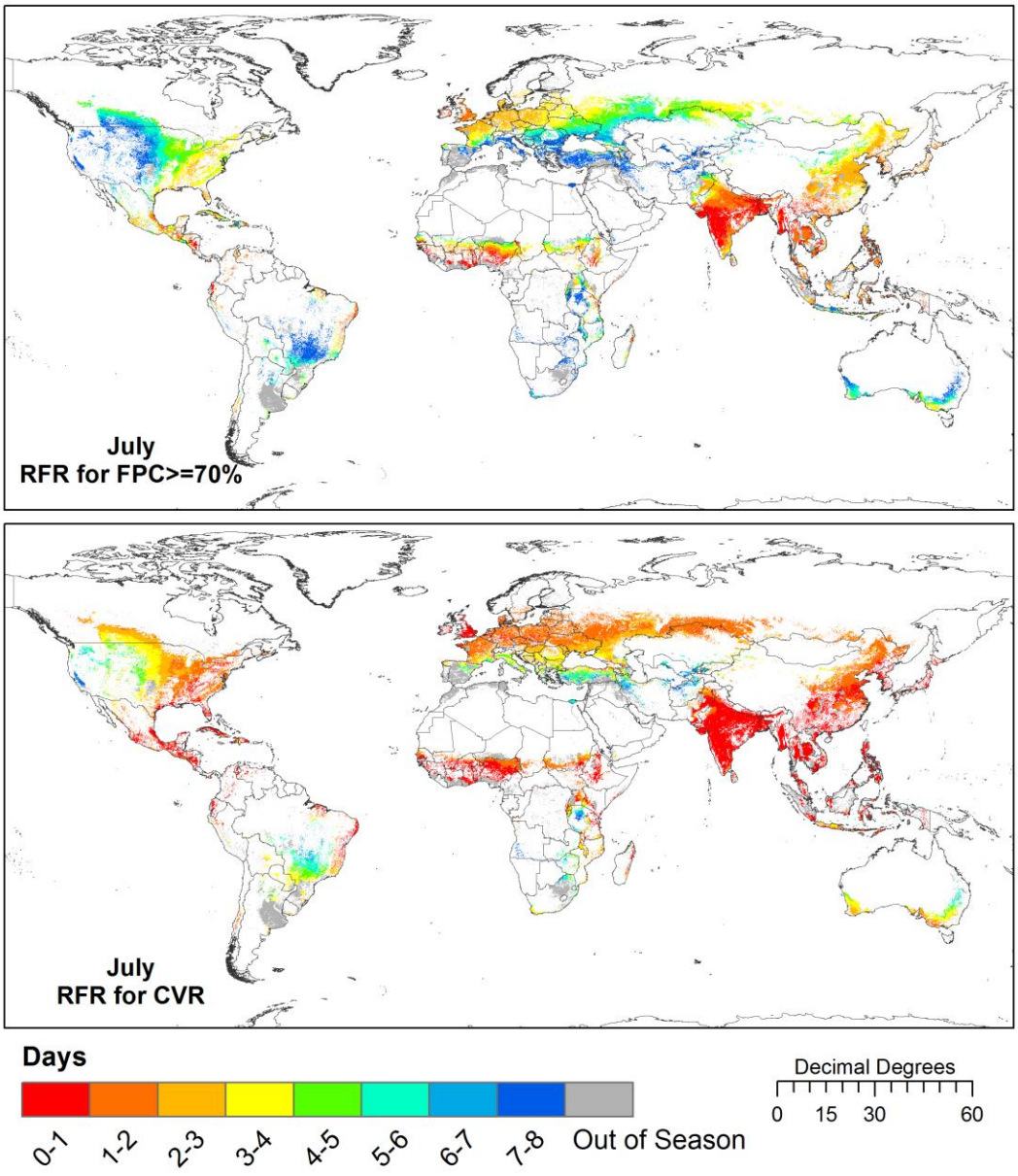

Figures 4.9a-b: The revisit frequency required to probabilistically yield, a) Top, a view at least 70%; or b) Bottom, a completely clear view (CVR), every 8 days during the month of July. Areas containing cropland out of season are shown in gray. Resolution is 0.05˚.

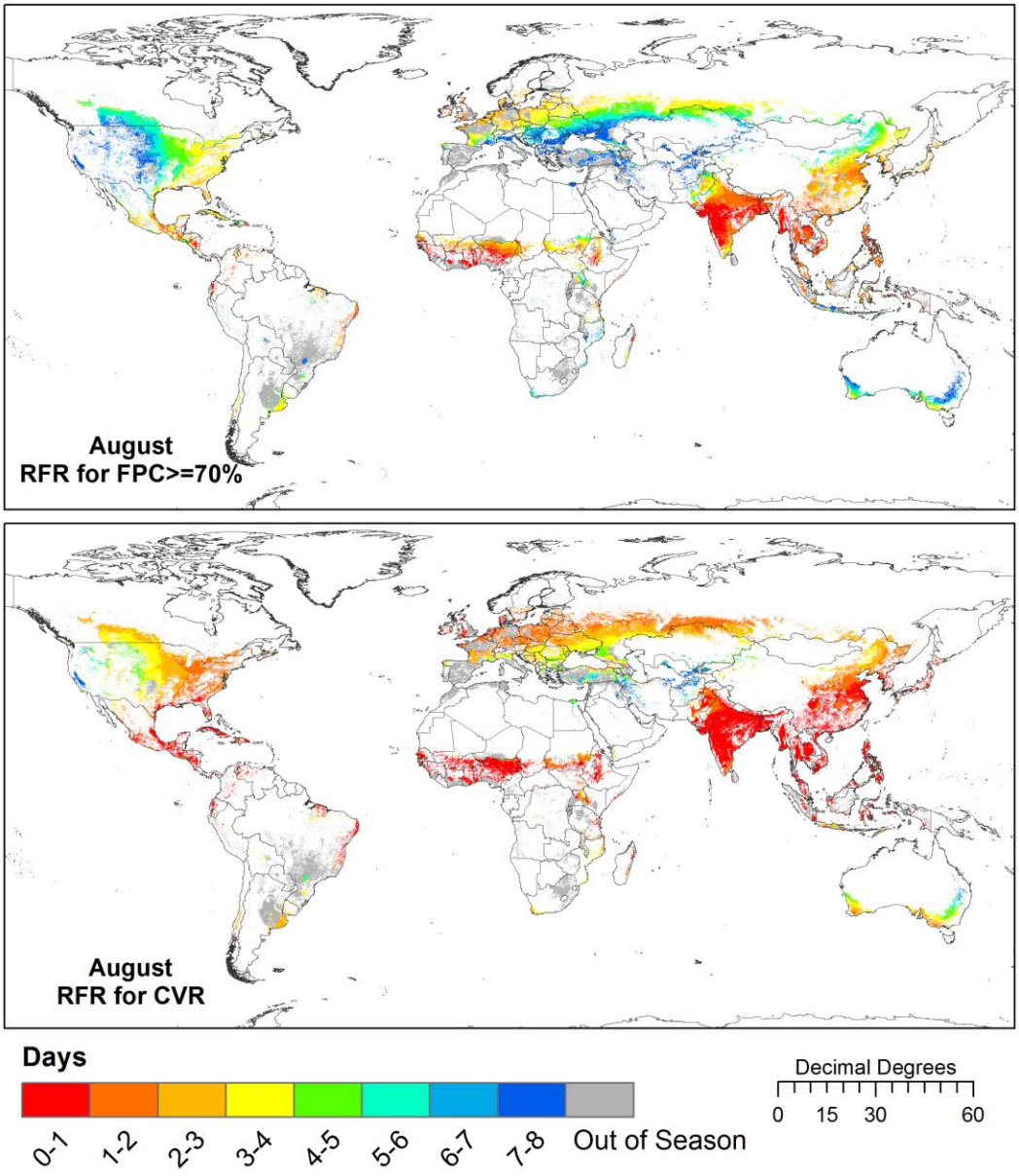

Figures 4.10a-b: The revisit frequency required to probabilistically yield, a) Top, a view at least 70%; or b) Bottom, a completely clear view (CVR), every 8 days during the month of August. Areas containing cropland out of season are shown in gray. Resolution is 0.05˚.

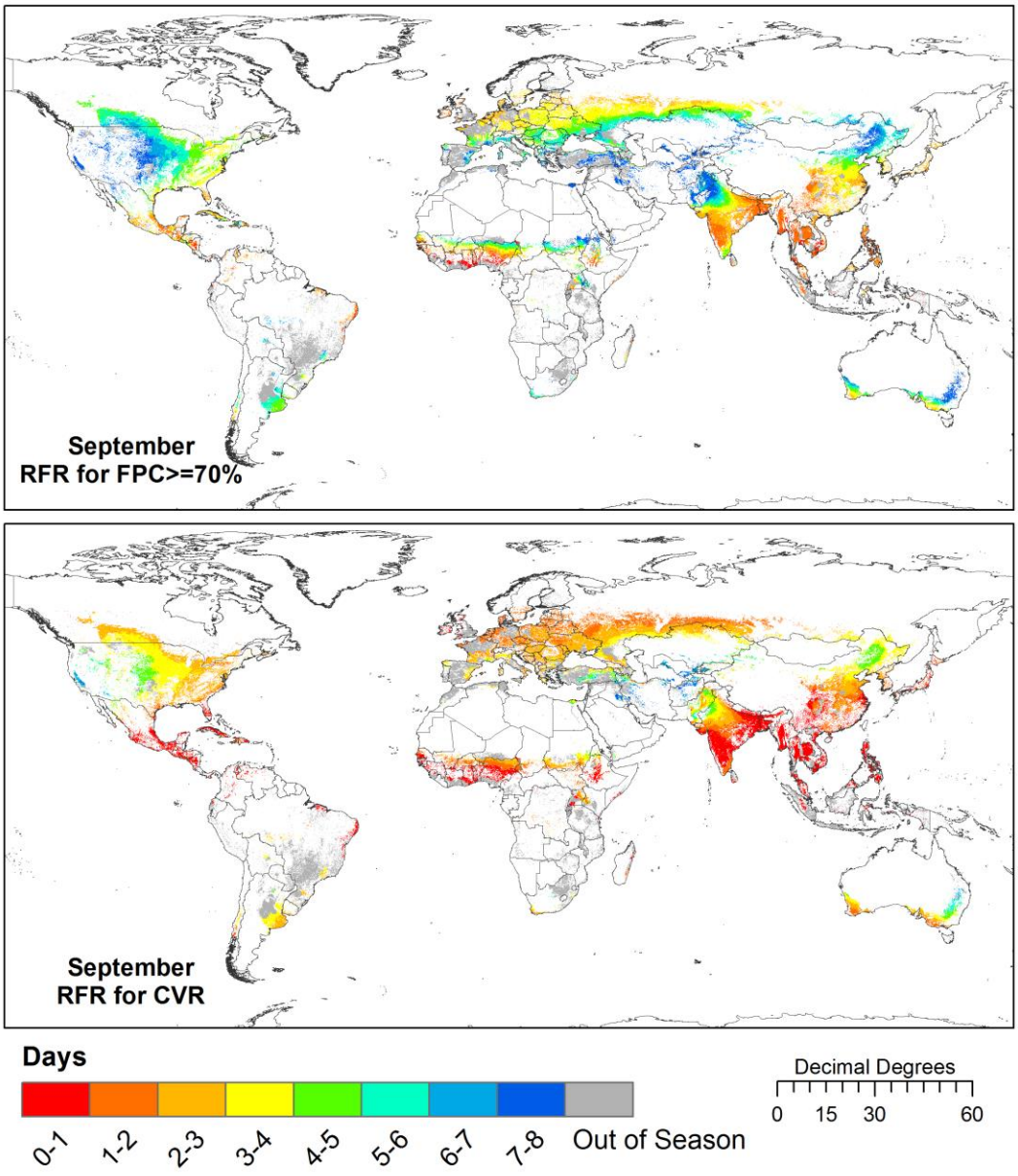

Figures 4.11a-b: The revisit frequency required to probabilistically yield, a) Top, a view at least 70%; or b) Bottom, a completely clear view (CVR), every 8 days during the month of September Areas containing cropland out of season are shown in gray. Resolution is 0.05˚.

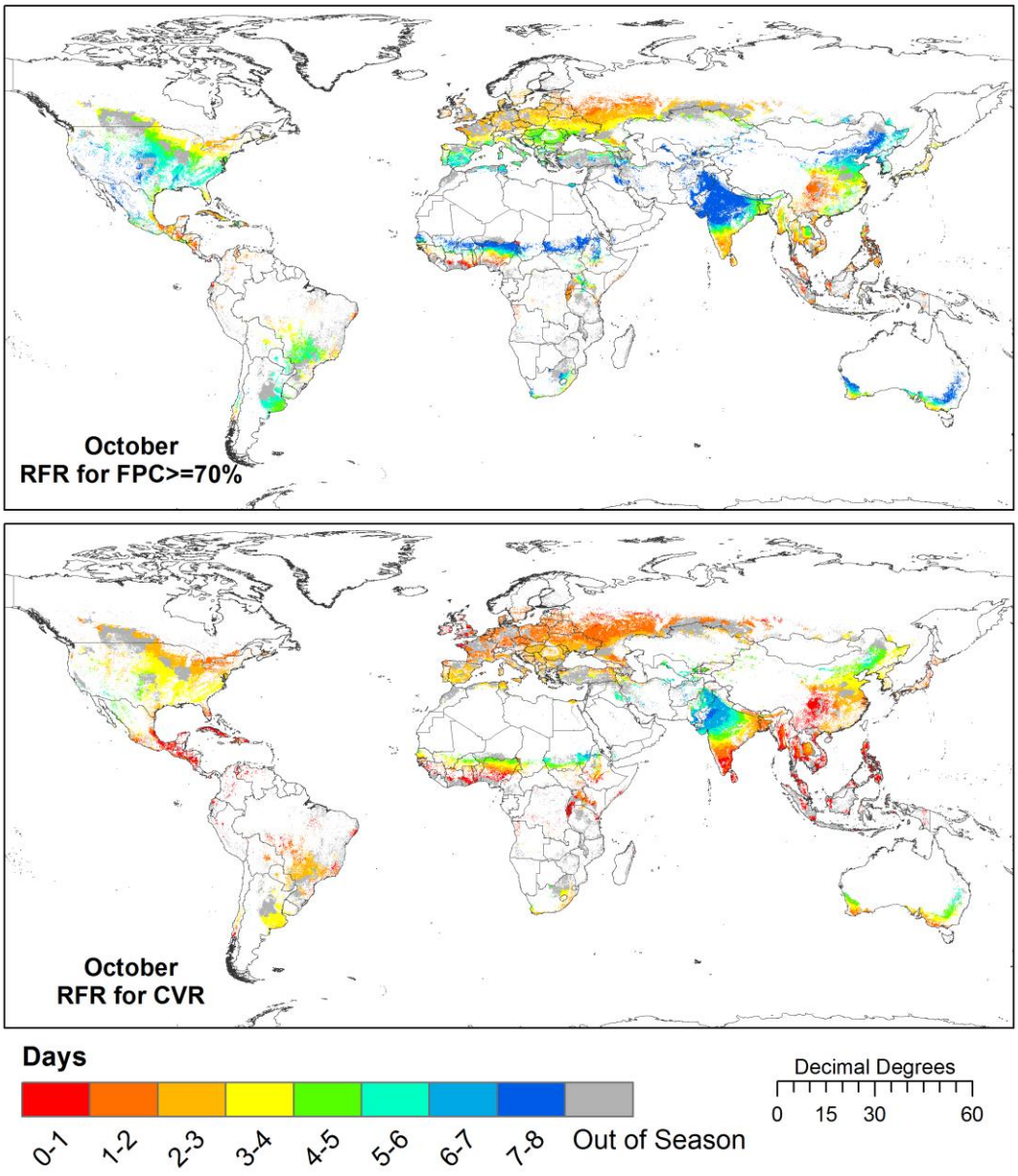

Figures 4.12a-b: The revisit frequency required to probabilistically yield, a) Top, a view at least 70%; or b) Bottom, a completely clear view (CVR), every 8 days during the month of October. Areas containing cropland out of season are shown in gray. Resolution is 0.05˚.

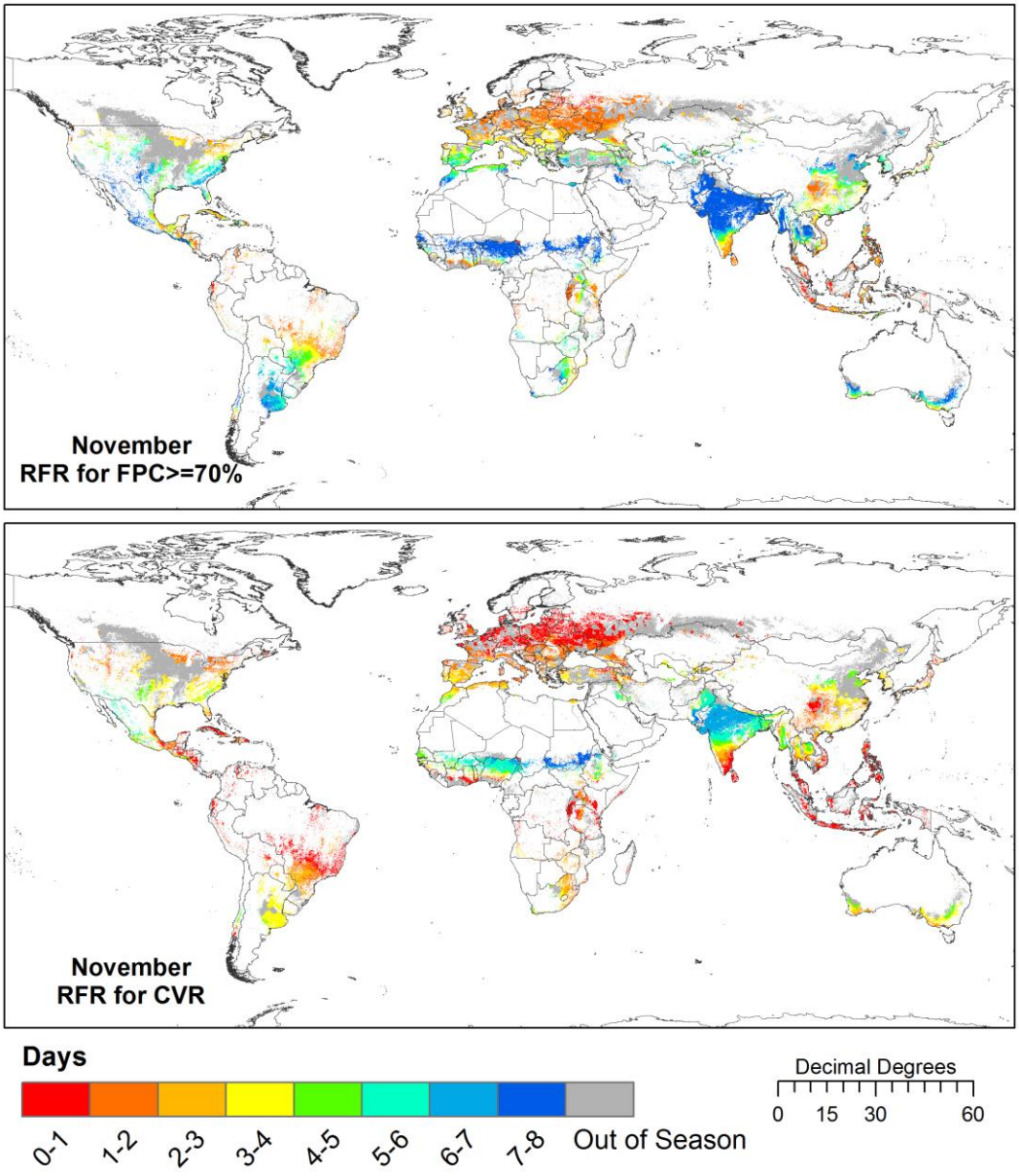

Figures 4.13a-b: The revisit frequency required to probabilistically yield, a) Top, a view at least 70%; or b) Bottom, a completely clear view (CVR), every 8 days during the month of November. Areas containing cropland out of season are shown in gray. Resolution is 0.05˚.

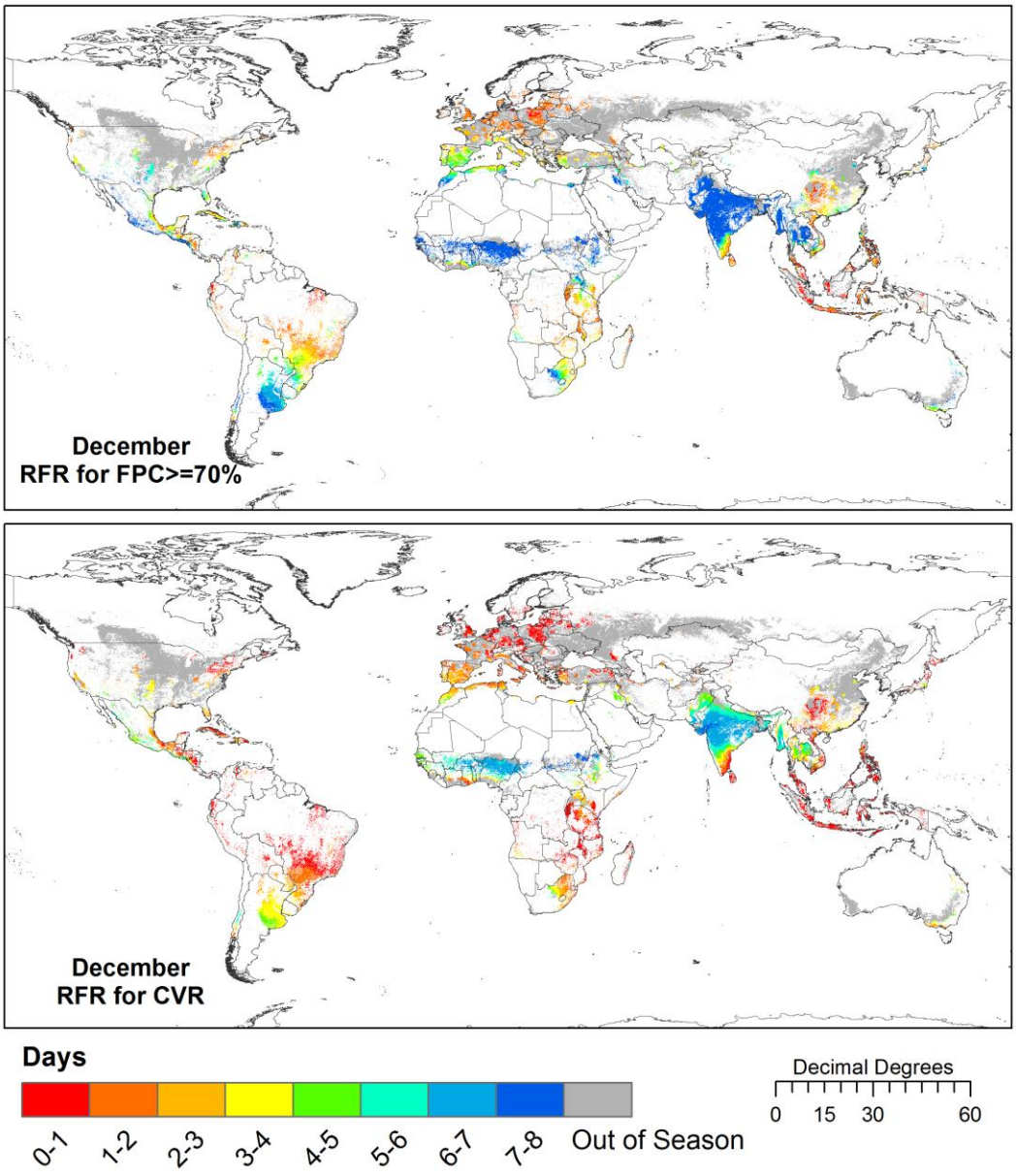

Figures 4.14a-b: The revisit frequency required to probabilistically yield, a) Top, a view at least 70%; or b) Bottom, a completely clear view (CVR), every 8 days during the month of December. Areas containing cropland out of season are shown in gray. Resolution is 0.05˚.

The revisit frequency required ranges from <1 day to exactly 8 days when the requirement is for a scene that has an FPC of at least 70%. Globally, the general pattern reveals that for November through February, a single revisit (RFR = 8 days) is

all that is required for 22-31% of actively cropped cells (Figure 4.15). This is owing to the Indian summer monsoon areas in these months are very clear. For April-June, 3-5 days is the most common revisit frequency required (20-31% of cells), while in March and July-October, required revisit frequency ranges broadly from 2-6 days. There are some cells for which a revisit rate of less than 1 day is required, but only during the months of July and August does this account for more than 4% of cells (8% and 9%, respectively). Globally, 44-55% of cells have a required revisit frequency of less than 4 days, while 7-23% of cells have a required revisit frequency of less than 2 days.

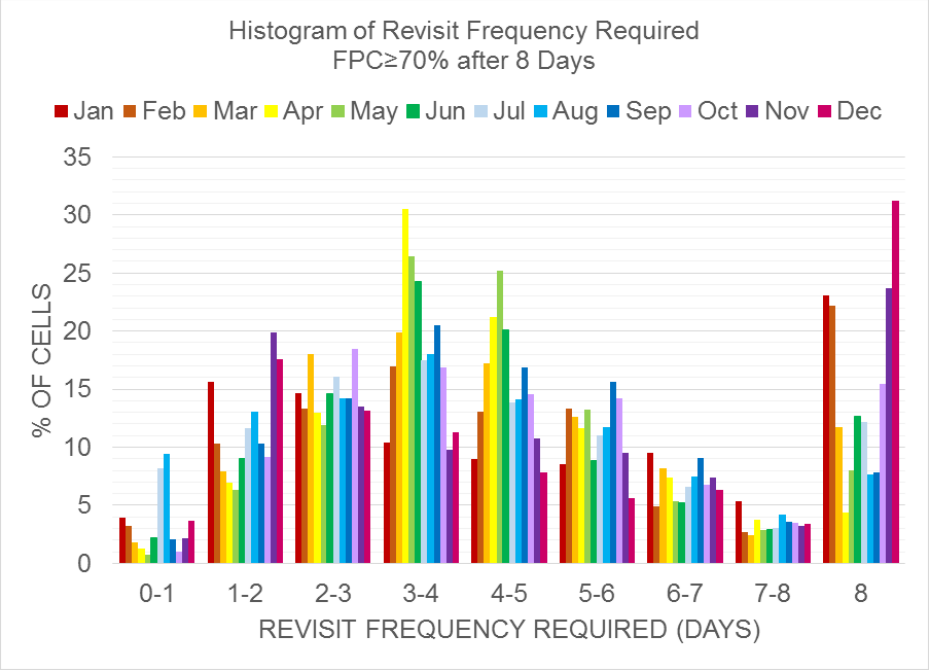

Figure 4.15: Histogram showing the revisit frequency required to yield a view at least 70% clear within 8 days over actively cropped cells during each month of the year.

This story is very different for the requirement for completely clear views, where for every month of the year, the most common revisit frequencies required fall in the 0-3 day range. In fact, 74-92% of cells have a required revisit frequency of less

than 4 days, while 38-60% of cells have a required revisit frequency of less than 2 days. As is visible in the map figures (4.3-4.14b), there is practically nowhere for which the revisit frequency is equivalent to the requirement (Figure 4.16), which is not surprising as the analysis would require an area to have 0% cloud cover probability during that month in order to meet a completely clear view. Again, the slightly increased average revisit rate pattern in November-February mentioned previously is present, although it is much lower in magnitude and has shifted to the 5-7 day range. In sum, rapid revisit rates would be required to meet an 8 day clear view requirement.

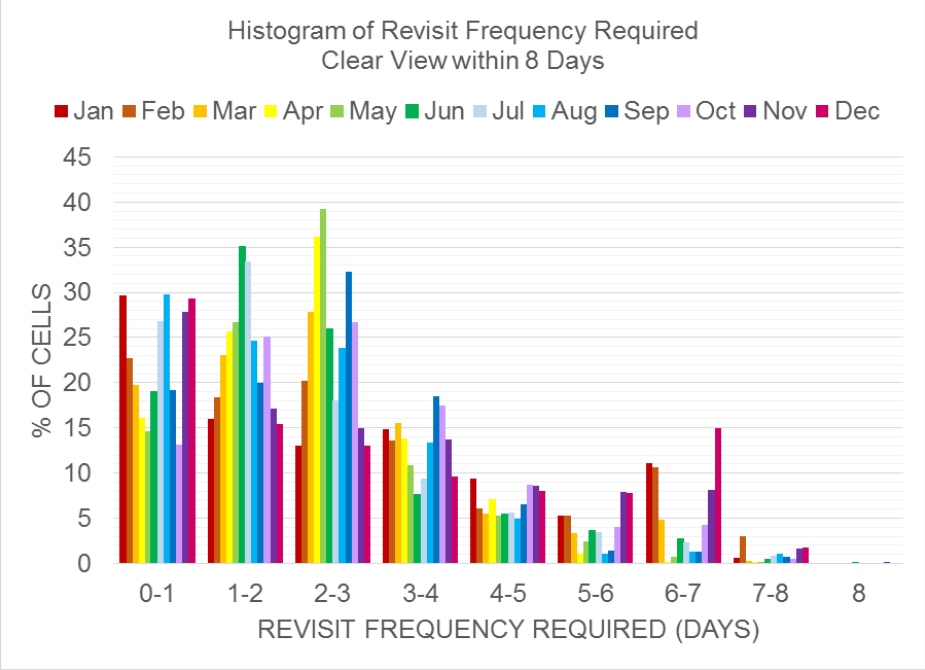

Figure 4.16: Histogram showing the revisit frequency required to yield a clear view every 8 days over actively cropped cells during each month of the year.

4.3.2 Requirement #5: 16 Day Reasonably Clear View Requirement

Recognizing that obtaining the revisit frequency required to meet the 8 day moderate resolution data requirement will be challenging with the current state of moderate resolution remote sensing (see Chapter 5 for full discussion), an analysis of the revisit frequency required to yield reasonably clear views of all croplands at least every 16 days throughout the AGS has also been performed. Similar patterns are followed in the revisit frequency required for an FPC of at least 70% for 16 days (Figure 4.17) as were exhibited and described for the 8 day requirement (Figure 4.15), with the November-February time frame again exhibiting a relatively infrequent revisit (16 days) required in 22-31% of cases yet again, and with the most common required revisit frequencies for April to June falling in the 6-9 day range. No month has more than 1% of cell requiring a revisit of less than 1 day, although >20% of cells during July-August and November-January require revisit rates more frequent than 4 days. Again, between 44-55% of cells require a revisit of less than 8 days.

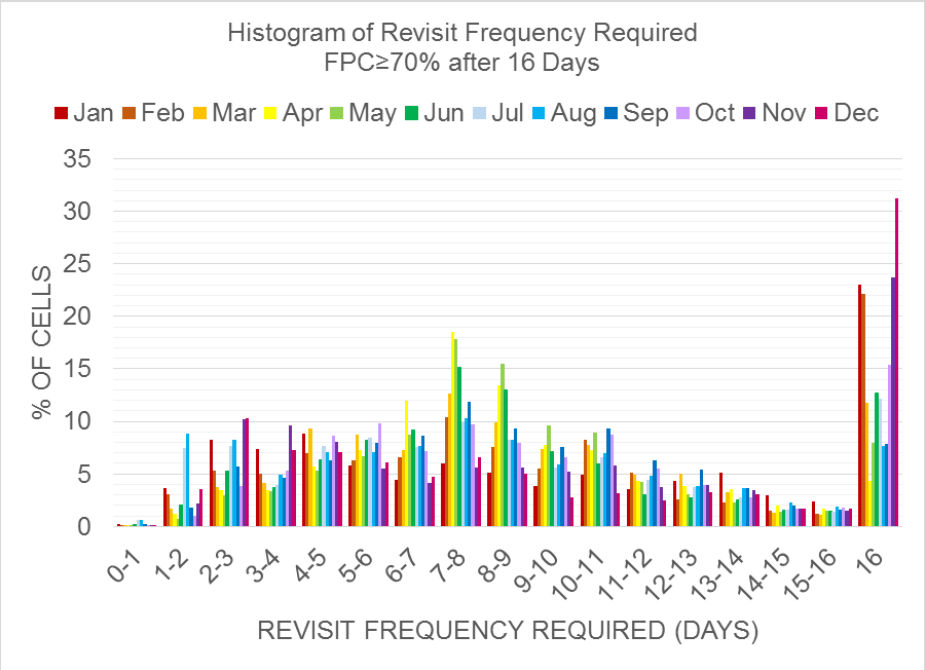

Figure 4.17: Histogram showing the revisit frequency required to yield a view at least 70% clear within 16 days over actively cropped cells during each month of the year.

Because of the simple linear relationship in Equation 3, the revisit frequency for a completely clear view within 16 days is simply half as frequent as for 8 days. In this case, 67-92% of actively cropped cells require a revisit frequency of less than 8 days (many of them in 4-5 day range), with 38-60% of cells requiring a revisit within 4 days (Figure 4.18).

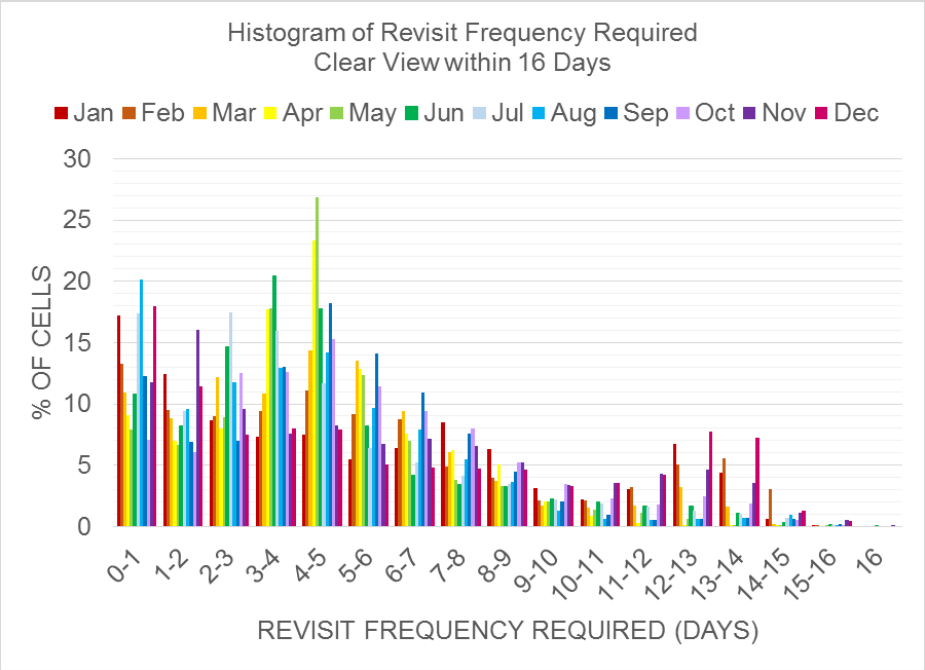

Figure 4.18: Histogram showing the revisit frequency required to yield a clear view within 16 days over actively cropped cells during each month of the year.

4.4 Discussion, Future Research, and Conclusions

The research has shown the revisit frequency required to probabilistically yield a clear view (or partially clear view – FPC ≥ 70%) within 8 or 16 days within the context of moderate spatial resolution EO requirements established by the GEO Agricultural Monitoring Community of Practice and the CEOS Ad Hoc Team for GEOGLAM (Table 4.1). These revisit frequency requirements are provided on a monthly basis for only those areas which are actively cropped (or *not* actively cropped in the case of those requirements for data outside of the AGS), and where appropriate, for areas which contain fields of the stated target size. The revisit frequency required varies temporally and geographically, with many areas requiring revisits more frequent than every 2 or 4 days in order to probabilistically meet a CVR or FPC requirement every 8 or 16 days, respectively.

As previously mentioned, the requirement evaluated (#5) is preferred for the full cropland extent, but may be taken on a sampled basis. It would perhaps be beneficial to design a sampling frame with these cloud constraints in mind. The implications of these required revisit frequencies will be discussed in depth in Chapter 5, wherein approaches to meeting these requirements will be presented and evaluated.

For over 40 years, moderate spatial resolution remote sensing instruments have passed over the earth at least every 16-18 days, with much of the Landsat program's history having 8-9 day overpass frequency, although data for most areas outside of the United States have not been systematically acquired at this rate (Ju & Roy, 2008; Wulder et al., 2008; Wulder, White, Masek, Dwyer, & Roy, 2011). In this context, it may seem surprising that the revisit frequency that is required to actually meet an 8 or 16 day requirement for (relatively or completely) cloud free data is in some areas less than 2 or 4 days, respectively. However, in the context of the global agricultural monitoring activities, such as crop yield forecasting, which have relied upon daily data since the launch of MODIS Terra in 1999, this revelation is not unexpected. In order to yield moderate resolution results at the regional to global scale, it is necessary to rethink the way in which we have historically approached moderate resolution systems' design and/or to consider a multi-mission constellation approach to monitoring (Goward et al., 2011; Hansen & Loveland, 2012).

The requirements articulated herein provide practical inputs into a data acquisition strategy for global agricultural monitoring. However, what remains is twofold. First, an investigation into our current, near-term, and mid-term EO systems

revisit capabilities would provide valuable insight into our missions' capacity to meet such requirements (Chapter 5). That many of the required revisit frequencies articulated herein are well beyond the capabilities of any single existing moderate resolution program or mission demonstrates that with current proven capabilities, a multi-mission, multi-space agency constellation approach is necessary for operational monitoring in the moderate resolution domain, although precisely how these constellations might operate requires further analysis (Chapter 5). Secondly, for the synthetic aperture radar (SAR) requirements detailed in Table 4.1, Req. 6 and 9, the "where" requirement identifies "persistently cloudy" areas. It is necessary to delineate precisely which regions are "persistently cloudy" and therefore require microwave SAR acquisitions, a topic which will also be addressed in Chapter 5.

Chapter 5: Meeting Earth Observations Requirements for Global Agricultural Monitoring: An Evaluation of the Revisit Capabilities of Current and Planned Moderate Resolution Optical & Thermal Infrared Earth Observing Missions

5.1 Introduction

The past decade for remote sensing has been described as the "MODIS Revolution," with nearly twice daily consistently high quality global observations available in near real time (NRT) being applied by researchers around the world to generate global scale science results (Justice et al., 1998; Justice, Vermote, Privette, & Sei, 2011). With the Landsat archive opening and computational resources growing, global scale analyses are poised to move into the moderate resolution domain (Goward et al., 2009, 2011, 2012; Wulder, Masek, Cohen, Loveland, & Woodcock, 2012; Roy et al., 2014), with regional to global datasets at 30m resolution already demonstrated (Gong et al., 2013; Hansen et al., 2013; Johnson, 2010; Roy et al., 2010; Yu et al., 2013). In the context of crop condition monitoring and yield forecasting, moderate resolution data have not yet achieved broad scale results across the globe, primarily due to the lack of consistent cloud free acquisitions with sufficiently high temporal resolution, although as demonstrated by the GEOGLAM requirements table (Table 4.1, especially Requirements #4-6), this is a priority growth area for analyses spanning the extent of cropland for fields of all sizes. Requirements for coarse resolution data are presently being met by the systematic acquisitions of systems like MODIS and its follow-on, the Visible Infrared Imaging Radiometer (VIIRS) Suite (Justice et al., 2013), as well as Proba-V and Sentinel-3. Yet, in terms

of moderate spatial resolution optical missions, no single observatory at present is capable of acquiring data with sufficient frequency to meet an eight day cloud free requirement over *all* croplands, much less one which makes data freely and openly available to science users. Still, the Landsat observatory has been used in many regional studies particularly for land cover and land use analyses (Homer et al., 2007; Johnson, 2010; Skole & Tucker, 1993; Vogelmann et al., 2001; Wulder et al., 2008). In the private sector, there are emerging options for both fine and moderate spatial resolution monitoring, such as Planet Labs and Disaster Modeling Constellation (Underwood et al., 2005). However, they are (or will be) fee-based, and are not yet established as a viable data source. For this reason, the focus herein will be on analyzing the capability of current and near-term moderate resolution civil space agency flown instruments to meet EO requirements for global agricultural monitoring.

Having articulated the temporal revisit requirements for moderate resolution O+TIR monitoring in Chapter 4, there remains the assessment of the capacity of our current and planned moderate resolution missions to meet the revisit requirements. This will be achieved by identifying candidate missions, modeling their coincident orbital overpasses, and comparing these multi-mission/multi-space agency constellations' combined revisit frequencies to show how and where we can (and cannot) meet our O+TIR EO requirements for monitoring. In those areas where we *cannot* meet our O+TIR requirements, alternative data types (namely, microwave synthetic aperture RADAR (SAR) data) should be considered instead. Requirement #6 found in Table 4.1 calls for SAR data on a weekly basis in areas which are

"persistently cloudy," in addition to rice cultivating areas. There is growing research in SAR algorithm development for rice and non-rice areas alike (Hong, Zhang, Zhou, & Brisco, 2014; Kussul, Skakun, Shelestov, Kravchenko, & Kussul, 2012; Leichtle, Schmitt, Roth, & Schardt, 2012; McNairn, Champagne, Shang, Holmstrom, & Reichert, 2009a; McNairn, Shang, Champagne, & Jiao, 2009b; McNairn, Shang, Jiao, & Champagne, 2009c; Torbick et al., 2011). The term "persistently cloudy" is qualitative but carries the implication that areas which fit this description are those for which current/planned O+TIR instrumentation are insufficient. Therefore, "persistently cloudy" will be defined herein as those areas and times of year which require a more frequent revisit in order to yield a (reasonably) clear view than our current/planned moderate resolution O+TIR missions are capable of delivering.

5.1.1 Identifying Candidate Missions

There are a number of moderate resolution optical plus thermal infrared (O+TIR) missions that are currently operating as well as several additional planned to launch in the next few years. At this time (early 2014), the only moderate resolution O+TIR missions with free and open data policies are Landsat 7 Enhanced Thematic Mapper (L7 ETM+) and the Landsat 8 Operational Land Imager and Thermal Infrared Sensor (L8 OLI and TIRS), which together have a combined revisit capability of 8 days (SLC-Off problems notwithstanding). However, due to onboard storage and downlinking limitations these missions do not acquire every land scene at every opportunity, although recent alterations to the missions' acquisition plans have greatly increased daily acquisitions to 550-600 daylit scenes per day for L8 and 400-450 for L7 (Eugene Fosnight, USGS, personal communication, 5 February 2014)

from the originally partitioned 250 best quality daylit, land-containing scenes, coming close to the acquiring all possible 540-630 daylit land-containing scenes within view of each sensor each day (Arvidson et al., 1999, 2001, 2006). The Indian Space Research Organization's (ISRO) Resourcesat-2 Advanced Wide Field Sensor (R2 AWiFS) is also currently operating, with a spatial resolution as fine as 55m and a repeat cycle of 24 days, although with its sensor engineering characteristics this permits a revisit capability on the order of 5 days. At present, ISRO does not provide this data freely to all, although there has been some suggestion that they may supply some free data for GEOGLAM activities in response to encouragement from CEOS (Brian Killough, personal communication, 10 February 2014). Agencies within the United States – namely, the Department of Agriculture – have purchased these data and found them to be valuable for cropland monitoring applications and compatible if not complementary to Landsat data, although some uncertainty about long term radiometric calibration stability remains (Boryan & Craig, 2005; Goward et al., 2012; Johnson, 2010). Meanwhile, planned for the near future is the European Space Agency's Sentinel-2 Earth observatory, comprised of two separate instruments (S2A, S2B), the first of which is set for launch in 2015. The two satellites together are purported to systematically acquire all data over land in the low-latitudes every 5 days and in the mid-latitudes on the order of 2-3 days (Drusch et al., 2012). The Sentinel-2 program also plans to employ a free and open data policy, and efforts are underway to cross-calibrate the instruments and ensure interoperability with Landsat (Jeff Masek, personal communication, October 2012). It should be noted that the Sentinel-2 missions do not include thermal bands. Thermal data in the agricultural

monitoring context are used primarily for evapotranspiration and water status (Anderson et al., 2011; Hain, Crow, Mecikalski, Anderson, & Holmes, 2011), and land surface temperature measurements (Tomlinson, Chapman, Thornes, & Baker, 2011; Weng, Fu, & Gao, 2014), as well as for atmospheric adjustment (Frey et al., 2008; Justice et al., 1998; Roy et al., 2014), although there is recent research suggesting their utility in yield forecasting (Johnson, 2014) as well as for crop type classification and residue mapping (Sullivan, Lee, Beasley, Brown, & Williams, 2008). Nevertheless, data from the visible, near-IR and shortwave IR are still the most broadly applied resource in the agricultural monitoring context. Therefore, due to the Sentinel-2 missions' high spatial and temporal resolution, their free and open data policy, their planned interoperability with the Landsat missions, and their otherwise well-placed spectral bands, they are included herein for analysis.

While there are other moderate resolution Earth observing missions in orbit or planned for launch within the next five years, these three observatories/five instruments have (or will have) the highest quality data, are (or are in the process of negotiating to be) available to the agricultural monitoring community for low to no cost, are being studied for interoperability, and are considered to be the most attainable and highest quality by the CEOS Ad Hoc Team for GEOGLAM. They therefore comprise the candidate missions analyzed for their combined revisit capabilities herein.

5.2 Methods

5.2.1 Overpass Analysis

The frequency with which a given area falls within the view of a satellite sensor is contingent upon the satellite's orbit, the field of view of the sensor, and the latitude of the target area. With polar orbiters, high latitudes are within view more frequently than Equatorial zones, and so the majority of the variability in combined revisit capabilities occurs on a latitudinal gradient. Different missions have different repeat cycles, which refers to the time it takes the satellite to repeat a full orbital cycle, to be distinguished from revisit capabilities – which is the amount of time until an area is within view of a sensor. As such it is necessary to evaluate the combined revisit capabilities of multiple sensors in a window of time ("scenario period") sufficient to allow for all considered missions to complete their respective full repeat cycles on the same day.

The Committee on Earth Observation Satellites has invested in the development of a visualization environment (COVE) that models the orbits and by extension the coincident overpasses of multiple missions (Chander, Killough, & Gowda, 2010; Kessler et al., 2013). In this analysis[6], the aforementioned five satellites have been combined to form seven hypothetical imaging moderate resolution O+TIR constellations (Table 5.1). The scenario periods range from 72-160 days, and each time a given area passes within view of one sensor in a hypothetical constellation is counted as an acquisition opportunity (AO). In order to yield the

[6] The modeled overpass analysis has been executed by the CEOS Systems Engineering Office (SEO) team under the leadership of Brian D. Killough at NASA Langley Research Center in Newport News, VA. I have requested the satellites to be included as well as their combinations for this study, and all subsequent analyses are my own.

average time to revisit for each 1˚ cell, at the end of the scenario period the number of AOs for each hypothetical constellation is divided by the number of days within the scenario period.

Table 5.1: The seven hypothetical constellations and their best and worst revisit capabilities

#	Satellites	Scenario Period – Days	Least AO	Mode AO	Most AO	Best Revisit - Days	Mode Revisit - Days	Worst Revisit - Days
1	L8, S2A, S2B, R2	160	150	288	312	0.94	1.80	1.95
2	L7, L8, S2A, R2	120	121	232	253	1.01	1.94	2.11
3	L7, L8, R2	72	91	173	192	1.26	2.40	2.67
4	L7, L8, S2A, S2B	80	123	246	246	1.54	3.08	3.08
5	L8, S2A, S2B	80	152	305	305	1.90	3.81	3.81
6	L7, L8, S2A	80	178	356	356	2.22	4.44	4.44
7	L7, L8	80	320	640	640	4.00	8.00	8.00

The actual interval between AOs is variable throughout the scenario period and will be shorter or longer than the average as the scenario period progresses. However, this temporal spacing is not consistently bound to any point in time or any specific location, and so for consistency, the average revisit time is maintained for each 1˚ grid cell. Additionally, within each scenario period, there is also some apparent longitudinal variability in revisit capability due to the initial conditions of the simulation (Paul Kessler & Shaun Deacon, personal communication, 10 March 2014). This banding can be considered an artifact of the simulation and is not significant (Figures 5.1-7). To reduce the presence of these artifacts, only data within the 5^{th} and 95^{th} percentile are maintained. To be consistent with the approach used so far, which situates the analysis in terms of "best" and "worst" case scenarios, I extract

and use in this analysis the best (5th percentile), mode, and worst (95th percentile) *average* revisit frequency over each 1˚ increment of latitude.

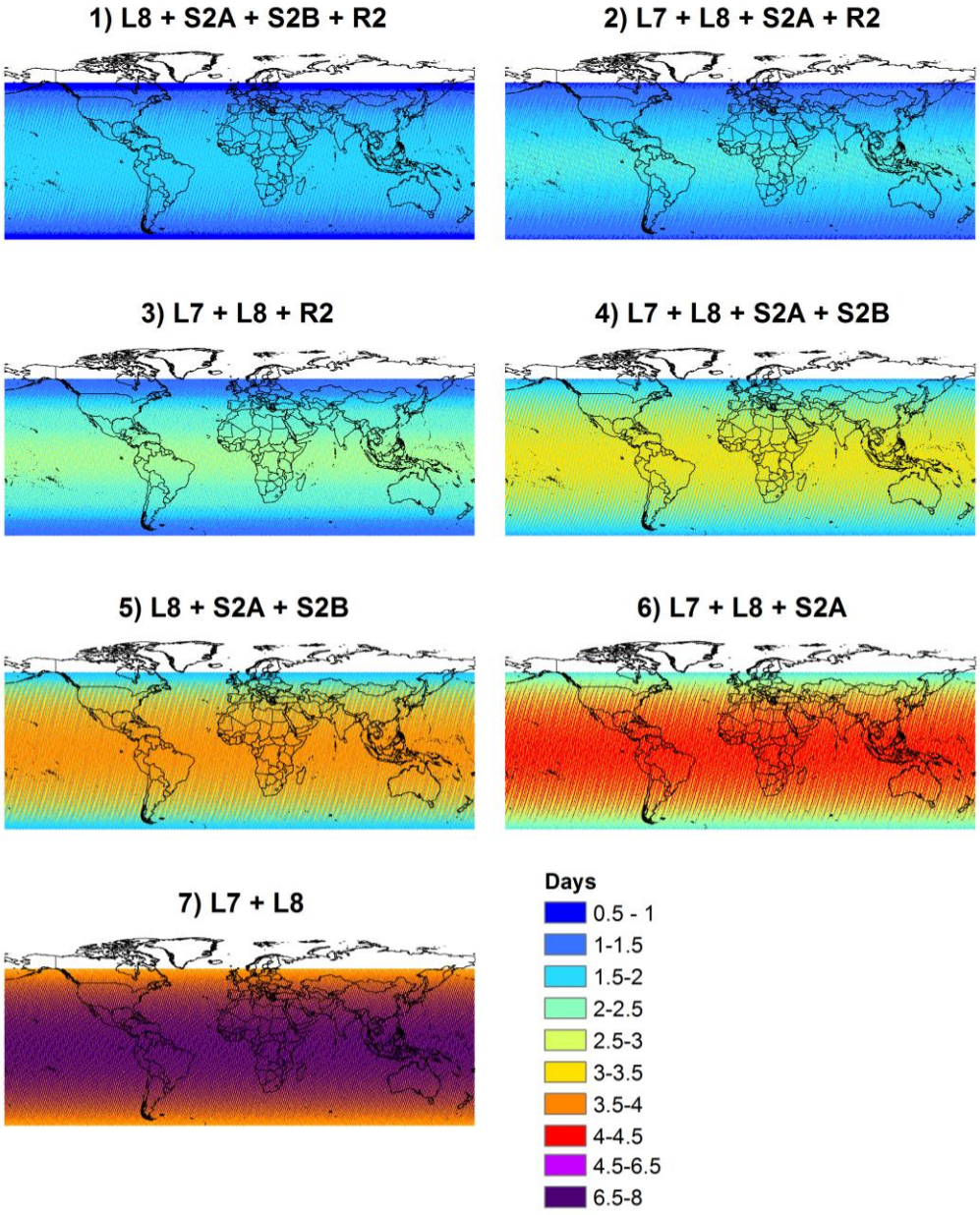

Figures 5.1-7: The average revisit capabilities of the seven hypothetical constellations analyzed herein. This is the "raw" revisit analysis, showing for each 1˚ cell the average revisit time observed over the scenario period. All seven constellations use the same legend for ease of intercomparison.

It bears noting that this analysis shows coincident overpasses and therefore acquisition opportunities from 60˚N to 60˚S (where the majority of croplands lie), but does not attempt to analyze actual *acquisition* frequencies. As previously mentioned, of the observatories incorporated in this analysis, only the Sentinel-2 program (S2A/S2B) plans to acquire every (low- and mid-latitude) land scene at every opportunity, and therefore an acquisition opportunity does not automatically mean that an image will be acquired. This analysis provides a baseline of what kind of performance by these missions is possible.

5.2.2 Comparing Overpass Capabilities with EO Requirements

Chapter 4 showed the revisit frequency required to yield both a cloud free clear view (CVR) and a final percentage clear (FPC) of at least 70% after a given number of days, thereby providing two scenarios and bounding a sort of "best case scenario" and "worst case scenario" for acquisition frequency. Herein, the 8 day requirement for O+TIR data is compared against the seven combined revisit capabilities described in the previous section. More precisely, the best/most frequent combined revisit for each 1˚ of latitude (resampled to 0.05˚) is compared against the revisit frequency required to yield an FPC of at least 70% over each 0.05˚ after 8 days, and the worst/least frequent combined revisit for each 1˚ of latitude (resampled to 0.05˚) is compared against the revisit frequency required to yield a clear view within 8 days. This bounds the upper and lower end of our ability to meet this 8 day requirement for (reasonably) clear O+TIR data. As the realistic performance is likely to fall somewhere between these two comparisons, I have provided summary statistics for two such analyses which estimate the "middle of the road" case as well:

the most common (mode) revisit for each 1˚ of latitude (resampled to 0.05˚) compared against both the requirement for an FPC of at least 70% as well as the requirement for clear views.

5.3 Results

5.3.1 Meeting the Requirement for a Reasonably Clear View every 8 Days

In Table 5.1, the constellations are numbered 1 through 7, denoting their rank in terms of revisit frequency. That is to say, anything that Constellation #7 can meet, so too can #1-6, anything Constellation #6 can meet, so too can #1-5 but not #7, et cetera. Meanwhile, a value of 0 (elsewhere denoted "None", as in Figures 5.8-5.19a-b) indicates that no constellation is capable of meeting the revisit frequency requirement, and denotes a time and area for which active microwave SAR data ought to be considered. A quick glance through the monthly maps showing which (if any) of the constellations are capable of meeting the less frequent (based on a final percentage clear requirement of at least 70%; Figures 5.8-5.19a) and the more frequent (based on a clear view requirement; Figures 5.8-5.19b) required revisit for that month shows that for most areas in most months, the former comparison (the "best case scenario") yields very high success rate with 6-7 different proposed constellations being capable of meeting the required revisit frequency. The same, however, cannot be said for the "worst case scenario" comparison, wherein many areas are met by only Constellations #1-3, and still many others are not viable candidates for the use of O+TIR data.

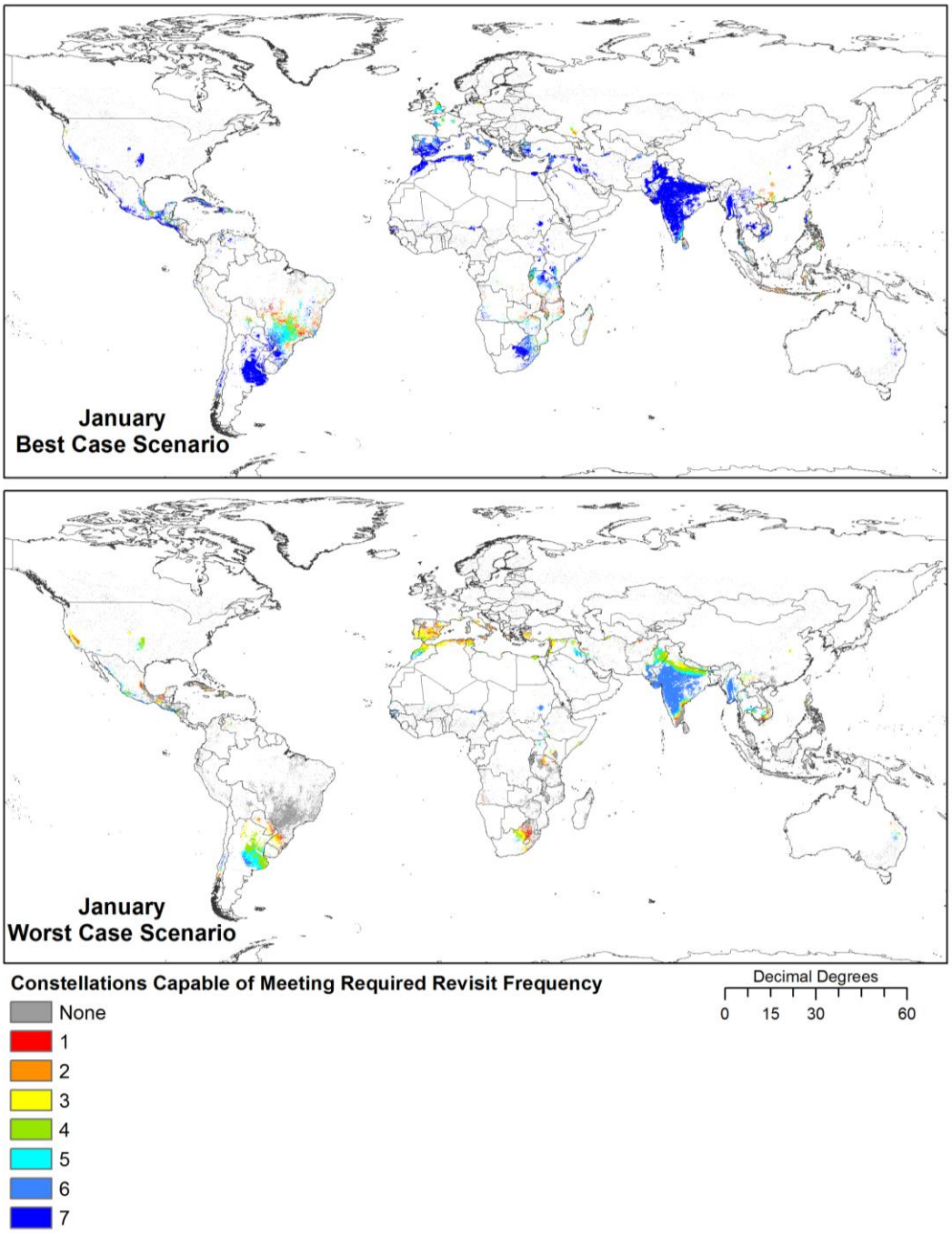

Figure 5.8a-b: Constellations capable of meeting the revisit frequency required to yield a view every 8 days during January that is, a) Top, at least 70% clear, and b) Bottom, 100% clear. The "best case scenario" (a) compares this less stringent clear view requirement with the best revisit observed at each 1˚of latitude, while the "worst case scenario" (b) compares the more stringent clear view requirement with the worst revisit observed at each 1˚of latitude. The missions included in Constellations #1-7 can be found in Table 5.1. Note that the constellations are ranked such that each requirement that can be met by #7 can be also met by 1-6, and so forth.

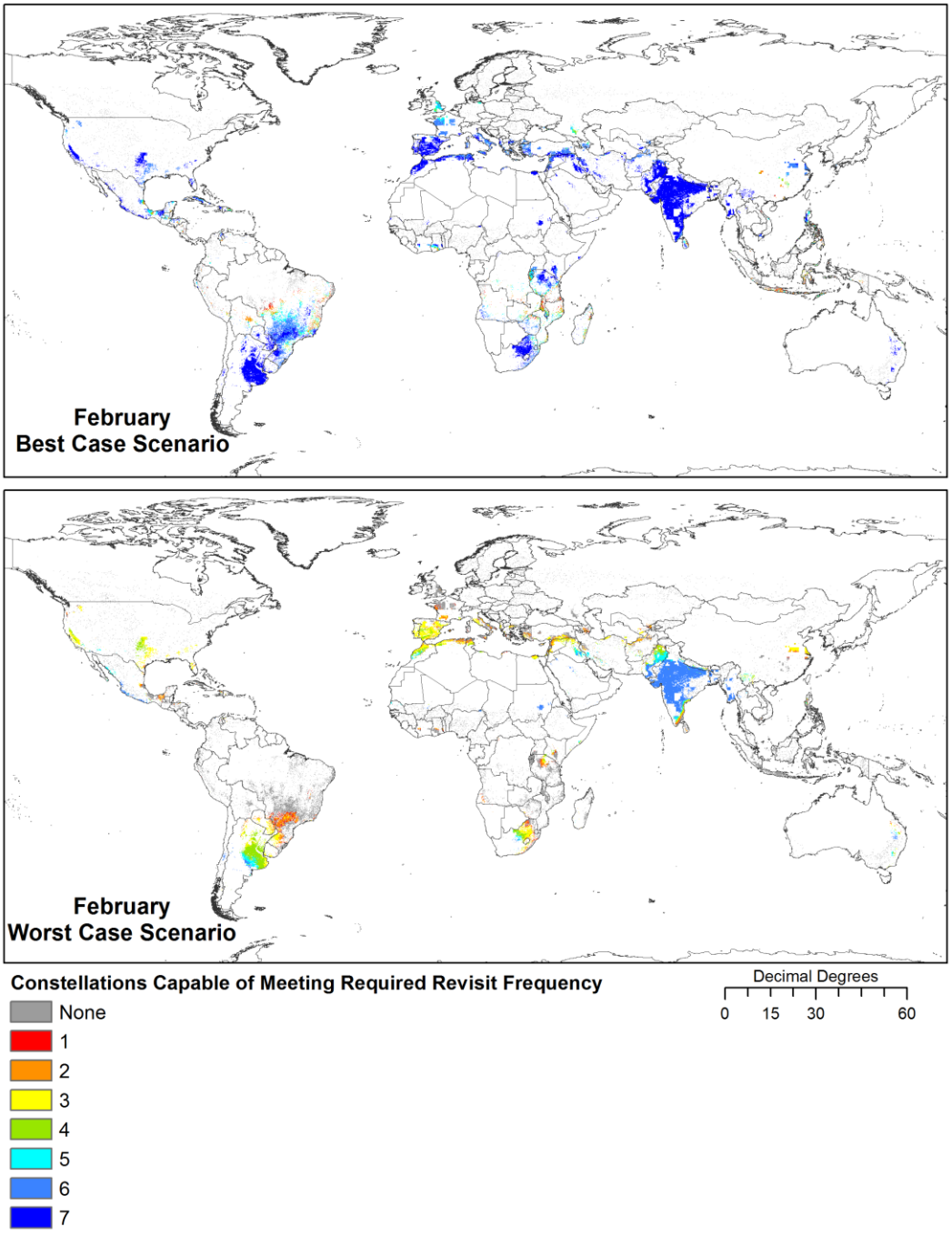

Figure 5.9a-b: Same as Figure 5.8a-b, but for February.

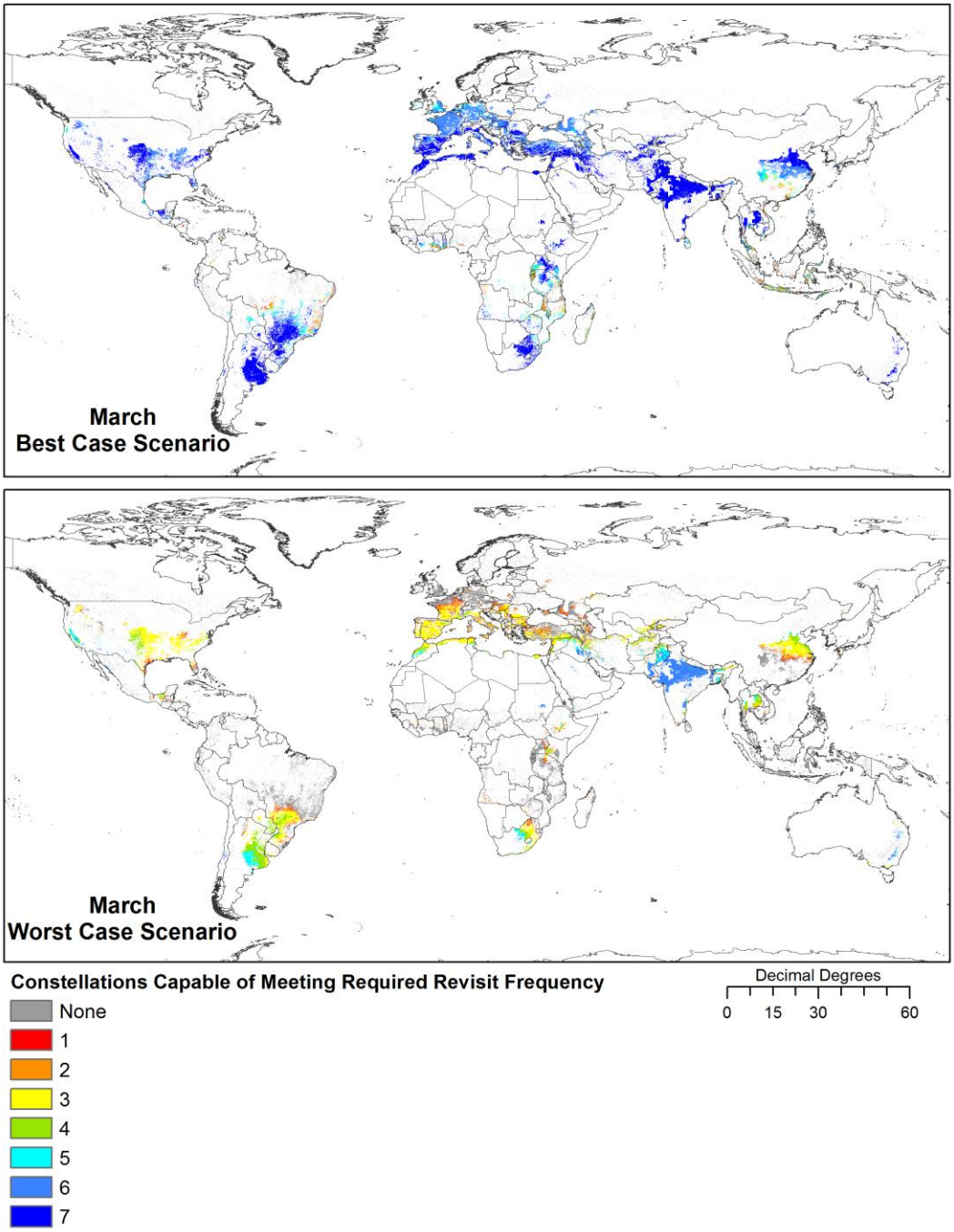

Figure 5.10a-b: Same as Figure 5.8a-b, but for March.

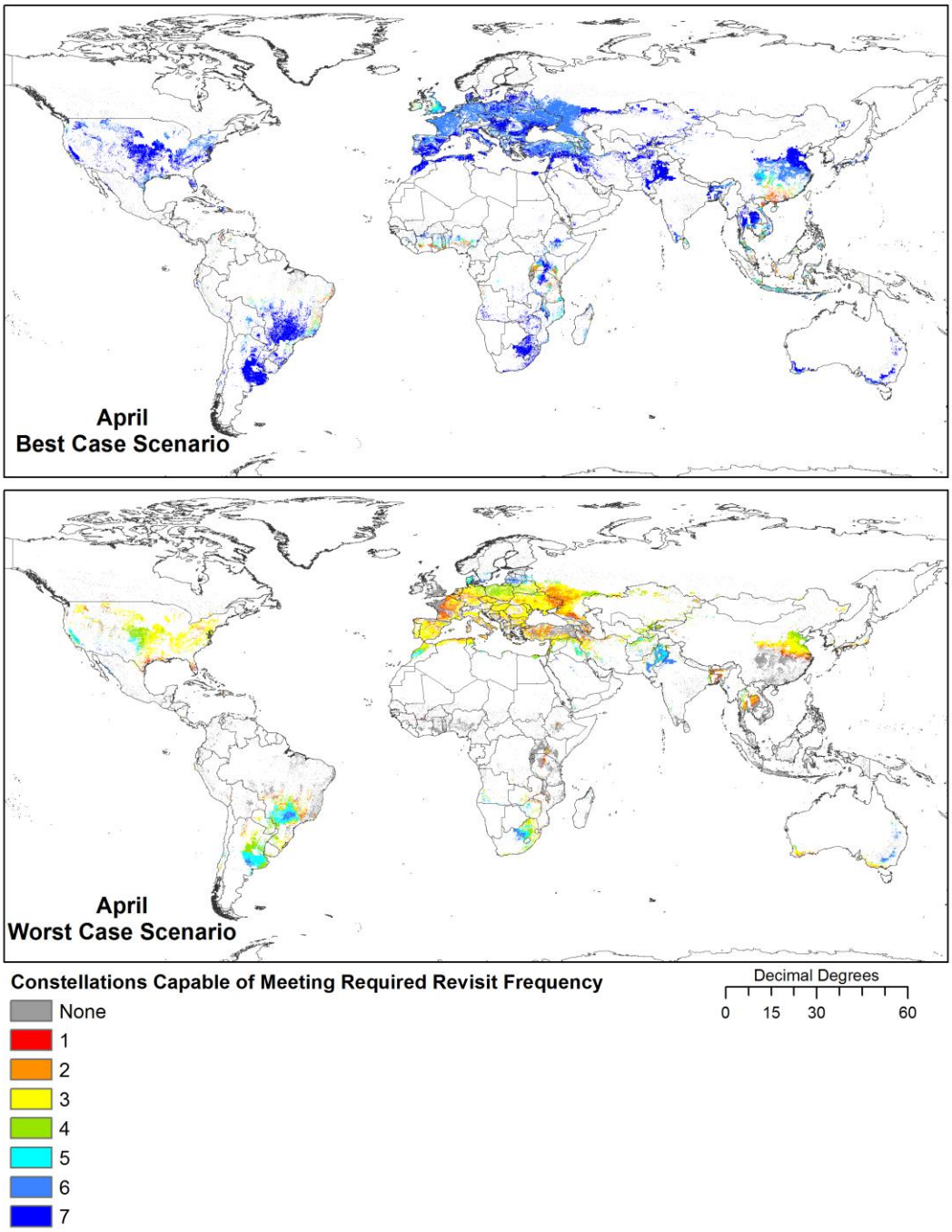

Figure 5.11a-b: Same as Figure 5.8a-b, but for April.

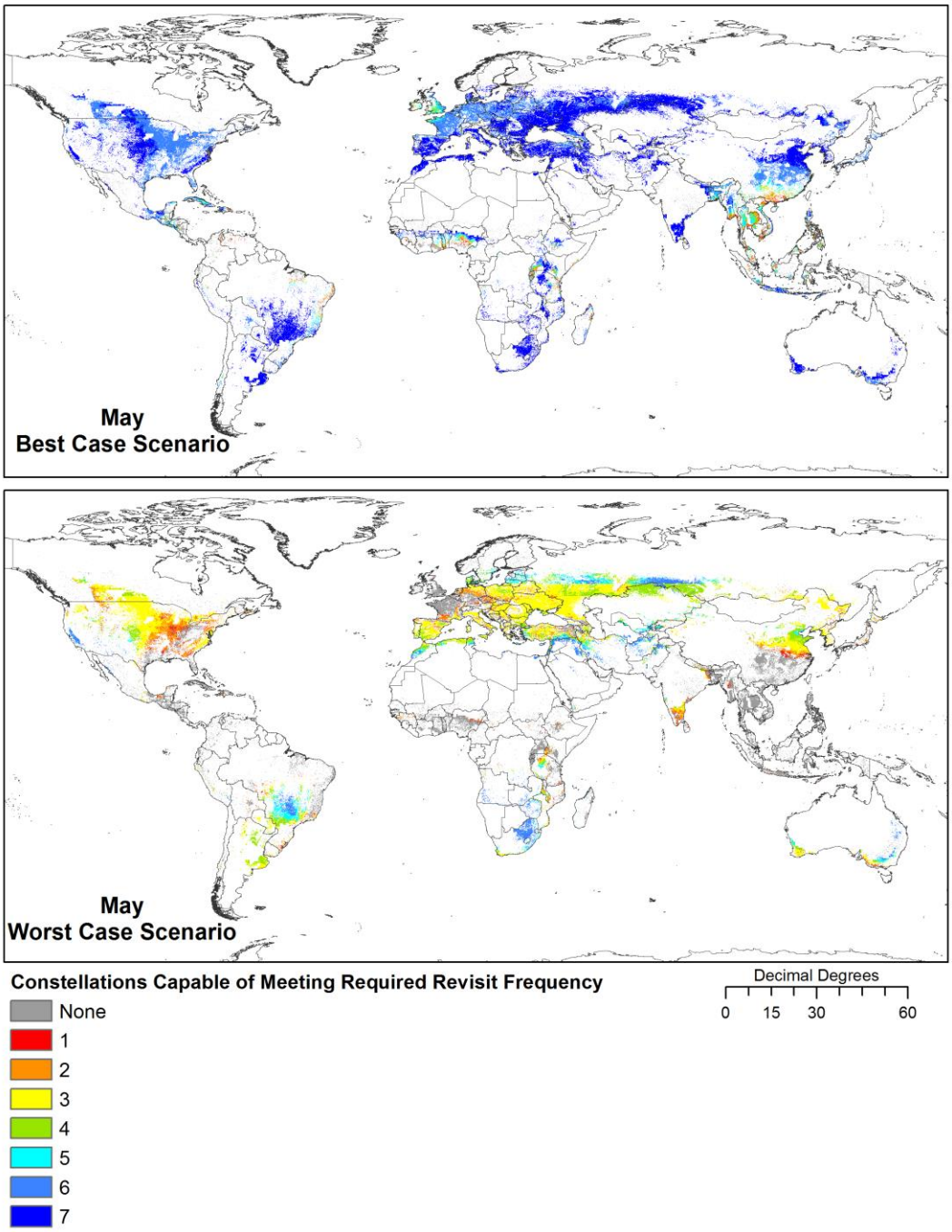

Figure 5.12a-b: Same as Figure 5.8a-b, but for May.

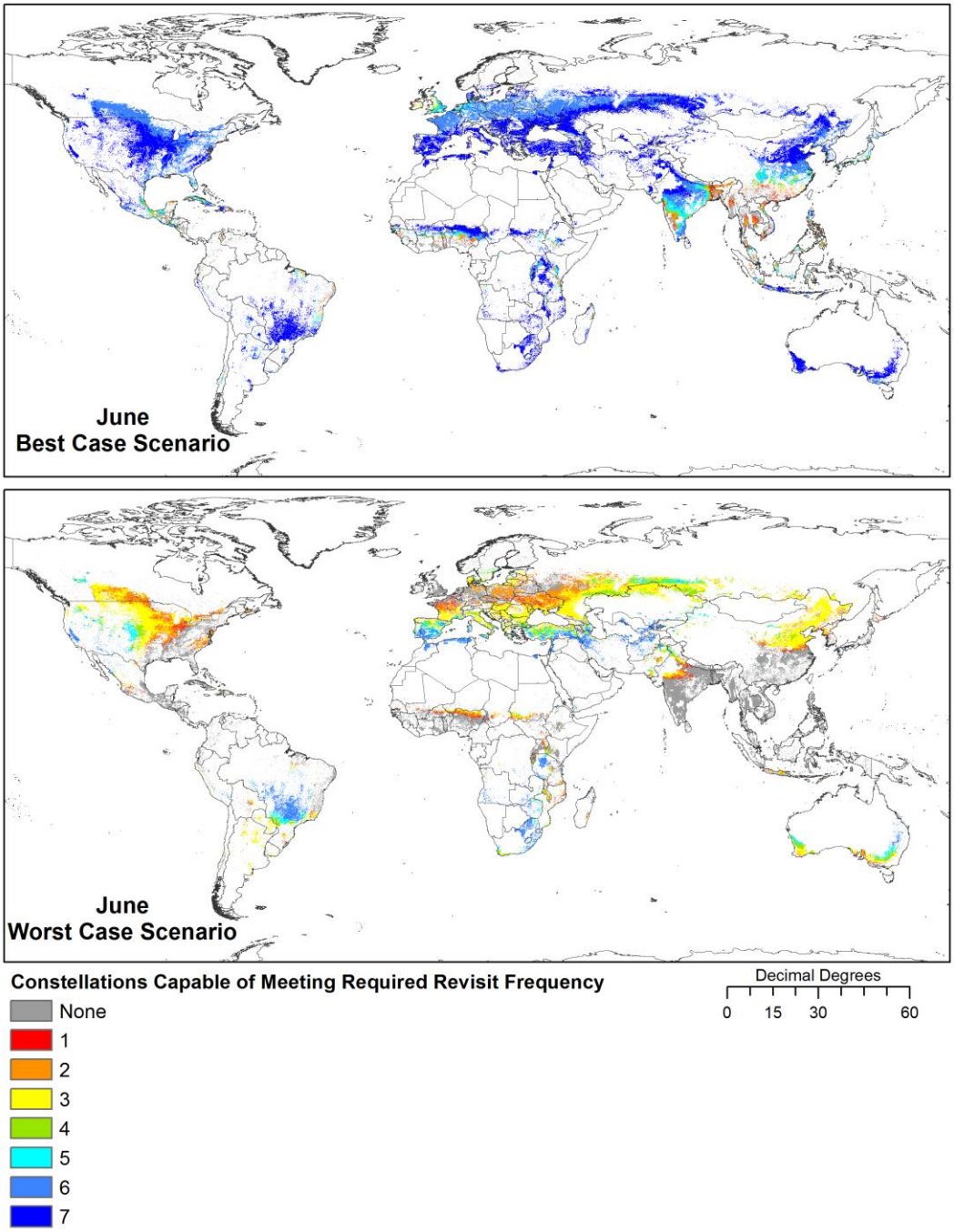

Figure 5.13a-b: Same as Figure 5.8a-b, but for June.

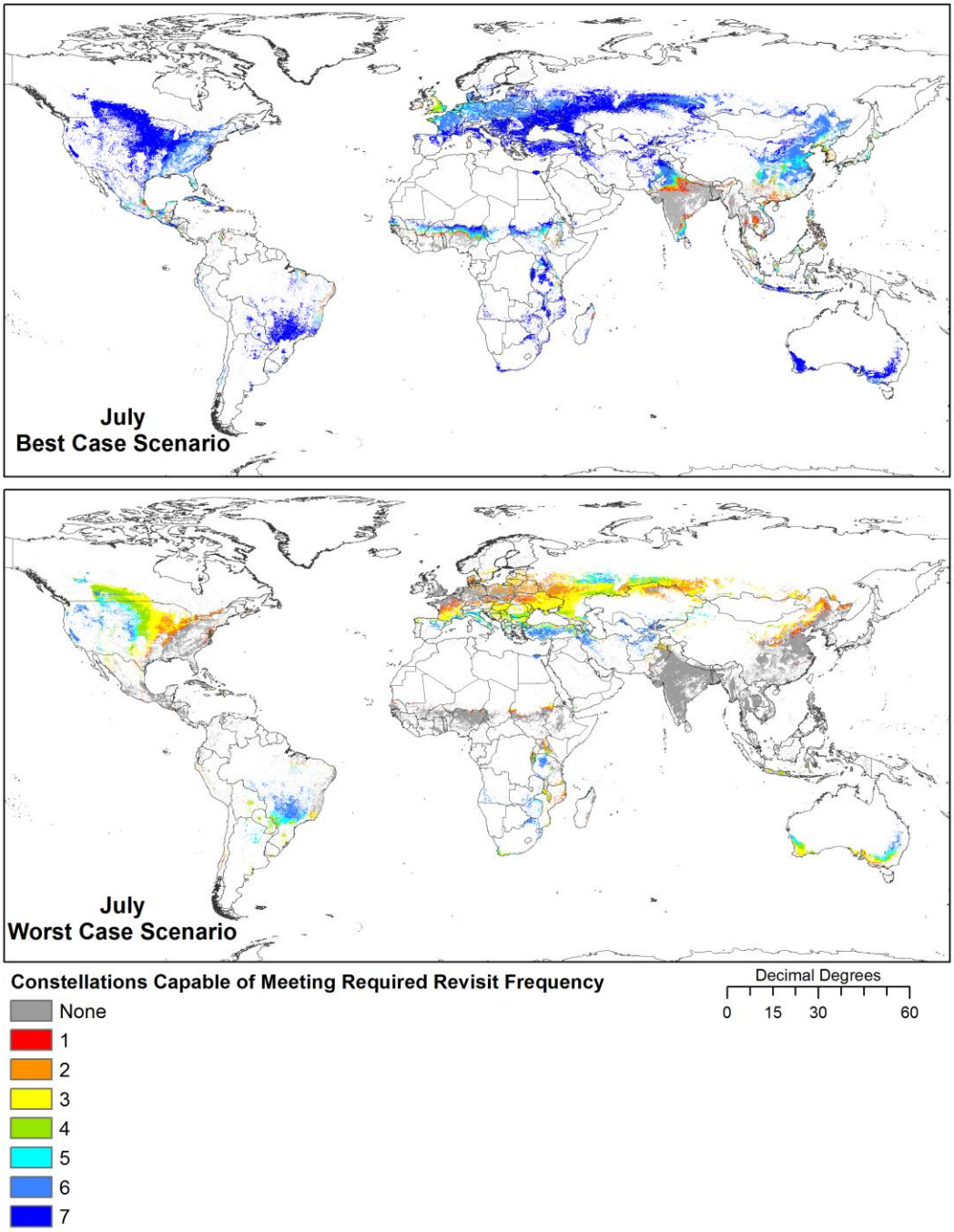

Figure 5.14a-b: Same as Figure 5.8a-b, but for July.

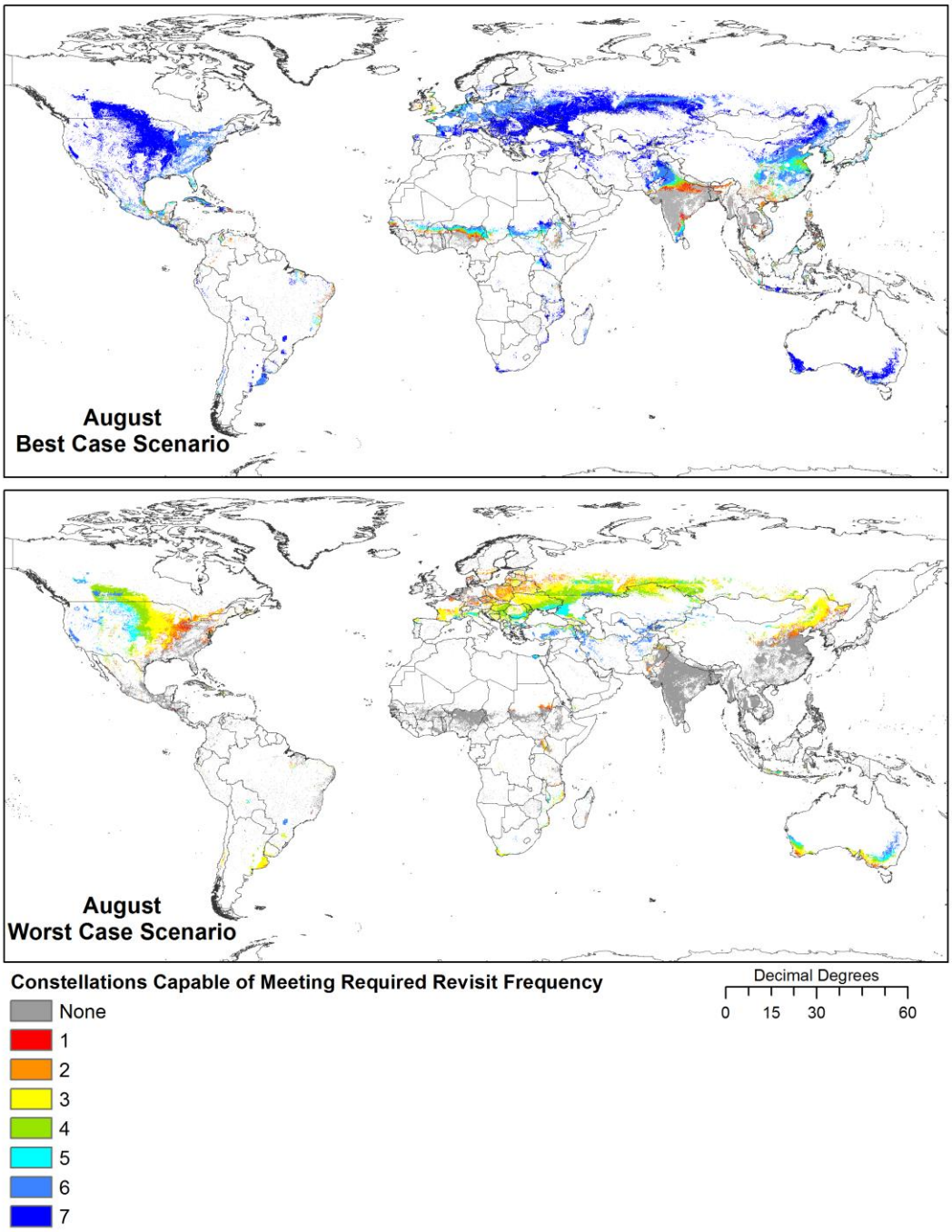

Figure 5.15a-b: Same as Figure 5.8a-b, but for August.

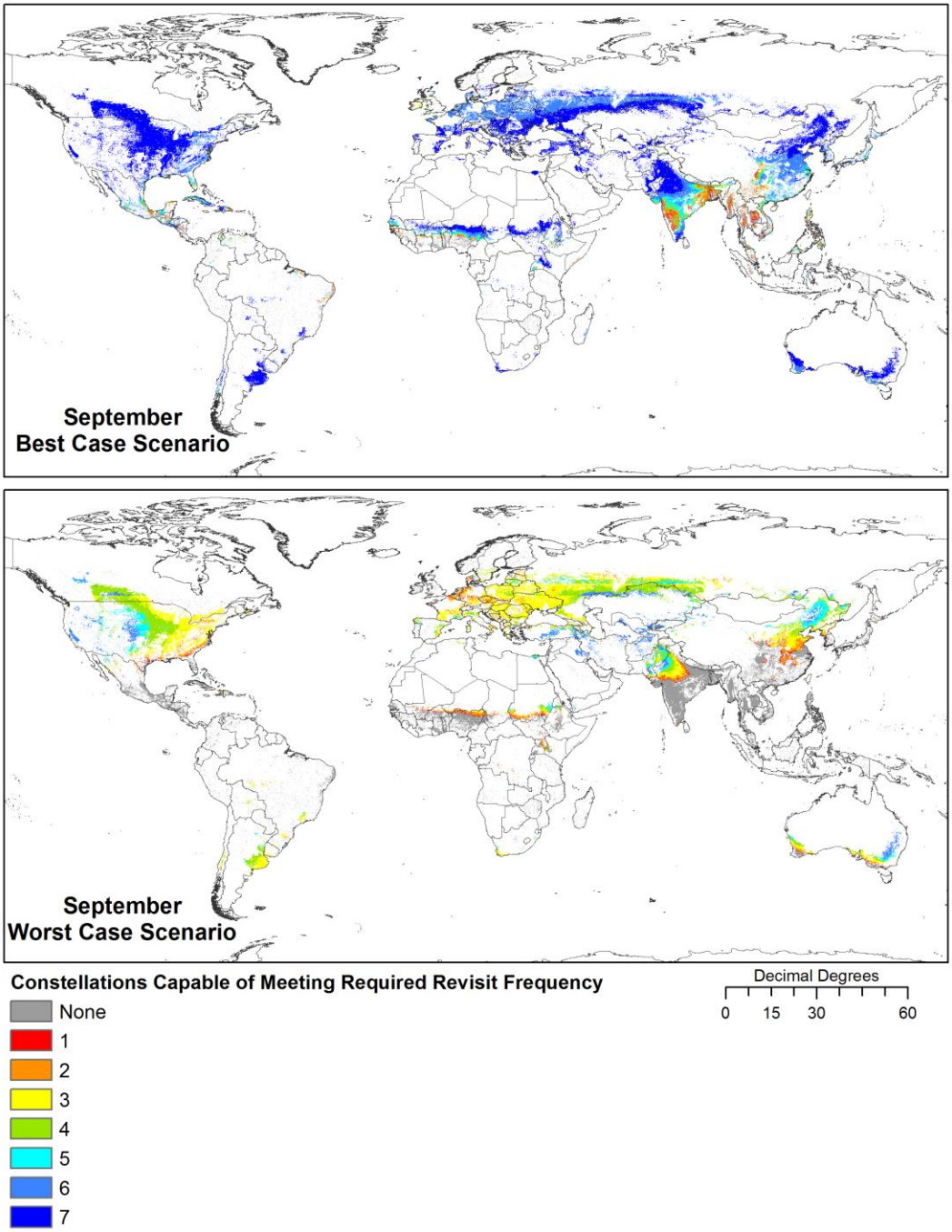

Figure 5.16a-b: Same as Figure 5.8a-b, but for September.

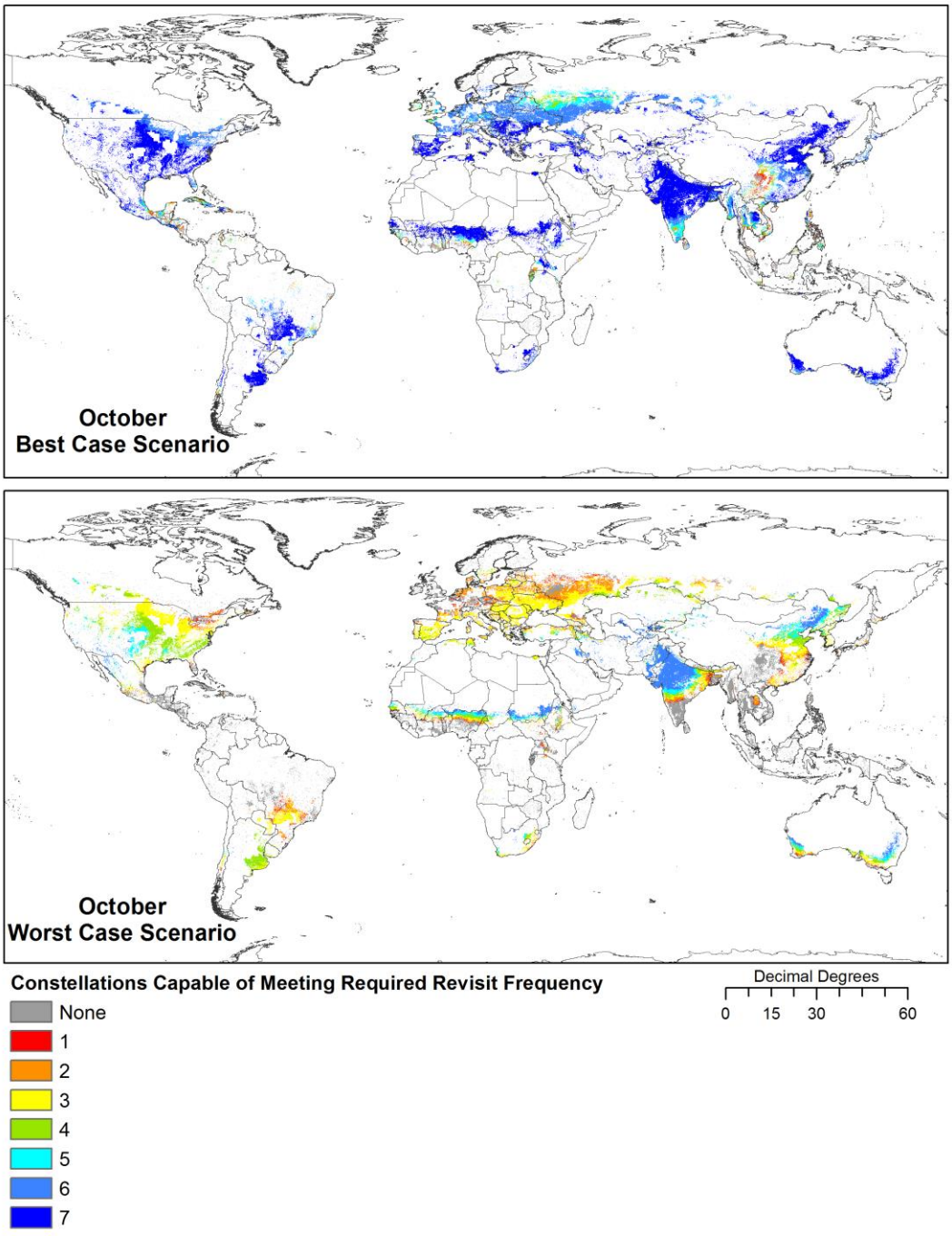

Figure 5.17a-b: Same as Figure 5.8a-b, but for October.

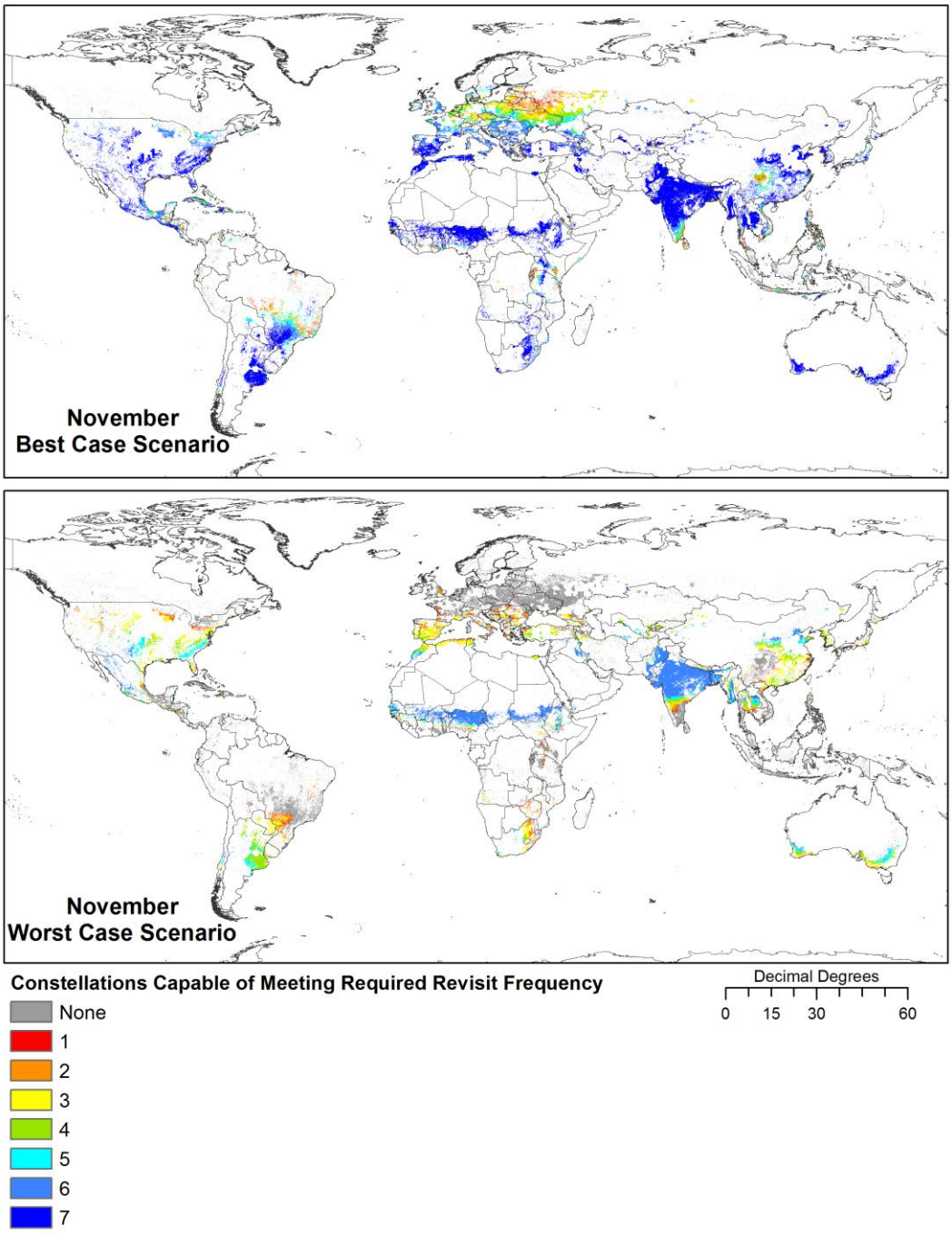

Figure 5.18a-b: Same as Figure 5.8a-b, but for November.

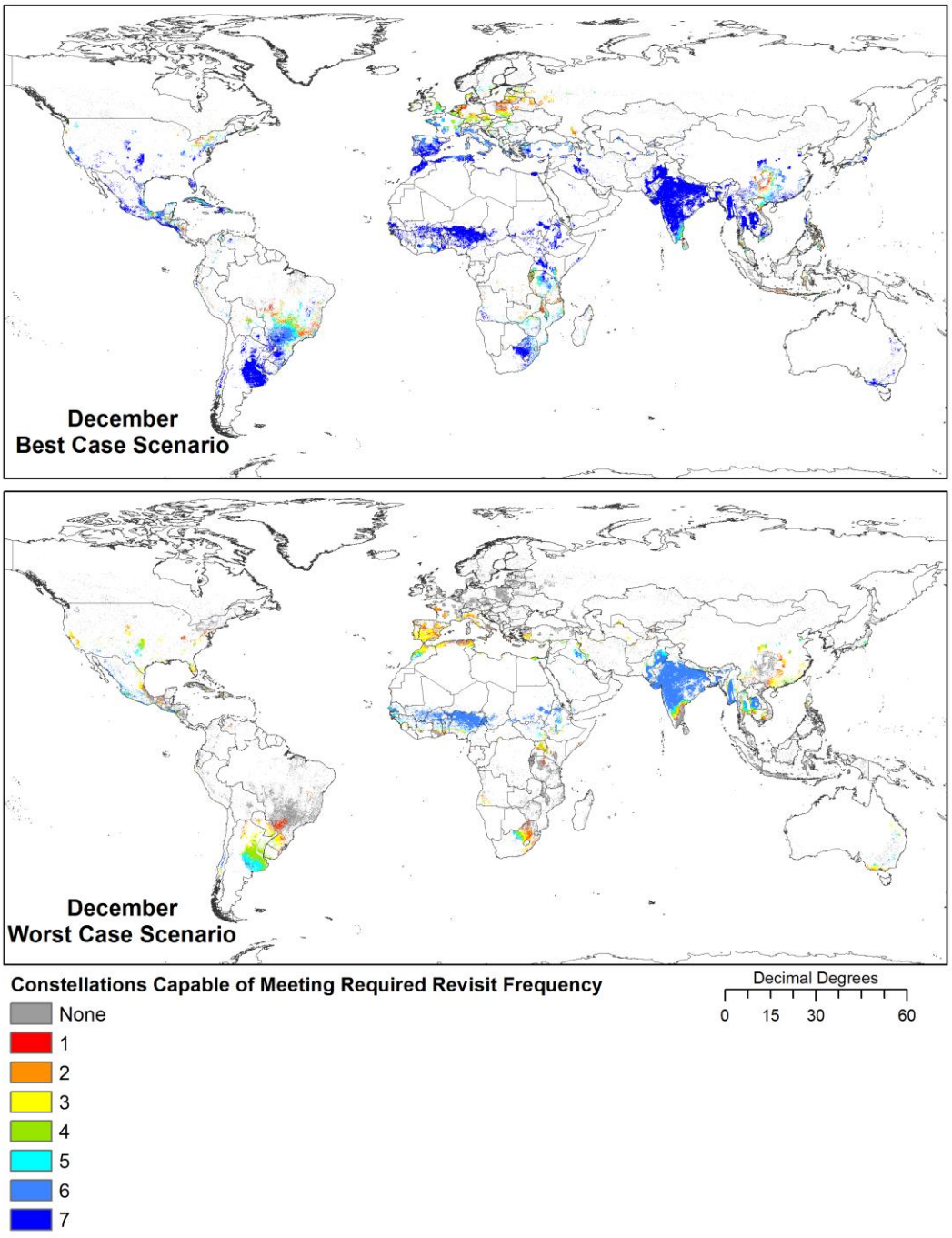

Figure 5.19a-b: Same as Figure 5.8a-b, but for December.

In fact, at the global level, one or more of these constellations is capable of probabilistically meeting an 8 day requirement for at least 70% cloud free data for between 77% (January) and 94% (May) of 0.05˚cells worldwide, assuming the best

revisit frequency (Figure 5.20). With the mode revisit frequency, between 71% and 91% of cells will be at least 70% clear, and between 48% and 76% of cells will probabilistically yield clear views, within 8 days. Meanwhile, assuming the worst revisit frequency, between 47% (January) and 73% (October) of 0.05˚cells worldwide can probabilistically have an 8 day requirement for completely clear data met with one or more of these seven constellations. Interestingly, when comparing these four scenarios, it becomes clear that the largest determinant of any constellation being capable of meeting a requirement is whether that requirement is for completely clear views (CVR) or partially clear views (FPC ≥ 70%), so the present discussion will focus on the best and worst case scenarios, acknowledging that the most likely scenario will lie somewhere between them.

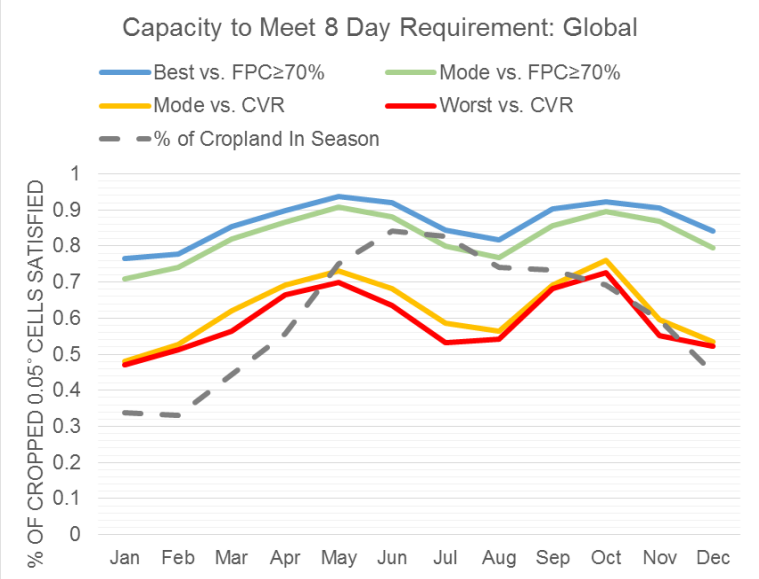

Figure 5.20: The overall capacity to meet an 8 day data requirement, considering different revisit capacities (best, mode, worst) of the constellations versus two acceptable clear view thresholds (70%, 100%). Capacity is presented as percentage of total actively cropped 0.05˚ cells which have their requirements met by at least one constellation. To provide perspective on the extent requiring imagery for each month, also plotted is the percent of cropland in season during each month.

At present (early 2014), Landsat 7 and Landsat 8 acquire the only freely and openly available moderate resolution data. Their combination, Constellation #7, even in the best case scenario can only meet an 8 day revisit requirement in 45-54% of actively cropped 0.05˚ grid cells (Figure 5.21). The addition of a Sentinel mission as in Constellation #6 (or both, as in Constellations #4-5) leads to a marked increase in the success rate in the best case scenario, although Constellation #4 peaks at a 37% success rate in the worst case scenario (Figure 5.22). The added value of Resourcesat-2 in terms of increasing revisit frequency at the global scale is more notable in the worst case than for the best case, where Constellations #1-3 add only a marginal increase in the success rate, while in the worst case, the addition of R2 makes a considerable difference in success rate (peaks at 73%).

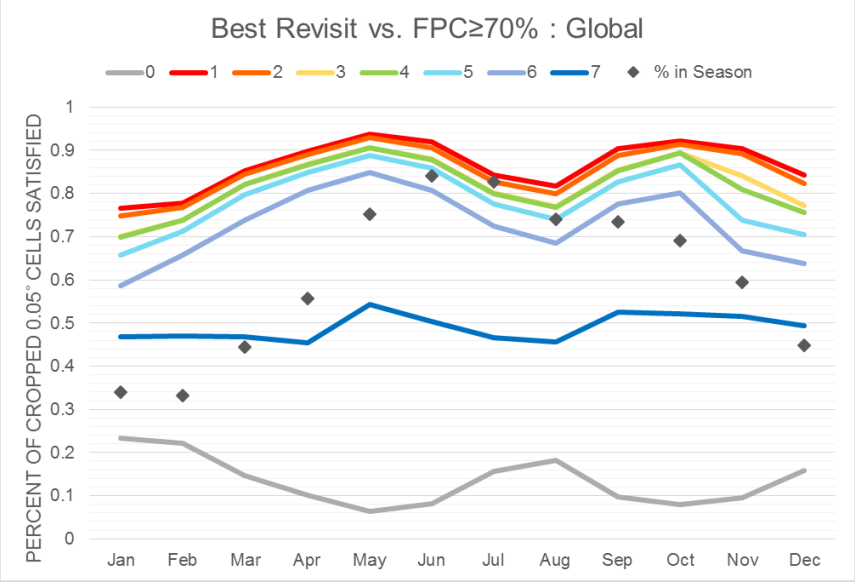

Figure 5.21: Globally, the percent of actively cropped 0.05˚ cells in each month having their requirement for at least 70% views every 8 days met by each constellation's best observed average revisit rate. This is the best case scenario. To provide perspective on the extent requiring imagery for each month, also plotted is the percent of cropland in season during each month.

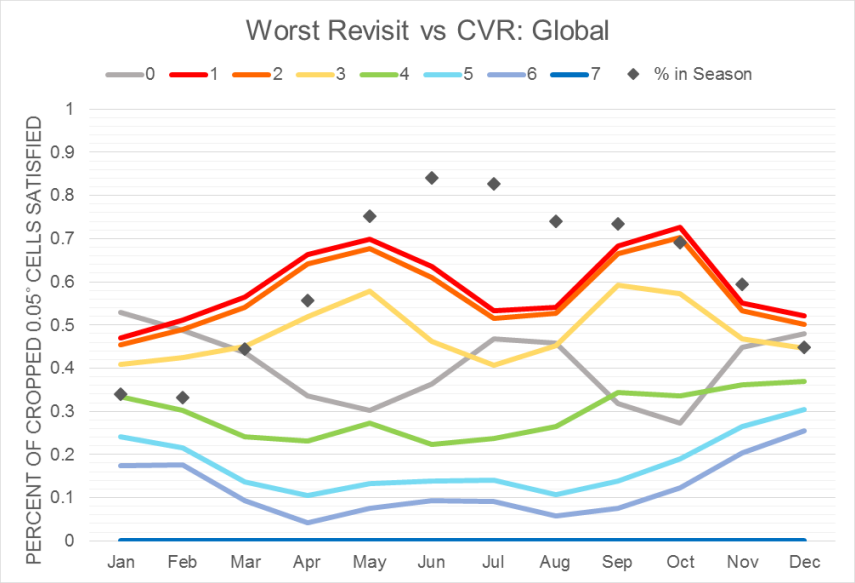

Figure 5.22: Globally, the percent of actively cropped 0.05˚ cells in each month having their requirement for completely clear data every 8 days met by each constellation's worst observed average revisit rate. This is the worst case scenario. To provide perspective on the extent requiring imagery for each month, also plotted is the percent of cropland in season during each month.

These success rates, of course, vary greatly when taking a regional perspective, as cloud cover's impacts on obtaining (reasonably) clear views varies geographically and revisit capability varies latitudinally. Looking at Europe (Figure 5.23), for example, Constellation #7 again has a somewhat low performance, although with larger monthly variability present. The overall success rate in the best case scenario is greatly increased by the incorporation of S2A alone (Constellation #6), with most other months having their success rate only marginally increased through the addition of other sensors. However, if the requirement is for clear views, and the worst revisit rate (which is 8 days – the same as the mode and worst revisit frequencies, and what we typically consider the revisit of the two combined Landsat missions to be) is examined, then Constellation #7 is completely incapable of yielding clear views within 8 days. This is not surprising as having a clear view requirement

exactly match revisit capability would require a 0% probability of cloud presence, something highly unlikely in cropland areas. The worst case scenario again emphasizes the value of adding R2 into an imaging constellation (Figure 5.24), with the most pervasively cropped months (April-October) reaching between 69-91% success rate even with Constellation #1. However, the uptick in cloudiness and subsequent decline the success rate for both scenarios in November may have some impact on end of season harvested area analyses.

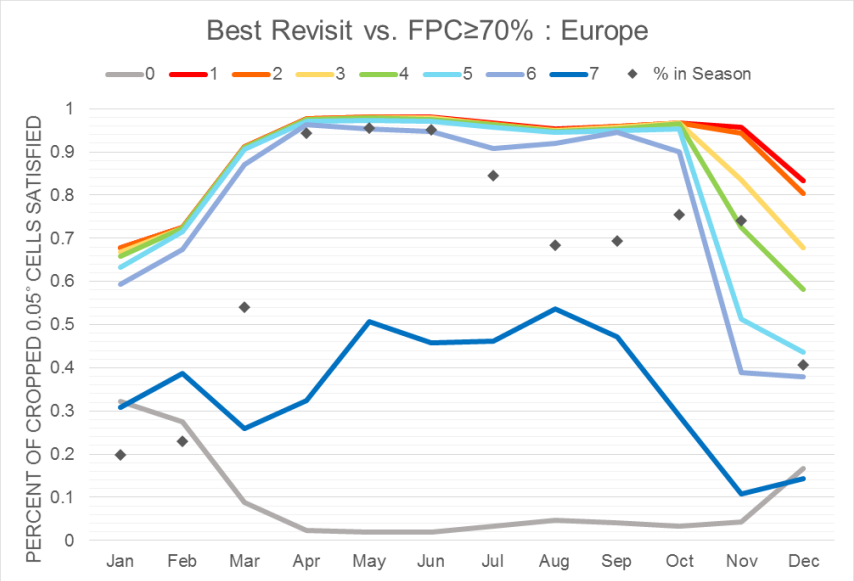

Figure 5.23: For Europe, the percent of actively cropped 0.05˚ cells in each month having their requirement for at least 70% views every 8 days met by each constellation's best observed average revisit rate. This is the best case scenario. To provide perspective on the extent requiring imagery for each month, also plotted is the percent of cropland in season during each month.

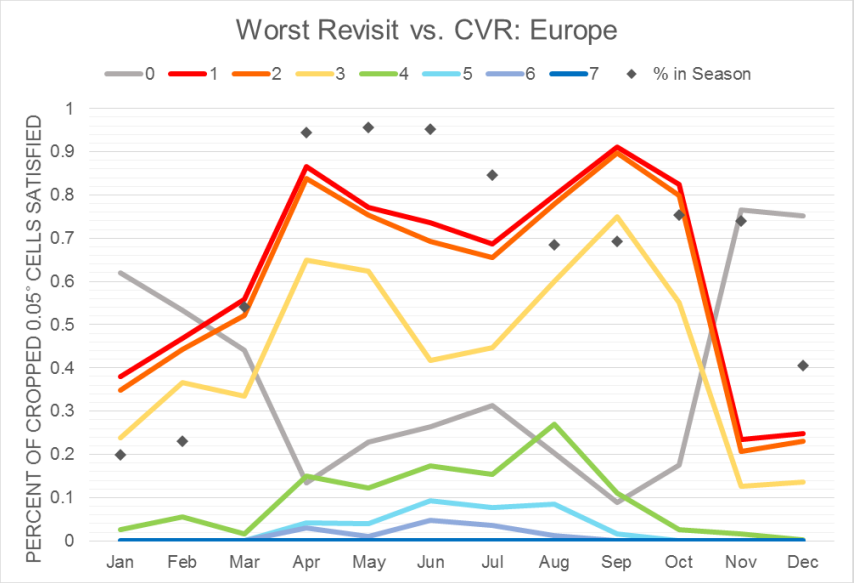

Figure 5.24: For Europe, the percent of actively cropped 0.05˚ cells in each month having their requirement for completely clear views every 8 days met by each constellation's worst observed average revisit rate. This is the worst case scenario. To provide perspective on the extent requiring imagery for each month, also plotted is the percent of cropland in season during each month.

An analysis of south and southeast Asia (including India, Nepal, Burma, Bhutan, Bangladesh, Vietnam, Laos, Thailand, Cambodia, and Malaysia, but excluding China) shows a very large difference between the best (Figure 5.25) and worst (Figure 5.26) case scenarios during the middle of the year (May-October), although the general shapes of the curves are similar. As seen in Figure 5.25, the success rate for the best revisit frequency for even Constellation #1 during July and August hovers around 30%, meaning approximately 70% of actively 0.05˚cells are left without a view that is at least 70% clear. Exacerbating this situation is the fact that July and August are amongst the most pervasively cropped months of the calendar year, meaning these requirements are missed not just at a higher rate but over a larger area. The outlook is even poorer in the worst case scenario, with what amounts to a cease of the utility of these O+TIR constellations between April and

September (although further refining the scale of analysis to the national level, by October much of India has its requirements met (Figure 5.17)).

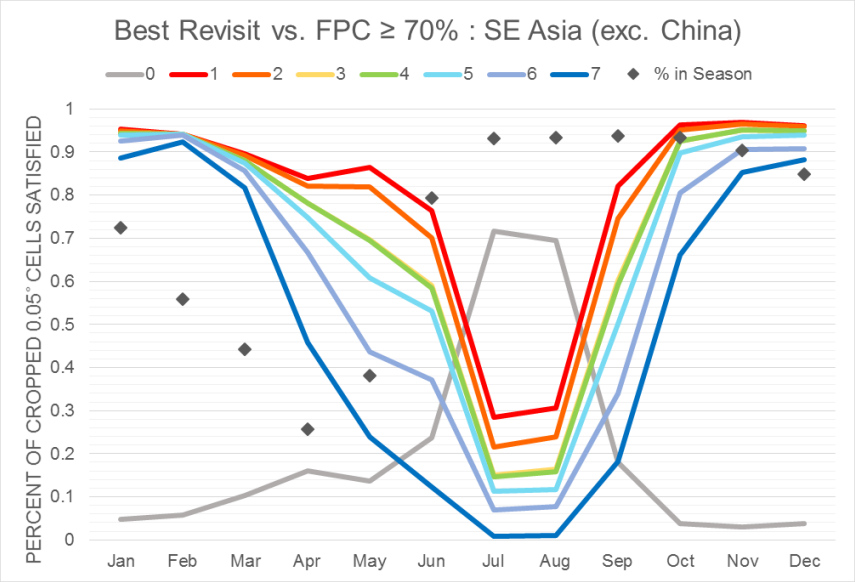

Figure 5.25: For Southeast Asia (excluding China), the percent of actively cropped 0.05˚ cells in each month having their requirement for at least 70% views every 8 days met by each constellation's best observed average revisit rate. This is the best case scenario. To provide perspective on the extent requiring imagery for each month, also plotted is the percent of cropland in season during each month.

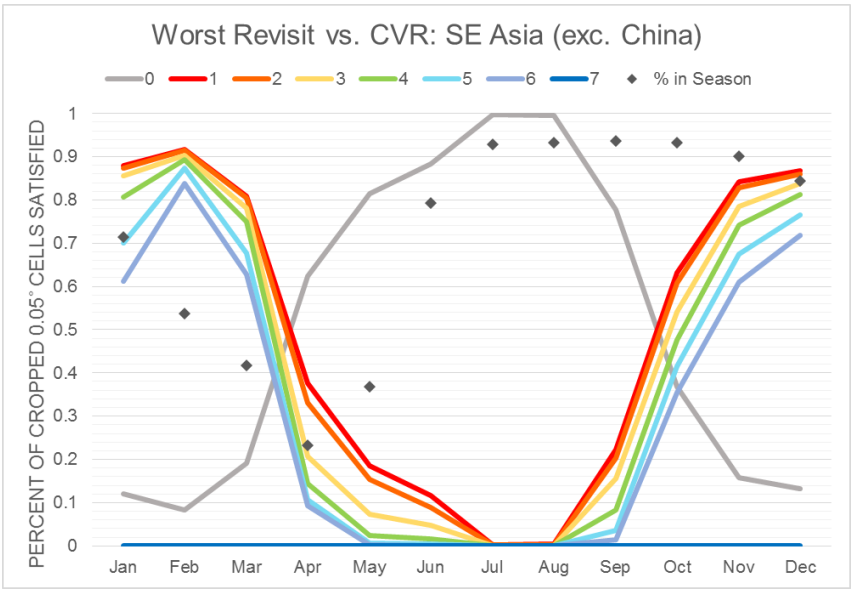

Figure 5.26: For Southeast Asia (excluding China), the percent of actively cropped 0.05˚ cells in each month having their requirement for completely clear views every 8 days met by each constellation's worst observed average revisit rate. This is the worst case scenario. To provide perspective on the extent requiring imagery for each month, also plotted is the percent of cropland in season during each month.

5.3.2 Meeting the Requirement for a Reasonably Clear View every 16 Days

Despite the fact that there is twice the amount of time to obtain an FPC of at least 70%, the overall success rate at the global scale is not that different from the 8 day case discussed in Section 5.3.1. The overall success rate is upped to between 83% (February) and 97% (June), as opposed to between 77-94% with the 8 day data. The largest difference, however, is in the performance of Constellation #7, the two Landsat missions (Figure 5.27). This constellation is capable of meeting 70-90% of requirements for data at least 70% clear every 16 days at the global scale, up from a yearly average of about 50% for 8 day data. Meanwhile, there still remain some 0.05˚ cells for which a requirement cannot be met (3-17%).

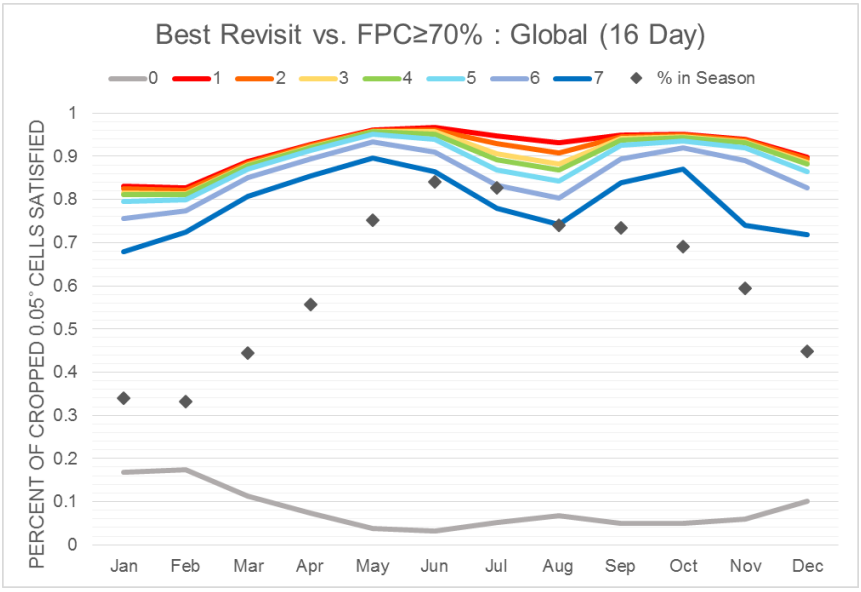

Figure 5.27: Globally, the percent of actively cropped 0.05˚ cells in each month having their requirement for at least 70% views every 16 days met by each constellation's best observed average revisit rate. This is the best case scenario. To provide perspective on the extent requiring imagery for each month, also plotted is the percent of cropland in season during each month.

Meanwhile, for the requirement for completely clear data within 16 days, the largest improvement in success rate relative to the 8 day "worst case scenario" are for Constellations #4-7 (Figure 5.28). Constellation #7 meets 9-29% of requirements, up from essentially 0%. Constellations #5-6 are capable of meeting 41-59% and 46-67%, respectively, of their requirements, each covering 20-52% additional actively cropped 0.05˚ cells with a 16 day requirement relative to the 8 day requirement. Meanwhile, overall success has increased, standing at 60-84%, but still leaves considerable gaps during certain areas during certain times of the year. The gaps in requirements met for both the best and worst case scenarios for 16 day reasonably clear views highlights that some areas are very persistently and pervasively cloudy, and O+TIR missions are simply not well suited for monitoring in these areas/times of year.

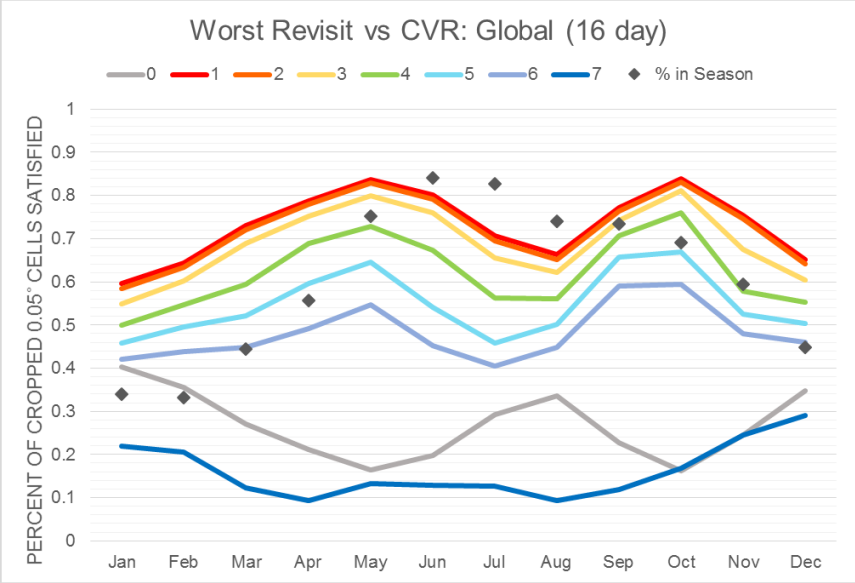

Figure 5.28: Globally, the percent of actively cropped 0.05˚ cells in each month having their requirement for completely clear views every 16 days met by each constellation's worst observed average revisit rate. This is the worst case scenario. To provide perspective on the extent requiring imagery for each month, also plotted is the percent of cropland in season during each month.

5.3.3 Persistently Cloudy Areas: Where Requirements are Unmet

As seen in Figures 5.8-5.26, there are a number of cells/times of year shown in gray (with value "0" or "None") for which none of the analyzed O+TIR hypothetical constellations have a combined revisit frequent enough to meet a reasonably cloud free requirement within 8 days. As seen in the requirements table (Table 4.1), moderate resolution microwave SAR data are required every 8 days in "persistently cloudy areas" (including/in addition to rice cultivating areas), which have been defined herein as those areas and times of year which require a more frequent revisit in order to yield a (reasonably) clear view than our current/planned moderate resolution polar orbiting O+TIR missions are capable of delivering. SAR data are not the only alternative – for example, data from geostationary satellites with multiple

observations per day have been used, but at rather coarse spatial resolution (Duveiller et al., 2013) – but they are currently most broadly available and applied non-polar orbiting moderate resolution data type. Figure 5.29 shows the extent and number of months for which SAR data may be required. In the best case, very few areas require microwave data for more than 3-4 months, with the majority of areas requiring SAR data for 2 months. These areas are concentrated in Southeast Asia, West Africa, and parts of Eastern Europe and the Equatorial Americas. However, in the worst case scenario, the extent of necessary SAR data is expanded both in space and time, with many areas throughout the world requiring more than six months of SAR data. This highlights the potential value of microwave SAR data in a global agricultural monitoring system.

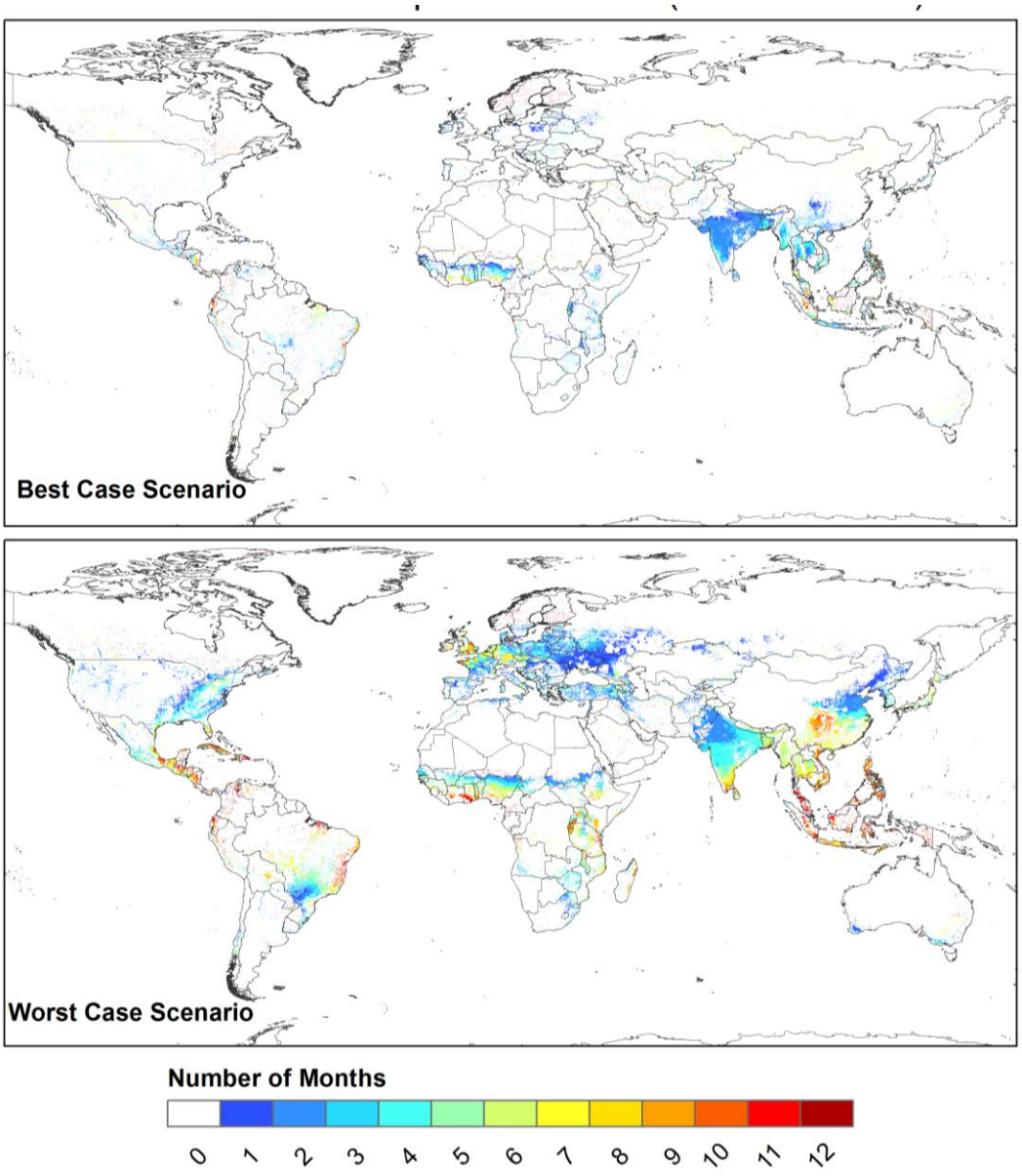

Figure 5.29: For the a) top, best case scenario (best revisit vs. requirement for 70% clear views), and b) bottom, worst case scenario (worst revisit vs. requirement for completely clear views), the number of months throughout the agricultural growing season for which an 8 day requirement cannot be met by any of the seven moderate resolution O+TIR constellations evaluated herein. These areas are too persistently and pervasively cloudy for these systems, and as such, alternatives for monitoring – principally, microwave SAR data (as in Table 4.1, Requirement #6) – should be considered.

5.4 Discussion

There are four primary insights gained from this analysis. First, although rather stringent, the requirement for clear views is not completely unreasonable in some areas during certain parts of the year. However, it certainly requires a constellation beyond that which is currently freely available (Constellation #7), and must be supplemented in other areas/times of year by partially clear views (or non-optical data). Second, accepting partially clear views, as seen in the best case scenario analysis for both 8 and 16 day requirements, provides a promising outlook for the capabilities of our current and near-term moderate O+TIR instruments for many areas throughout the year. Areas wherein clear views are not probable, but at least one constellation is capable of yielding a view that is at least 70% clear, are good candidates for an image compositing approach, although concerns about this approach's likelihood to underestimate the impacts of cloud cover as well as miss changes in crop condition and progress during the compositing period should be kept in mind (Chapter 3).

A third point is that simply adding more sensors does not necessarily improve coverage. At the global level in the case of the 8 day requirement, the two Landsat missions combined (Contsellation #7, the only currently available satellites with a free and open data policy) are capable of delivering views that are at least 70% clear over 45-54% of actively cropped areas throughout the year. The addition of one Sentinel satellite (S2A; Constellation #6) ups the success rate to 59-85%. Adding the S2B in (Constellation #4) increases the success rate to 70-91% with its four satellites. However, the addition of just R2 to the two Landsat missions (as seen in

Constellation #3) results in a practically identical success rate (70-91%) as does Constellation #4 with its four satellites. In fact, R2 has the largest effect on increasing revisit frequency of any single satellite analyzed herein due to its very wide swath, albeit with a relatively lower spatial resolution (56m). What these points suggest is that adding more satellites is not the only way to increase revisit frequency; rather, sensor architecture and alternative designs can and should be considered in the future, although this should be weighed against other factors such as the ground distortion at the edge of wide swath (Verma, Garg, & Garg, 2009).

A fourth finding is that in both scenarios for both the 8 and 16 day reasonably clear data requirement, there are still areas and times for which our current and near-term O+TIR instrumentation cannot yield a sufficient revisit frequency to overcome the presence and pervasiveness of cloud cover. This is related to the third point – space agencies can deploy a veritable cadre of polar orbiting O+TIR missions, but little difference will be made in areas that are frequently and pervasively occluded by clouds. These areas, as shown in Figure 5.27, are poorly suited for polar orbiting O+TIR imaging, and alternative data sources, particularly microwave SAR data, should be considered instead. If willing to accept O+TIR data which are at least 70% clear, that leaves between 6-23% percent of 0.05° cells globally, depending on month, which can be characterized as requiring microwave SAR. However, if clear cells are required, this leaves between 27-53% of cells worldwide, a considerable quantity pointing at the value of investing in research related to using data from alternatives to polar orbiting O+TIR instruments.

5.4.1 Considerations and Limitations

There are a few caveats to consider in this analysis. First, pinning down the exact combined revisit frequency for each constellation is very challenging due to the repeat cycles of each component mission being out of sync with one another. For example, if there are 80 revisits within 120 days, it can only be said that the *average* combined revisit frequency is 1.5 days. All of the satellites discussed herein are sun-synchronous with overpass times at (or projected to be at) 10:30 am, and so a revisit of 1.5 days is actually impossible. How precisely this impacts the success rate is unknown, and merits further research, but is beyond the scope of this analysis.

An additional note is on the spatial unit of analysis: 0.05˚, which translates to about 5.6 km at the Equator. The final percentage clear analysis (FPC) is easily scalable to any unit of analysis, but the clear view requirement (CVR) is intimately tied to this native spatial unit. That is to say, while only 50% of a 0.05˚cells may be capable of meeting a clear view requirement, a finer resolution analysis might increase the apparent success rate. As stated in Chapter 3, the CVR analysis is likely to overestimate the impact of cloud cover, and therefore the worst case scenario analysis herein is likely particularly pessimistic. On the other hand, the constellations rarely deliver their best possible revisit frequency, and assumptions about spatial and temporal correlation within the FPC analysis (Roy et al., 2006) lead to the best case scenario being optimistic. In reality, the type of performance to be expected from current and near-term missions will likely fall somewhere in between these two scenarios.

Finally, it is worth noting that Landsat 7 has had a scan-line corrector (SLC) mirror failure since 2003, resulting in the absence of a considerable amount of data (22%) in stripes throughout the scene (Scaramuzza et al., 2004). The data are still valuable and usable (Maxwell, Schmidt, & Storey, 2007), but this will impact the apparent revisit frequency, because even if the data are acquired (which is not a certitude, as systematic acquisitions are only planned for S2A+S2B), 22% of data will be missing from each L7 acquisition.

5.5 Conclusions & Future Research

The analysis presented herein shows the strength of combining multiple satellite missions to form an imaging constellation. Combining missions from two or three different space agencies leads to greatly improved revisit frequencies and an improvement in our ability to meet our EO requirements for agricultural monitoring, although key gaps exist in pervasively and persistently cloudy regions. Future research might continue the investigation initiated by Gao et al. (2006) regarding the utility of a moderate resolution MODIS type system (with daily or even twice daily revisit capability) for meeting EO requirements for agriculture and other societal benefit areas. Such a revisit frequency could prove particularly useful for yield forecasting with its reliance on very frequent data, but it is possible that an investment in such a system would experience diminishing marginal returns due to persistent cloud cover. For this reason, an increased investment in SAR systems and related algorithm development would be well-placed, as would a continued focus on SAR-optical data fusion (Hong et al., 2014; Torbick et al., 2011).

Lastly, it is important to reiterate that an acquisition opportunity, as shown in this analysis, is just that – an opportunity, but not a *fait accompli,* in terms of acquisition or in terms of data availability. To date, agricultural analysts in many parts of the world have been hesitant to rely more fully upon a remote sensing based monitoring system due to concerns about data access, availability, interoperability, and continuity. Systematic acquisitions over actively cropped agricultural areas as well as a policy which guarantees continuous access to high quality, interoperable data are essential in the effort to meet EO requirements for agricultural monitoring (Atzberger, 2013).

Chapter 6: Discussion, Conclusions, & Future Research

6.1 Overview & Main Findings

This research has provided new findings describing the temporal, spatial, and spectral resolution Earth observations requirements for a variety of agricultural monitoring applications. Each subsequent chapter in the work has built upon the previous contribution, first detailing the formulation of the requirements and generation and assemblage of supporting datasets, and then assessing our current and planned capabilities for meeting the 8 and 16 day reasonably clear view requirements for moderate spatial resolution optical plus thermal data. Ultimately, it has provided spatially explicit insight into where, when, and how frequently we require different scales and types of data as well as information on where and when our O+TIR instrumentation is insufficient and alternative data types must be considered instead. This work has provided baseline results and key inputs into an image acquisition strategy for global agricultural monitoring

This dissertation began by taking ten years of MODIS Terra surface reflectance (MOD09) data converted to NDVI together with a variety of cropland masks, and extracted the timing of the agricultural growing season, including the phenological transition dates start of season, peak of season, and end of season for cropped areas around the world at 0.5˚ (Chapter 2). Preliminary comparison against existing crop calendars and crop progress data from USDA-NASS for the CONUS, as well as vetting with regional agricultural experts indicate that this approach has characterized cropland phenology well. This spatially explicit information on the

timing of the AGS – herein referred to as "growing season calendars" – breaks down the calendar year into periods during which different types and frequencies of EO data are required, with more frequently sampled data required during the AGS than when crops are out of season (Table 4.1). Next, the impact of cloud cover frequency and amount on passive O+TIR remote sensing instruments' capability throughout the AGS to obtain reasonably clear views of the Earth's surface was analyzed. Toward this end, daily cloud flags from MOD09 from 2000-2012, compiled to show average daily cloud presence probability (*P*(cloud)) and daily cloud extent (APCloud), were averaged over different segments of the AGS based on the PTDs described in Chapter 2. It was shown (Chapter 3) that the early and middle portion of the AGS experience both more frequent and more pervasive cloud cover at nearly every latitude, that high cloud amount/frequency often coincide with broad cropland cultivation, that the morning is generally less impacted by cloud cover than is the afternoon, and that cloud occlusion is a factor that must be considered when articulating temporal resolution requirements for O+TIR data.

General data requirements were characterized in Chapter 4 in Table 4.1. The table described the necessary spatial, spectral, and temporal resolutions for data to be used as inputs for a variety of agricultural monitoring applications including crop area, type, calendar, condition, yield, biophysical variables, and practices, as well as general environmental variables. These descriptive requirements were placed concretely in the spatial context (Chapter 4) through the inclusion of the growing season calendars from Chapter 2 (*when to image*), a "best available" cropland mask (Fritz et al., 2013) and field size distribution layer (Fritz et al., unpublished; *where*

[fine vs. moderate vs. coarse] data are required), and the cloud cover information from Chapter 3 (*how frequently to image*). This latter input revealed the *actual* temporal resolution (revisit frequency) that would be required in order to probabilistically yield a reasonably (≥70%) or completely clear view within a given time period during each month for actively cropped areas at 0.05˚, providing a "best" and "worst" case scenario for revisit frequency required. In this chapter, the minimum (16 day) and preferred (8 day) requirement for reasonably clear moderate spatial resolution data (Table 4.1; Requirement #5) were introduced. The 8 day reasonably clear view requirement was specifically highlighted, as agricultural monitoring scientists and practitioners have indicated that increased *effective* temporal resolution (rate of reasonably clear views) at moderate resolution (10-70m) is paramount in operational agricultural monitoring. This analysis showed that if data that are at least 70% clear are required within a given period, then 44-55% of global cells require a revisit frequency less than half the length of that given period (i.e. <4 days for 8 day and <8 day for 16 day reasonably clear view), although between 22-31% of cells could be satisfied by only a single revisit within the given period (i.e. every 8 or 16 days, respectively). The revisit frequency required to yield a completely clear view, however, was less than half the length of the total period in 74-92% and 67-92% of actively cropped 0.05˚ grid cells, for 8 day and 16 day periods, respectively, and in practically no location would just a single revisit be sufficient to probabilistically yield a completely clear view.

However, there remained the question of whether our current and near-term planned moderate resolution instruments would be capable of a revisit frequent

enough to meet these actual temporal resolution requirements. Chapter 5 responded directly to that by comparing the requirements articulated in Chapter 4 with seven hypothetical multi-mission, multi-space agency moderate resolution constellations based off of five instruments. These analyses, in the end, confirmed the long-held notion that no single mission is capable of delivering high quality data at the regional or global scale at a revisit rate frequent enough to be used for agricultural monitoring applications which rely on phenological tracking (e.g. crop type or yield). It showed that two Landsat missions together, with a revisit of 8 days, are capable of yielding views that are at least 70% clear for between 45-54% (depending on month) of actively cropped 0.05˚ grid cells for an 8 day requirement and 70-90% for a 16 day requirement. Meanwhile, the two Landsat missions were completely incapable of meeting a clear view requirement anywhere during any month of the year for the 8 day requirement, although for 9-29% of actively cropped 0.05˚ cells, the two sensors could probabilistically yield a completely clear view within 16 days. However, the addition of missions from other space agencies, namely Resourcesat-2 AWiFS, Sentinel-2A, and Sentinel-2B, could result in 77-94% of actively cropped areas being at least 70% clear, and 47-73% of areas being completely clear, each within 8 days (83-97% and 60-84% for 16 days, respectively). It also showed that these success rates are regionally and seasonally variable, with certain areas having some imaging requirements met throughout the year and others (particularly Southeast Asia, West Africa, Northern Europe, and the Equatorial Americas) facing such total cloud obscuration during certain parts of the year that O+TIR data are rendered practically useless for agricultural monitoring purposes. There remained 6-23% or 27-53% of

areas for which no hypothetical polar orbiting O+TIR imaging constellation was capable of yielding a reasonably clear view within 8 days. These are areas/periods of time for which alternatives to polar orbiting O+TIR data should be considered, particularly microwave SAR or possibly geostationary O+TIR instrumentation.

6.1.1 Implications

This research provides concrete evidence for an imaging constellation approach to moderate resolution remote sensing, enlisting multiple missions and even multiple spectral ranges of data to form an integrated monitoring system. Specific to agriculture, neither the problem of food insecurity nor the impact of increased agricultural market volatility are likely to disappear. As such, it is crucial to acquire EO data of sufficient quantity, quality, and accessibility to generate informational products about local, regional, and global food supply. This research has shown that neither at present, nor in the near term, are we capable of meeting at the global level *all* requirements for the reasonably clear 8 or 16 day moderate spatial resolution O+TIR data which would be used across all monitoring activities: crop area, type, calendar, yield, condition, biophysical variables, or system. Fortunately, through an imaging constellation approach as proposed and demonstrated in Chapter 5, we would be able to meet the requirements for a great majority of cropped areas, a promising finding for the generation of regional results.

There are some areas of the world and times of year for which cloud cover is simply too pervasive and persistent to be monitored by O+TIR data, and this research has highlighted with a high degree of spatial precision (0.05˚) where those areas and times of year lie. Through the incorporation of microwave SAR data with cloud

penetrating capabilities, these persistently cloudy areas could be monitored as well, providing the opportunity for consistent regional to global scale results. Such a constellation approach, however, would require considerable data coordination (Section 6.2.1).

Beyond this broader implication for agricultural monitoring using satellite EO, this research responds to a long-standing need for spatially explicit cropland phenology information through the generation of 0.5˚ agricultural growing season calendars (Chapter 2). While these GSCs are still in the process of being thoroughly vetted by regional agricultural monitoring experts, their comparison against known crop calendars in the corn and soy cultivating Corn Belt of the CONUS, their sensitivity to interannual and within region variations in growing season timing, as well as their approval by experts from Australia, Canada, Argentina, Uruguay, Ukraine, Spain, and Russia, all point to a successful product.

6.2 Considerations and Future Research

At present, a major dearth in agricultural monitoring is spatially explicit crop specific phenology and interannual variability, their absence being the largest source of uncertainty in a number of agricultural monitoring applications (Wu et al., 2013b). The growing season calendar methodology presented in Chapter 2 has been developed in such a way that it could be adapted to generate spatially explicit crop specific calendars at whatever spatial resolution desired. This activity would require crop specific masks, something that is presently being developed for the major crops (wheat, rice, corn, and soybean) in the context of GEOGLAM at the MODIS resolution for many areas around the world.

Not analysed herein is the capability of coarse, fine, or very fine spatial resolution optical systems to meet the requirements established. As discussed in Chapter 5, the major area for improvement, both in terms of available systems and the magnitude of science and operational monitoring results, is in moderate spatial resolution remote systems. In the case of coarse data (>100m), there are already a number of systems in place or planned that have (near) daily temporal resolution, such as MODIS Terra/Aqua, S-NPP and JPSS VIIRS, SPOT-5 VGT-2, Sentinel-3A SLSTR, and Proba-V VGT-P. Several of these have or plan to have free and open data policies, and so as long as the spatial, spectral, temporal, and radiometric quality of these missions are maintained, the requirements can be met, although efforts at enabling interoperability are crucial as well. Meanwhile, in the case of fine (5-10m) and very fine (<5m) spatial resolution data, despite the pointing capabilities of the sensors and the resultant relatively frequent revisit rate possible (on the order of 1-5 days), there is still uncertainty about whether or not these systems can deliver such a frequent revisit rate in multiple areas at the same time , or if acquisitions in one area would come at the expense of another. An evaluation of these capabilities and potential trade-offs would prove useful and valuable. Additionally, these fine and very fine data are entirely fee based, and a cost-benefit analysis of the areas wherein this considerable financial investment could be best placed, in light of cloud cover constraints and the degree of spatial heterogeneity of the landscape (Duveiller & Defourny, 2010), would be beneficial.

Herein, “reasonably cloud free” has been taken to mean at least 70% cloud free/clear. This means that as much as 30% of a view may be occluded by clouds, and

as briefly discussed, this may be too great an amount for certain monitoring applications. Future research should investigate the utility and limitations of different acceptable thresholds of cloud cover (including the 70% threshold), particularly in the context of the specific agricultural monitoring applications listed in Table 4.1. Different agricultural monitoring applications may tolerate different quantities or frequencies of cloud cover, and research should be conducted to analyse how these variable cloud cover amounts impact the production of each target product.

In this vein, a useful area of future research would be to analyse the requirements for each target product (moving down the columns in Table 4.1) rather than to analyse the requirements for each data type (moving along rows in Table 4.1), as is presented in this dissertation. It would be useful to understand how close we are to meeting the data requirements to derive crop yield versus cropland mask, and so forth. Identifying which *thematic* and *geographical* areas will probabilistically not have their requirements met will identify important paths and areas for research. Simply stating that requirements cannot be met is insufficient – but identifying gaps will pave the way for the research community to develop new methods of working with the data to which we do have access.

There are three main aspects of EO requirements which are not at present discussed in this work or articulated in the requirements table (Table 4.1). First, there is no mention of radiometric resolution in the requirements table, largely because the assumption is that the current standard of systems with 8-12 bits radiometric resolution will be maintained from here forward. However, if alternative sensor architecture is considered (as mentioned in Section 5.4) to improve temporal and/or

spatial resolution of an Earth observing instrument, this may come at the cost of other elements of the instrument in order to reduce data volume. It would be worthwhile, then, to explicitly outline the minimum precision for each requirement/agricultural monitoring application. Second, Table 4.1 also neglects to explicitly mention the EO specifications for the spectral bands which are needed to atmospherically adjust the data. This requirement is not included explicitly as the initial formulation of the requirements considered only data directly used to extract crop specific parameters. In general, and since the early days of the Landsat program, the spectral band placement for moderate resolution EO systems has been made for the purpose of vegetation discrimination and monitoring in mind (Goward & Williams, 1997; Mika, 1997). However, the absence of well-placed spectral bands (both in the cloud screening process [e.g. cirrus, thermal bands], and vegetation discrimination [e.g. red edge]), would greatly impact the accuracy and reliability of derived informational products, and as such there is already discussion within the CEOS Ad Hoc Team for GEOGLAM to correct this omission.

Third, the requirements table identifies the need for SAR data, but that is a broad category with a range of additional instrument specifications possible. At the outset of the observation requirements development, there was some discussion about the polarization and specific radar bands desired, but the group acknowledged that more research was needed. Early research has shown both C-Band multi-polarization SAR data fused with optical data as well as C-Band and L-Band SAR-only analyses to be useful for crop type discrimination (McNairn et al., 2009a, 2009c; Torbick et al., 2011). In light of the barrier that cloud cover provides for optical imaging

(Chapters 3-5), further research into the utilization of SAR data on its own, as well as its fusion with optical data, for agricultural monitoring purposes would be very well placed. This research and development of SAR data methodologies and algorithms should be conducted in a variety of agricultural systems and for different crops, as applicability of the data is expected to change with the specific landscape under study.

6.2.1 From requirements to data acquisition: strategic considerations

These requirements will require updating over time to keep pace with agricultural land use change and shifting "best practices" for agricultural monitoring. The former case requires an updating of base layers, primarily the cropland masks and field size information, but also growing season calendars, tasks that will become more easily implementable due to the increased quantity of VFTM EO data that are purported to be made available through the acquisition strategy into which this thesis provides input. In fact, the data requested by the requirements table themselves are meant to be used to generate crop area and crop type masks, as well as crop calendars, and so updating could be done on a yearly basis in highly dynamic areas. The purported increase in access to high quality data may also impact the rate at which methodologies to monitor agriculture evolve (which may impact the data requirements), as will the expanding breadth and depth of EO-based agricultural monitoring expertise.

When these EO requirements are converted into a strategy, there may be a few ways to optimize them. First, as seen in the requirements table (Table 4.1), there are certain spatial/spectral ranges that occupy two separate records (e.g. Requirements

#4-5, Requirements #7-8) due to variable extent and effective temporal resolutions. Requirement #5, for example, asks for 10-70m O+TIR data roughly weekly (no more than 16 days) on a sampled (prefer cropland extent) basis. With a higher temporal resolution (although potentially for only a subset of areas), this requirement could satisfy part of Requirement #4. The same is true of Requirement #8 partially satisfying Requirement #7. Through harmonizing these requirements, the overall quantity of data needed would be reduced.

A second factor which merits further investigation when translating the requirements into actual data acquisitions is whether and where requirements could be smoothed spatially to reduce power cycling burden for remote sensing devices. For example, if there is a small strip in the along-track direction that is out of season between two areas which are in season, it may make sense to acquire data for that intermediate strip as well. Similarly, if a small area is in season surrounded by many areas which are out of season, it may be worth performing a cost/benefit analysis of acquiring that data versus power cycling impacts on the sensing device.

Third, at present, the requirements are considered as necessary from the SOS to EOS. This makes logical sense for spring and summer crops that grow without interruption, however for winter crop cultivating areas, there is often a period after the SOS during which a plant becomes dormant and active generation of above ground biomass temporarily ceases (Miller, 1999). During this period, it is not clear that there is a need for image acquisitions, and removing these from the analysis would potentially improve the apparent success rate (Chapter 5) and would certainly reduce the total number of acquisitions needed.

6.2.2 Uncertainty and error quantification

Not included in this dissertation is the quantification of error in these analyses. Each chapter builds upon the work of the previous, with the error propagating throughout, and as such, future work should quantify the error both within each analysis as well as how it propagates through into the final products (Chapters 4-5; Congalton et al., 1991). Ultimately, two of the most important questions to answer are: a) *how likely is it that the revisit frequency required (as articulated in Chapter 4) will return a (reasonably) clear view every 8 or 16 days?;* and b) *how accurate are the success rates presented in Chapter 5?* Answering such questions is beyond the scope of this immediate research, although identifying the sources of error is an important first step.

The sources of error in Chapter 2 come from errors in the cropland masks used which may result in the inclusion of non-crop pixels in the aggregation process, and their signals' consideration in the derivation of the PTDs. Error in the GSCs comes also from the PTD detection algorithm itself, which assumes a given threshold of the NDVI can be attributed to non-crop background vegetation (e.g. weeds), and which allows for the mixing of multiple crop types within each 0.5˚ cell. While 10 years of dates (2001 through 2010) were detected for each season, a median was extracted and used in Chapters 3-5. Land cover or land use change that may have occurred during those years could provide a source of error in subsequent chapters as well.

In Chapter 3, as briefly discussed, error will come from the MODIS surface reflectance flags themselves, although they have been extensively validated

(Kotchenova, Vermote, Matarrese, & Klemm Jr, 2006; Kotchenova & Vermote, 2007; Vermote & Kotchenova, 2008).These analyses are based on 10-13 years, which is a relatively short record as clouds do experience interannual variability. The extent to which this subset of time is representative of cloud cover conditions moving forward is also a source of uncertainty. This analysis is particularly vulnerable to resolution dependent error due to both the initial resolution of the base data (1 km) as well as the resolution of analysis (0.05˚, or 5.6 km at the Equator). In the *P*(clear) analysis, the aggregation from 1 km to 0.05˚ based on a binary cloud/no cloud distinction means that it is possible to have *P*(clear) be zero, but cloud cover could also be as little as approximately 4%, or even less (Figure 3.1) as the 1 km pixels flagged as cloudy may actually have only a very small quantity of cloud within them. This results in a particularly conservative estimate of clouds. On the other hand, as stated in Roy et al. (2006), on which the FPC analysis is based, the assumption that there is no temporal or spatial correlation in cloud cover will result in an underestimation of the time to any given FPC, providing a more optimistic outlook than is likely realistic. An analysis of how optimistic or pessimistic the input cloud datasets and resultant analyses are would be very beneficial in planning required acquisition frequency (Chapters 3-5).

The cropland mask introduced and applied in Chapter 4 onward (Fritz et al., 2013) will have its own user and producer accuracies and errors of commission/omission, affecting the areas flagged as requiring observations. For analyses in both Chapters 4 and 5, there is no attempt to derive the probability that each subsequent requirement period (herein, 8 or 16 days) would result in a

reasonably clear view. This provision of some form of confidence interval around securing clear views in consecutive periods would be useful. In Chapter 5, the overpass analysis itself has certain artifacts resulting from its initial model conditions which may increase or decrease the number of acquisition opportunities in the scenario period. This has been partially mitigated by bounding the analysis to the 5^{th} and 95^{th} percentiles of acquisition opportunities. However, also at hand as a source of uncertainty is the implicit assumption that the revisit frequency capability of a constellation is simply the number of acquisition opportunities divided by the number of days in the scenario period, resulting in non-integer revisit frequencies. In fact, all considered missions are sun-synchronous and pass over a given area of the Earth at the same time each day, meaning non-integer revisit frequencies are impossible. An error assessment should also take this into account.

6.3 Concluding Thoughts

Perhaps the greatest strength of the use of remotely sensed data for operational agricultural monitoring is that it provides timely and synoptic coverage at multiple scales and allows for repeatable methods and analyses. Conversely, the greatest challenges to date have largely been related to data availability and by association, the lack of EO data coordination: data acquisitions are uneven throughout space and time (Hansen & Loveland, 2012; Wulder et al., 2008), leaving gaps that can prevent the data from being implemented broadly and adopted operationally; many data policies are closed, resulting in data being inaccessible and/or very expensive to use; and data from different instruments are not interoperable, due in part to the lack of pre-processing standards, meaning there is a lack of consistency between datasets

(Duveiller et al., 2013; Wu et al., 2013b). Also at hand (although beyond the scope of this research) is the capacity of agricultural monitoring agencies around the world to download and manage EO data. The data volumes required for operational crop monitoring are too large for local download in most countries of the world, and considerable training is necessary in order to utilize EO data. The research presented here has articulated EO requirements for global agricultural monitoring and provided key inputs into a data acquisition strategy, but efforts to address these other crucial aspects of data coordination are also necessary. Ensuring free and open access to high quality, interoperable data that are pre-processed at a standard level will pave the way toward an operational global agricultural monitoring program that leverages and engages talent from around the world.

Glossary

AGS: Agricultural growing season; the period during which crops are in season. Bounded by SOS and EOS (see below).

AO: Acquisition opportunity; occurs when a satellite passes over a given area of the Earth, allowing for an acquisition to be obtained.

APClear: Average percentage clear. Refers to the average percentage of 1 km pixels within a 0.05˚ cell which are cloud free.

APCloud: Average percentage cloudy. Refers to the average percentage of 1 km pixels within a 0.05˚ cell which contain cloud.

CONUS: Conterminous United States; the lower 48 states, excluding Alaska and Hawaii.

CVR: Clear view requirement; referenced in the usage of the probability of a clear view product (*P*(clear)) to yield a completely 100% cloud free clear view.

EO: Earth observations. Herein, refers to satellite remote sensing based observations of the Earth's surface, encompassing multiple spatial, spectral, temporal, and radiometric resolutions. Elsewhere, can refer to in situ observations as well.

EOS: End of agricultural growing season. The termination of photosynthetic activity.

FAO: Food and Agricultural Organization of the United Nations.

FPC: Final percentage clear, the percentage of a spatial unit (herein, 0.05˚) that is cloud free/clear within a certain number of days or after a certain number of observations; referenced in the usage of the average percentage clear product (APClear).

GEO: Group on Earth Observations, an intergovernmental organization that coordinates efforts amongst international space and monitoring agencies to build a Global Earth Observation System of Systems. Established officially in 2005 after conception in 2003, it focuses on nine societal benefit areas, including agriculture.

GEOGLAM: GEO's Global Agricultural Monitoring Initiative. Mandated in 2011 by the G20 agricultural ministers to build upon GEO activities in the agriculture society benefit area. Has six primary components, one of which is the coordination of EO data for agricultural monitoring.

G20: Group of 20; consortium of finance ministers from the 20 of the largest economic powers in the world, collectively accounting for 80% of world trade.

GSCs: Growing season calendars; spatially explicit (0.05˚) characterization of the agricultural growing season.

HIRS: High-resolution Infrared Radiation Sounder; a multi-channel infrared scanning radiometer which has been broadly used to monitor cloud cover and other atmospheric constituents.

ISCCP: International Satellite Cloud Climatology Project; initiated in 1982, an effort to derive information on global distribution of clouds as well as their diurnal, seasonal, and interannual cycles from satellite radiance measurements.

LAI: Leaf area index, a dimensionless quantity that describes the one-sided green leaf area per unit ground surface area.

L7: Landsat 7. A satellite launched in 1999, jointly flown and operated by NASA and USGS. Contains one sensor: the Enhanced Thematic Mapper, which since 2003 has had a failure of its scan-line corrector, resulting in a data gap of 22% of each acquired scene.

L8: Landsat 8. A satellite launched in 2013, jointly flown and operated by NASA and USGS. Contains two sensors: the Operational Land Imager, covering the visible and reflected infrared, and the Thermal Infrared Sensor, collecting data in the thermal portion of the Electromagnetic Spectrum.

MODIS: Moderate Resolution Imaging Spectrometer. Consists of two missions: MODIS Terra, aka EOS AM, launched in 1999, and MODIS Aqua, aka EOS PM, launched in 2002. Operated by NASA, it has 36 spectral bands, and has paved the way for global scale observations of terrestrial and atmospheric processes.

MOD09: The MODIS Terra derived surface reflectance product.

NASA: The United States' National Aeronautics and Space Administration. NASA operates a number of Earth observing missions, and also provides research funding and opportunities for the application of EO data. Their fellowship program funded this dissertation research.

NDVI: The normalized difference vegetation index. A dimensionless ratio that incorporates data from the red and near-infrared, and that has been shown to correlate highly with leaf area index. It ranges from -1 to +1, with a low NDVI indicating relatively little green leaf area, and a high NDVI indicating relatively dense green leaf area.

Non-AGS: The non-agricultural growing season; the period during which crops are out of season, occupying the period between the EOS and SOS.

O+TIR: Optical plus thermal infrared. Refers specifically to the visible, reflected infrared, and thermal infrared portions of the Electromagnetic Spectrum, to which most clouds are opaque.

***P*(clear)**: The probability of a cloud free clear view, with an entire 0.05˚cell being completely cloud free. A dataset derived from 10-12 year of MODIS surface reflectance data for both the morning (MODIS Terra) and afternoon (MODIS Aqua). Provides insight into cloud absence frequency.

***P*(cloud)**: The probability of the view of a 0.05˚cell containing any quantity of cloud. The inverse of *P*(clear), this provides insight into a cloud presence frequency.

POS: Peak of season; the annual NDVI maximum.

PPE: Peak period end; the point following the NDVI maximum (POS) that is greater than 70% of the annual range in NDVI. Indicates the end of the period within which the NDVI maximum is likely to occur.

PPS: Peak period start; the point preceding the NDVI maximum (POS) that is greater than 70% of the annual range in NDVI. Indicates the beginning of the period within which the NDVI maximum is likely to occur.

RFR: Revisit frequency required; refers to the frequency with which a data acquisition would been to occur to probabilistically yield a (reasonably) cloud free view within a given number of days.

R2: Resourcesat-2, and satellite flown by the Indian Space Research Organization. It contains three multispectral cameras on board, although the focus herein has been on the Advanced Wide-Field Sensor (AWiFS) sensor.

SAR: Synthetic Aperture Radar, a form of radio detection and ranging that, through the electronic simulation of a very large antenna, is able to obtain finer spatial resolution images than are conventional radar systems. Herein, microwave SAR data, with their cloud penetrating capabilities, are presented as alternatives O+TIR data in areas frequently occluded by cloud cover.

SOS: Start of season; the beginning of the agricultural growing season, at which point above ground green biomass begins to accumulate.

S2A: Sentinel-2A, the first of the two planned European Space Agency moderate spatial resolution Sentinel missions. It is purported to launch in late 2014, and have a revisit capability of 10 days. Coupled with a spatial resolution of 10-20 m, this mission will provide a key asset for agricultural monitoring.

S2B: Sentinel-2B, the second of the two planned European Space Agency moderate spatial resolution Sentinel missions. It is purported to launch sometime in 2015, and will have the same spatial and temporal resolution capabilities as the S2A mission, meaning together they will provide a revisit capability of 5 days.

USDA: The United States Department of Agriculture.

USDA-FAS: The United States Department of Agriculture's Foreign Agricultural Service. This portion of the agency deals primarily with international agricultural production, agricultural systems, and markets.

USDA-NASS: The United States Department of Agriculture's National Agricultural Statistics Service. This portion of the agency deals primarily with domestic crop production, agricultural systems, and markets.

USGS: The United States Geological Survey.

VFTM: Very fine to moderate spatial resolution data, falling roughly between <5 m – 100m. Traditionally, 250 m to even 1000 m data have been considered moderate, but as instrumentation has improved, so too have the definition adjusted. VFTM data are currently not acquired in a systematic manner (as opposed to coarse resolution data like MODIS), and require coordination in order for their potential to be fully realized, providing context for this research.

Scholarly References

Allen, R., Hanuschak, G., & Craig, M. (2002). *History of remote Sensing for crop acreage in USDA's National Agricultural Statistics Service*. NASS.

Anderson, J. E., & Kalcic, M. T. (1982). Analysis of thematic mapper simulator data acquired during winter season over Pearl River, MS Test Site. Retrieved from http://agris.fao.org/agris-search/search/display.do?f=1989/US/US89520.xml;US8840888

Anderson, M. C., Hain, C., Wardlow, B., Pimstein, A., Mecikalski, J. R., & Kustas, W. P. (2011). Evaluation of Drought Indices Based on Thermal Remote Sensing of Evapotranspiration over the Continental United States. *Journal of Climate*, *24*(8).

Arvidson, T., Gasch, J., & Goward, S. N. (1999). Pleasing all of the people most of the time: Planning Landsat 7 acquisitions for the US archive. In *Proceedings of Pecora* (Vol. 14, pp. 154–162).

Arvidson, T., Gasch, J., & Goward, S. N. (2001). Landsat 7's long-term acquisition plan—An innovative approach to building a global imagery archive. *Remote Sensing of Environment*, *78*(1), 13–26.

Arvidson, T., Goward, S., Gasch, J., & Williams, D. (2006). Landsat-7 long-term acquisition plan: Development and validation. *Photogrammetric Engineering and Remote Sensing*, *72*(10), 1137.

Atzberger, C. (2013). Advances in remote sensing of agriculture: Context description, existing operational monitoring systems and major information needs. *Remote Sensing*, *5*(2), 949–981.

Baker, D. N., Whisler, F. D., Parton, W. J., Klepper, E. L., Cole, C. V., Willis, W. O., … Bauer, A. (1985). The development of winter wheat: a physical physiological process model. *ARS United States Department of Agriculture, Agricultural Research Service*. Retrieved from http://agris.fao.org/agris-search/search/display.do?f=2012/OV/OV2012063600636.xml;US19860082050

Baret, F., & Guyot, G. (1991). Potentials and limits of vegetation indices for LAI and APAR assessment. *Remote Sensing of Environment*, *35*(2), 161–173.

Bastiaanssen, W. G., Molden, D. J., & Makin, I. W. (2000). Remote sensing for irrigated agriculture: examples from research and possible applications. *Agricultural Water Management*, *46*(2), 137–155.

Becker-Reshef, I., Justice, C., Doorn, B., Reynolds, C., Anyamba, A., Tucker, C. J., & Korontzi, S. (2009). NASA's contribution to the Group on Earth Observations (GEO) Global Agricultural Monitoring System of Systems. *NASA Earth Observer*, *21*, 24–29.

Becker-Reshef, I., Justice, C., Sullivan, M., Vermote, E., Tucker, C., Anyamba, A., … Schmaltz, J. (2010a). Monitoring global croplands with coarse resolution earth observations: The Global Agriculture Monitoring (GLAM) project. *Remote Sensing*, *2*(6), 1589–1609.

Becker-Reshef, I., Vermote, E., Lindeman, M., & Justice, C. (2010b). A generalized regression-based model for forecasting winter wheat yields in Kansas and Ukraine using MODIS data. *Remote Sensing of Environment*, *114*(6), 1312–1323.

Biradar, C. M., & Xiao, X. (2011). Quantifying the area and spatial distribution of double- and triple-cropping croplands in India with multi-temporal MODIS imagery in 2005. *International Journal of Remote Sensing*, *32*(2), 367–386. doi:10.1080/01431160903464179

Boatwright, G. O., Ravet, F. W., & Taylor, T. W. (1985). Development of early warning models. *ARS-United States Department of Agriculture, Agricultural Research Service (USA)*. Retrieved from http://agris.fao.org/agris-search/search/display.do?f=1986/US/US86205.xml;US8637128

Boken, V. K., & Shaykewich, C. F. (2002). Improving an operational wheat yield model using phenological phase-based Normalized Difference Vegetation Index. *International Journal of Remote Sensing*, *23*(20), 4155–4168.

Bolton, D. K., & Friedl, M. A. (2013). Forecasting crop yield using remotely sensed vegetation indices and crop phenology metrics. *Agricultural and Forest Meteorology*, *173*, 74–84. doi:10.1016/j.agrformet.2013.01.007

Boryan, C., & Craig, M. (2005). Multiresolution Landsat TM and AWiFS sensor assessment for crop area estimation in Nebraska. *Proceedings from Pecora*, *16*, 22–27.

Boryan, C., Yang, Z., Mueller, R., & Craig, M. (2011). Monitoring US agriculture: the US department of agriculture, national agricultural statistics service, cropland data layer program. *Geocarto International*, *26*(5), 341–358.

Bossard, M., Feranec, J., & Otahel, J. (2000). *CORINE land cover technical guide: Addendum 2000*. European Environment Agency Copenhagen. Retrieved from http://www.dmu.dk/fileadmin/Resources/DMU/Udgivelser/CLC2000/technical_guide_addenum.pdf

Bréon, F.-M., & Vermote, E. (2012). Correction of MODIS surface reflectance time series for BRDF effects. *Remote Sensing of Environment*, *125*, 1–9.

Brisco, B., & Brown, R. J. (1995). Multidate SAR/TM synergism for crop classification in western Canada. *Photogrammetric Engineering and Remote Sensing*, *61*(8), 1009–1014.

Brisson, N., Mary, B., Ripoche, D., Jeuffroy, M. H., Ruget, F., Nicoullaud, B., … Durr, C. (1998). STICS: a generic model for the simulation of crops and their water and nitrogen balances. I. Theory and parameterization applied to wheat and corn. *Agronomie*, *18*(5-6), 311–346.

Cairns, B. (1995). Diurnal variations of cloud from ISCCP data. *Atmospheric Research*, *37*(1–3), 133–146. doi:10.1016/0169-8095(94)00074-N

Chander, G., Killough, B., & Gowda, S. (2010). An overview of the web-based Google Earth coincident imaging tool. In *Geoscience and Remote Sensing Symposium (IGARSS), 2010 IEEE International* (pp. 1679–1682). IEEE. Retrieved from http://ieeexplore.ieee.org/xpls/abs_all.jsp?arnumber=5652852

Chang, J., Hansen, M. C., Pittman, K., Carroll, M., & DiMiceli, C. (2007). Corn and Soybean Mapping in the United States Using MODIS Time-Series Data Sets. *Agronomy Journal*, *99*(6), 1654.

Chen, P.-Y., Fedosejevs, G., Tiscareño-LóPez, M., & Arnold, J. G. (2006). Assessment of MODIS-EVI, MODIS-NDVI and VEGETATION-NDVI Composite Data Using Agricultural Measurements: An Example at Corn Fields in Western Mexico. *Environmental Monitoring and Assessment*, *119*(1-3), 69–82. doi:10.1007/s10661-005-9006-7

Chernokulsky, A. V., & Mokhov, I. I. (2009). Comparison of global cloud climatologies. *Current Issues of Remote Sensing of Earth from Space*, *6*(2), 235–243.

Doraiswamy, P. C., Hatfield, J. L., Jackson, T. J., Akhmedov, B., Prueger, J., & Stern, A. (2004). Crop condition and yield simulations using Landsat and MODIS. *Remote Sensing of Environment*, *92*(4), 548–559.

Drusch, M., Del Bello, U., Carlier, S., Colin, O., Fernandez, V., Gascon, F., … Bargellini, P. (2012). Sentinel-2: ESA's Optical High-Resolution Mission for GMES Operational Services. *Remote Sensing of Environment*, *120*, 25–36. doi:10.1016/j.rse.2011.11.026

Duveiller, G., Baret, F., & Defourny, P. (2011). Crop specific green area index retrieval from MODIS data at regional scale by controlling pixel-target adequacy. *Remote Sensing of Environment*, *115*(10), 2686–2701.

Duveiller, G., Baret, F., & Defourny, P. (2012). Remotely sensed green area index for winter wheat crop monitoring: 10-Year assessment at regional scale over a fragmented landscape. *Agricultural and Forest Meteorology*, *166*, 156–168.

Duveiller, G., & Defourny, P. (2010). A conceptual framework to define the spatial resolution requirements for agricultural monitoring using remote sensing. *Remote Sensing of Environment*, *114*(11), 2637–2650.

Duveiller, G., Defourny, P., & Gérard, B. (2008). A method to determine the appropriate spatial resolution required for monitoring crop growth in a given agricultural landscape. In *Geoscience and Remote Sensing Symposium, 2008. IGARSS 2008. IEEE International* (Vol. 3, pp. III–562). Retrieved from http://ieeexplore.ieee.org/xpls/abs_all.jsp?arnumber=4779409

Duveiller, G., López-Lozano, R., Seguini, L., Bojanowski, J. S., & Baruth, B. (2013). Optical remote sensing requirements for operational crop monitoring and yield forecasting in Europe. In *Proceedings of Sentinel-3 OLCI/SLSTR and MERIS/(A) ATSR Workshop, Frascati, Italy (ESA SP-711*. Retrieved from http://www.researchgate.net/publication/235968254_Optical_Remote_Sensing_Requirements_for_Operational_Crop_Monitoring_and_Yield_Forecasting_in_Europe/file/3deec514f64c07ff5c.pdf

FAOSTAT, F. (2012). Agriculture Organization of the United Nations. *Statistical Database*.

Fischer, A. (1994). A model for the seasonal variations of vegetation indices in coarse resolution data and its inversion to extract crop parameters. *Remote Sensing of Environment*, *48*(2), 220–230. doi:10.1016/0034-4257(94)90143-0

Frey, R. A., Ackerman, S. A., Liu, Y., Strabala, K. I., Zhang, H., Key, J. R., & Wang, X. (2008). Cloud detection with MODIS. Part I: Improvements in the MODIS cloud mask for Collection 5. *Journal of Atmospheric & Oceanic Technology*, *25*(7).

Friedl, M. A., McIver, D. K., Hodges, J. C., Zhang, X. Y., Muchoney, D., Strahler, A. H., … Cooper, A. (2002). Global land cover mapping from MODIS: algorithms and early results. *Remote Sensing of Environment*, *83*(1), 287–302.

Fritz, S., McCallum, I., Schill, C., Perger, C., Grillmayer, R., Achard, F., … Obersteiner, M. (2009). Geo-Wiki. Org: The use of crowdsourcing to improve global land cover. *Remote Sensing*, *1*(3), 345–354.

Fritz, S., McCallum, I., Schill, C., Perger, C., See, L., Schepaschenko, D., … Obersteiner, M. (2012). Geo-Wiki: An online platform for improving global land cover. *Environmental Modelling & Software*, *31*, 110–123.

Fritz, S., See, L., You, L., Justice, C., Becker-Reshef, I., Bydekerke, L., … Woodcock, C. (2013). The Need for Improved Maps of Global Cropland. *Eos*,

Transactions American Geophysical Union, *94*(3), 31–32. doi:10.1002/2013EO030006

Galford, G. L., Mustard, J. F., Melillo, J., Gendrin, A., Cerri, C. C., & Cerri, C. E. (2008). Wavelet analysis of MODIS time series to detect expansion and intensification of row-crop agriculture in Brazil. *Remote Sensing of Environment*, *112*(2), 576–587.

Gao, F., Masek, J., Schwaller, M., & Hall, F. (2006). On the blending of the Landsat and MODIS surface reflectance: Predicting daily Landsat surface reflectance. *Geoscience and Remote Sensing, IEEE Transactions on*, *44*(8), 2207–2218.

Gong, P., Wang, J., Yu, L., Zhao, Y., Zhao, Y., Liang, L., … Chen, J. (2013). Finer Resolution Observation and Monitoring of Global Land Cover: First Mapping Results with Landsat TM and ETM+ Data. *Int. J. Remote Sens.*, *34*(7), 2607–2654. doi:10.1080/01431161.2012.748992

Goward, S., Chander, G., Pagnutti, M., Marx, A., Ryan, R., Thomas, N., & Tetrault, R. (2012). Complementarity of ResourceSat-1 AWiFS and Landsat TM/ETM+ sensors. *Remote Sensing of Environment*, *123*, 41–56.

Goward, S. N., Arvidson, T., Williams, D. L., Irish, R., & Irons, J. R. (2009). *Moderate spatial resolution optical sensors*. SAGE Publications Ltd.: London, UK. Retrieved from http://books.google.fr/books?hl=fr&lr=&id=uIv82prTp4IC&oi=fnd&pg=PA123&dq=Goward,+S.N.,+2009&ots=Q7gUx-hBWm&sig=rS4YRIHrWu7o-171Ad5oec84eII

Goward, S. N., Tucker, C. J., & Dye, D. G. (1985). North American vegetation patterns observed with the NOAA-7 advanced very high resolution radiometer. *Plant Ecology*, *64*(1), 3–14.

Goward, S. N., & Williams, D. L. (1997). Landsat and earth systems science: development of terrestrial monitoring. *Photogrammetric Engineering and Remote Sensing*, *63*(7), 887–900.

Goward, S., Williams, D., Arvidson, T., & Irons, J. (2011). The Future of Landsat-Class Remote Sensing. In *Land Remote Sensing and Global Environmental Change* (pp. 807–834). Springer. Retrieved from http://link.springer.com/chapter/10.1007/978-1-4419-6749-7_35

Guindin-Garcia, N., Gitelson, A. A., Arkebauer, T. J., Shanahan, J., & Weiss, A. (2012). An evaluation of MODIS 8- and 16-day composite products for monitoring maize green leaf area index. *Agricultural and Forest Meteorology*, *161*, 15–25. doi:10.1016/j.agrformet.2012.03.012

Gunderson, A., & Chodas, M. (2011). An investigation of cloud cover probability for the HyspIRI mission using MODIS cloud mask data. In *Aerospace*

Conference, 2011 IEEE (pp. 1–14). Retrieved from http://ieeexplore.ieee.org/xpls/abs_all.jsp?arnumber=5747393

Hain, C. R., Crow, W. T., Mecikalski, J. R., Anderson, M. C., & Holmes, T. (2011). An intercomparison of available soil moisture estimates from thermal infrared and passive microwave remote sensing and land surface modeling. *Journal of Geophysical Research: Atmospheres (1984–2012), 116*(D15). Retrieved from http://www.agu.org/pubs/crossref/2011/2011JD015633.shtml

Han, W., Yang, Z., Di, L., & Mueller, R. (2012). CropScape: A Web service based application for exploring and disseminating US conterminous geospatial cropland data products for decision support. *Computers and Electronics in Agriculture*, *84*, 111–123.

Hansen, M. C., Roy, D. P., Lindquist, E., Adusei, B., Justice, C. O., & Altstatt, A. (2008). A method for integrating MODIS and Landsat data for systematic monitoring of forest cover and change in the Congo Basin. *Remote Sensing of Environment*, *112*(5), 2495–2513.

Hansen, M. C., & Loveland, T. R. (2012). A review of large area monitoring of land cover change using Landsat data. *Remote Sensing of Environment*, *122*, 66–74.

Hansen, M. C., Potapov, P. V., Moore, R., Hancher, M., Turubanova, S. A., Tyukavina, A., … Loveland, T. R. (2013). High-Resolution Global Maps of 21st-Century Forest Cover Change. *Science*, *342*(6160), 850–853.

Homer, C., Dewitz, J., Fry, J., Coan, M., Hossain, N., Larson, C., … Wickham, J. (2007). Completion of the 2001 National Land Cover Database for the Counterminous United States. *Photogrammetric Engineering and Remote Sensing*, *73*(4), 337.

Hong, G., Zhang, A., Zhou, F., & Brisco, B. (2014). Integration of optical and synthetic aperture radar (SAR) images to differentiate grassland and alfalfa in Prairie area. *International Journal of Applied Earth Observation and Geoinformation*, *28*, 12–19.

Huete, A., Didan, K., Miura, T., Rodriguez, E. P., Gao, X., & Ferreira, L. G. (2002). Overview of the radiometric and biophysical performance of the MODIS vegetation indices. *Remote Sensing of Environment*, *83*(1), 195–213.

Irish, R. R., Barker, J. L., Goward, S. N., & Arvidson, T. (2006). Characterization of the Landsat-7 ETM+ automated cloud-cover assessment (ACCA) algorithm. *Photogrammetric Engineering and Remote Sensing*, *72*(10), 1179.

Jackson, T. J. (1986). Soil water modeling and remote sensing. *Geoscience and Remote Sensing, IEEE Transactions on*, (1), 37–46.

Johnson, D. M. (2008). A comparison of coincident Landsat-5 TM and Resourcesat-1 AWiFS imagery for classifying croplands. *Photogrammetric Engineering and Remote Sensing*, *74*(11), 1413–1423.

Johnson, D. M. (2010). The 2007 Cropland Data Layer. Retrieved from https://www.farmfoundation.org/news/articlefiles/941-johnson.pdf

Johnson, D. M. (2014). An assessment of pre-and within-season remotely sensed variables for forecasting corn and soybean yields in the United States. *Remote Sensing of Environment*, *141*, 116–128.

Jones, J. W., Hoogenboom, G., Porter, C. H., Boote, K. J., Batchelor, W. D., Hunt, L. A., … Ritchie, J. T. (2003). The DSSAT cropping system model. *European Journal of Agronomy*, *18*(3), 235–265.

Jönsson, P., & Eklundh, L. (2004). TIMESAT—a program for analyzing time-series of satellite sensor data. *Computers & Geosciences*, *30*(8), 833–845.

Ju, J., & Roy, D. P. (2008). The availability of cloud-free Landsat ETM+ data over the conterminous United States and globally. *Remote Sensing of Environment*, *112*(3), 1196–1211.

Justice, C. O., & Becker-Reshef, I. (2007). Report from the Workshop on Developing a Strategy for Global Agricultural Monitoring in the framework of Group on Earth Observations (GEO). *UN FAO, July*.

Justice, C. O., Román, M. O., Csiszar, I., Vermote, E. F., Wolfe, R. E., Hook, S. J., … Miura, T. (2013). Land and cryosphere products from Suomi NPP VIIRS: Overview and status. *Journal of Geophysical Research: Atmospheres*, *118*(17), 9753–9765.

Justice, C. O., Vermote, E., Privette, J., & Sei, A. (2011). The evolution of US moderate resolution optical land remote sensing from AVHRR to VIIRS. In *Land Remote Sensing and Global Environmental Change* (pp. 781–806). Springer. Retrieved from http://link.springer.com/chapter/10.1007/978-1-4419-6749-7_34

Justice, C. O., Vermote, E., Townshend, J. R. G., DeFries, R., Roy, D. P., Hall, D. K., … Barnsley, M. J. (1998). The Moderate Resolution Imaging Spectroradiometer (MODIS): land remote sensing for global change research. *IEEE Transactions on Geoscience and Remote Sensing*, *36*(4), 1228 –1249. doi:10.1109/36.701075

Kaufman, Y. J., Remer, L. A., Tanré, D., Li, R.-R., Kleidman, R., Mattoo, S., … Ichoku, C. (2005). A critical examination of the residual cloud contamination and diurnal sampling effects on MODIS estimates of aerosol over ocean. *Geoscience and Remote Sensing, IEEE Transactions on*, *43*(12), 2886–2897.

Kauth, R. J., & Thomas, G. S. (1976). The tasselled cap–a graphic description of the spectral-temporal development of agricultural crops as seen by Landsat. In *LARS Symposia* (p. 159). Retrieved from http://docs.lib.purdue.edu/cgi/viewcontent.cgi?article=1160&context=lars_symp

Kessler, P. D., Killough, B. D., Gowda, S., Williams, B. R., Chander, G., & Qu, M. (2013). CEOS Visualization Environment (COVE) Tool for Intercalibration of Satellite Instruments. Retrieved from http://ieeexplore.ieee.org/xpls/abs_all.jsp?arnumber=6459582

Kotchenova, S. Y., & Vermote, E. F. (2007). Validation of a vector version of the 6S radiative transfer code for atmospheric correction of satellite data. Part II. Homogeneous Lambertian and anisotropic surfaces. *Applied Optics*, *46*(20), 4455–4464.

Kotchenova, S. Y., Vermote, E. F., Matarrese, R., & Klemm Jr, F. J. (2006). Validation of a vector version of the 6S radiative transfer code for atmospheric correction of satellite data. Part I: Path radiance. *Applied Optics*, *45*(26), 6762–6774.

Kussul, N., Skakun, S., Shelestov, A., Kravchenko, O., & Kussul, O. (2012). Crop Classification in Ukraine Using Satellite Optical and SAR Images. *INFORMATION MODELS & ANALYSES*, 118.

Leichtle, T., Schmitt, A., Roth, A., & Schardt, M. (2012). On the capability of different SAR polarization combinations for agricultural monitoring. In *Geoscience and Remote Sensing Symposium (IGARSS), 2012 IEEE International* (pp. 3752–3755). IEEE. Retrieved from http://ieeexplore.ieee.org/xpls/abs_all.jsp?arnumber=6350501

Li, A., Liang, S., Wang, A., & Qin, J. (2007). Estimating crop yield from multi-temporal satellite data using multivariate regression and neural network techniques. *Photogrammetric Engineering and Remote Sensing*, *73*(10), 1149.

Liu, J., Liu, M., Tian, H., Zhuang, D., Zhang, Z., Zhang, W., … Deng, X. (2005). Spatial and temporal patterns of China's cropland during 1990–2000: an analysis based on Landsat TM data. *Remote Sensing of Environment*, *98*(4), 442–456.

Lloyd, D. (1990). A phenological classification of terrestrial vegetation cover using shortwave vegetation index imagery. *Remote Sensing*, *11*(12), 2269–2279.

Lobell, D. B., & Asner, G. P. (2004). Cropland distributions from temporal unmixing of MODIS data. *Remote Sensing of Environment*, *93*(3), 412–422.

MacDonald, R. B., & Hall, F. G. (1980). Global crop forecasting. *Science*, *208*, 670–679.

MacDonald, R. B., Hall, F. G., & Erb, R. B. (1975). The use of Landsat data in a large area crop inventory experiment (LACIE). Retrieved from http://docs.lib.purdue.edu/lars_symp/46/

Maxwell, S. K., Schmidt, G. L., & Storey, J. C. (2007). A multi-scale segmentation approach to filling gaps in Landsat ETM+ SLC-off images. *International Journal of Remote Sensing*, *28*(23), 5339–5356.

McNairn, H., Champagne, C., Shang, J., Holmstrom, D., & Reichert, G. (2009a). Integration of optical and Synthetic Aperture Radar (SAR) imagery for delivering operational annual crop inventories. *ISPRS Journal of Photogrammetry and Remote Sensing*, *64*(5), 434–449.

McNairn, H., Shang, J., Champagne, C., & Jiao, X. (2009b). TerraSAR-X and RADARSAT-2 for crop classification and acreage estimation. In *Geoscience and Remote Sensing Symposium, 2009 IEEE International, IGARSS 2009* (Vol. 2, pp. II–898). IEEE. Retrieved from http://ieeexplore.ieee.org/xpls/abs_all.jsp?arnumber=5418243

McNairn, H., Shang, J., Jiao, X., & Champagne, C. (2009c). The contribution of ALOS PALSAR multipolarization and polarimetric data to crop classification. *Geoscience and Remote Sensing, IEEE Transactions on*, *47*(12), 3981–3992.

Meng, J., & Wu, B. (2008). Study on the crop condition monitoring methods with remote sensing. *International Archives of the Photogrammetry, Remote Sensing and Spatial Information Sciences*, *37*(B8), 945–950.

Mercury, M., Green, R., Hook, S., Oaida, B., Wu, W., Gunderson, A., & Chodas, M. (2012). Global cloud cover for assessment of optical satellite observation opportunities: A HyspIRI case study. *Remote Sensing of Environment*, *126*, 62–71.

Mika, A. M. (1997). Three decades of Landsat instruments. *Photogrammetric Engineering and Remote Sensing*, *63*(7), 839–852.

Miller, T. D. (1999). *Growth stages of wheat: identification and understanding improve crop management. Texas agricultural extension service, the Texas A&M university system*. SCS-1999-16.

Minnis, P. (1989). Viewing zenith angle dependence of cloudiness determined from coincident GOES East and GOES West data. *Journal of Geophysical Research: Atmospheres (1984–2012)*, *94*(D2), 2303–2320.

Minnis, P., & Harrison, E. F. (1984). Diurnal variability of regional cloud and clear-sky radiative parameters derived from GOES data. Part I: Analysis method. *J. Climate Appl. Meteor*, *23*, 993–1011.

Minnis, P., Sun-Mack, S., Young, D. F., Heck, P. W., Garber, D. P., Chen, Y., … Smith, W. L. (2011). CERES Edition-2 cloud property retrievals using TRMM VIRS and Terra and Aqua MODIS Data—Part I: Algorithms. *Geoscience and Remote Sensing, IEEE Transactions on*, *49*(11), 4374–4400.

Minnis, P., Trepte, Q. Z., Sun-Mack, S., Chen, Y., Doelling, D. R., Young, D. F., … Brown, R. R. (2008). Cloud detection in nonpolar regions for CERES using TRMM VIRS and Terra and Aqua MODIS data. *Geoscience and Remote Sensing, IEEE Transactions on*, *46*(11), 3857–3884.

Monfreda, C., Ramankutty, N., & Foley, J. A. (2008). Farming the planet: 2. Geographic distribution of crop areas, yields, physiological types, and net primary production in the year 2000. *Global Biogeochemical Cycles*, *22*(1), GB1022.

Moulin, S., Kergoat, L., Viovy, N., & Dedieu, G. (1997). Global-scale assessment of vegetation phenology using NOAA/AVHRR satellite measurements. *Journal of Climate*, *10*(6), 1154–1170.

Mueller, R., & Seffrin, R. (2006). New methods and satellites: a program update on the NASS cropland data layer acreage program. *Remote Sensing Support to Crop Yield Forecast and Area Estimates, ISPRS Archives*, *36*(8), W48.

Naylor, R. (2011). Expanding the boundaries of agricultural development. *Food Security*, *3*(2), 233–251.

Odenweller, J. B., & Johnson, K. I. (1984). Crop identification using Landsat temporal-spectral profiles. *Remote Sensing of Environment*, *14*(1), 39–54.

Ozdogan, M. (2010). The spatial distribution of crop types from MODIS data: Temporal unmixing using Independent Component Analysis. *Remote Sensing of Environment*, *114*(6), 1190–1204.

Ozdogan, M., & Woodcock, C. E. (2006). Resolution dependent errors in remote sensing of cultivated areas. *Remote Sensing of Environment*, *103*(2), 203–217.

Pan, Y., Li, L., Zhang, J., Liang, S., Zhu, X., & Sulla-Menashe, D. (2012). Winter wheat area estimation from MODIS-EVI time series data using the Crop Proportion Phenology Index. *Remote Sensing of Environment*, *119*, 232–242.

Pax-Lenney, M., & Woodcock, C. E. (1997). The effect of spatial resolution on the ability to monitor the status of agricultural lands. *Remote Sensing of Environment*, *61*(2), 210–220.

Pinter, P. J., Hatfield, J. L., Schepers, J. S., Barnes, E. M., Moran, M. S., Daughtry, C. S. ., & Upchurch, D. R. (2003). Remote sensing for crop management. *Photogrammetric Engineering and Remote Sensing*, *69*(6), 647–664.

Pittman, K., Hansen, M. C., Becker-Reshef, I., Potapov, P. V., & Justice, C. O. (2010). Estimating global cropland extent with multi-year MODIS data. *Remote Sensing*, *2*(7), 1844–1863.

Portmann, F. T., Siebert, S., & Döll, P. (2010). MIRCA2000—Global monthly irrigated and rainfed crop areas around the year 2000: A new high-resolution data set for agricultural and hydrological modeling. *Global Biogeochemical Cycles*, *24*(1), GB1011.

Reed, B. C., Brown, J. F., VanderZee, D., Loveland, T. R., Merchant, J. W., & Ohlen, D. O. (1994). Variability of land cover phenology in the United States. *Journal of Vegetation Science*, *5*, 703–714.

Reed, B. C., Schwartz, M. D., & Xiao, X. (2009). Remote Sensing Phenology. *Phenology of Ecosystem Processes*, 231–246.

Rossow, W. B., & Schiffer, R. A. (1999). Advances in understanding clouds from ISCCP. *Bulletin of the American Meteorological Society*, *80*(11), 2261–2287.

Rouse, J. W., Haas, R. H., Schell, J. A., Deering, D. W., & Harlan, J. C. (1974). *Monitoring the vernal advancement and retrogradation (greenwave effect) of natural vegetation*. Texas A & M University, Remote Sensing Center. Retrieved from http://library.wur.nl/WebQuery/clc/154154

Roy, D. P., Ju, J., Kline, K., Scaramuzza, P. L., Kovalskyy, V., Hansen, M., … Zhang, C. (2010). Web-enabled Landsat Data (WELD): Landsat ETM+ composited mosaics of the conterminous United States. *Remote Sensing of Environment*, *114*(1), 35–49.

Roy, D. P., Lewis, P., Schaaf, C. B., Devadiga, S., & Boschetti, L. (2006). The global impact of clouds on the production of MODIS bidirectional reflectance model-based composites for terrestrial monitoring. *Geoscience and Remote Sensing Letters, IEEE*, *3*(4), 452–456.

Roy, D. P., Wulder, M. A., Loveland, T. R., Allen, R. G., Anderson, M. C., Helder, D., … Scambos, T. A. (2014). Landsat-8: Science and product vision for terrestrial global change research. *Remote Sensing of Environment*, *145*, 154–172.

Sacks, W. J., Deryng, D., Foley, J. A., & Ramankutty, N. (2010). Crop planting dates: an analysis of global patterns. *Global Ecology and Biogeography*, *19*(5), 607–620. doi:10.1111/j.1466-8238.2010.00551.x

Sakamoto, T., Gitelson, A. A., & Arkebauer, T. J. (2013). MODIS-based corn grain yield estimation model incorporating crop phenology information. *Remote Sensing of Environment*, *131*, 215–231. doi:10.1016/j.rse.2012.12.017

Sakamoto, T., Wardlow, B. D., Gitelson, A. A., Verma, S. B., Suyker, A. E., & Arkebauer, T. J. (2010). A two-step filtering approach for detecting maize and soybean phenology with time-series MODIS data. *Remote Sensing of Environment*, *114*(10), 2146–2159.

Sakamoto, T., Yokozawa, M., Toritani, H., Shibayama, M., Ishitsuka, N., & Ohno, H. (2005). A crop phenology detection method using time-series MODIS data. *Remote Sensing of Environment*, *96*(3), 366–374.

Scaramuzza, P., Micijevic, E., & Chander, G. (2004). SLC gap-filled products phase one methodology. *Landsat Technical Notes*. Retrieved from http://landsat7.usgs.gov/documents/SLC_Gap_Fill_Methodology.pdf

Sellers, P. J. (1985). Canopy reflectance, photosynthesis and transpiration. *International Journal of Remote Sensing*, *6*(8), 1335–1372.

Sims, D. A., Rahman, A. F., Vermote, E. F., & Jiang, Z. (2011). Seasonal and inter-annual variation in view angle effects on MODIS vegetation indices at three forest sites. *Remote Sensing of Environment*, *115*(12), 3112–3120.

Singh Parihar, J., Justice, C., Soares, J., Leo, O., Kosuth, P., Jarvis, I., … Becker-Reshef, I. (2012). GEO-GLAM: A GEOSS-G20 initiative on Global Agricultural Monitoring. In *39th COSPAR Scientific Assembly. Held 14-22 July 2012, in Mysore, India. Abstract D2.2-9-12, p.1451* (Vol. 39, p. 1451). Retrieved from http://adsabs.harvard.edu/abs/2012cosp...39.1451S

Skole, D., & Tucker, C. (1993). Tropical deforestation and habitat fragmentation in the Amazon. Satellite data from 1978 to 1988. *Science(Washington)*, *260*(5116), 1905–1910.

Stehfest, E., Heistermann, M., Priess, J. A., Ojima, D. S., & Alcamo, J. (2007). Simulation of global crop production with the ecosystem model DayCent. *Ecological Modelling*, *209*(2–4), 203–219. doi:10.1016/j.ecolmodel.2007.06.028

Steven, M. D. (1993). Satellite remote sensing for agricultural management: Opportunities and logistic constraints. *ISPRS Journal of Photogrammetry and Remote Sensing*, *48*(4), 29–34.

Stubenrauch, C. J., Rossow, W. B., Kinne, S., Ackerman, S., Cesana, G., Chepfer, H., … Heidinger, A. (2013). ASSESSMENT OF GLOBAL CLOUD DATASETS FROM SATELITES. *Bulletin of the American Meteorological Society*, *94*(7).

Sullivan, D. G., Lee, D., Beasley, J., Brown, S., & Williams, E. J. (2008). Evaluating a crop residue cover index for determining tillage regime in a cotton-corn peanut rotation. *Journal of Soil and Water Conservation*, *63*(1), 28–36.

Tomlinson, C. J., Chapman, L., Thornes, J. E., & Baker, C. (2011). Remote sensing land surface temperature for meteorology and climatology: a review. *Meteorological Applications*, *18*(3), 296–306.

Torbick, N., Salas, W., Xiao, X., Ingraham, P., Fearon, M., Biradar, C., … Zhao, Y. (2011). Integrating SAR and optical imagery for regional mapping of paddy rice attributes in the Poyang Lake Watershed, China. *Canadian Journal of Remote Sensing*, *37*(1), 17–26.

Townshend, J. R. G., & Justice, C. O. (1988). Selecting the spatial resolution of satellite sensors required for global monitoring of land transformations. *International Journal of Remote Sensing*, *9*(2), 187–236.

Tucker, C. J. (1979). Red and photographic infrared linear combinations for monitoring vegetation. *Remote Sensing of Environment*, *8*(2), 127–150.

Tucker, C. J., Grant, D. M., & Dykstra, J. D. (2004). NASA's global orthorectified Landsat data set. *Photogrammetric Engineering and Remote Sensing*, *70*(3), 313–322.

Tucker, C. J., Holben, B. N., Elgin, J. H., & McMurtrey, J. E. (1981). Remote sensing of total dry-matter accumulation in winter wheat. *Remote Sensing of Environment*, *11*, 171–189.

Underwood, C., Machin, S., Stephens, P., Hodgson, D., da Silva Curiel, A., & Sweeting, M. (2005). Evaluation of the utility of the Disaster Monitoring Constellation in support of Earth observation applications. In *Small Satellites for Earth Observation: Selected Proceedings of the 5th International Symposium of the International Academy of Astronautics, Berlin, April 4-8 2005* (p. 436). Walter de Gruyter.

USDA-NASS. (1997). Harvesting Dates for US Field Crops. *US Department of Agriculture National Agricultural Statistics Service*.

USDA-NASS. (2010). *Usual Planting and Harvesting Dates for US Field Crops*.

USDA-NASS. (2013). *Quick Stats 2.0*.

Verma, N., Garg, P., & Garg, R. (2009). Evaluation of Geometric Properties of AWiFS images: a comparative study. *Geomatics Engineering*. Retrieved from http://www.csre.iitb.ac.in/~csre/conf/wp-content/uploads/fullpapers/OS1/OS1_1.pdf

Vermote, E. F., El Saleous, N. Z., & Justice, C. O. (2002). Atmospheric correction of MODIS data in the visible to middle infrared: first results. *Remote Sensing of Environment*, *83*(1), 97–111.

Vermote, E. F., & Kotchenova, S. (2008). Atmospheric correction for the monitoring of land surfaces. *Journal of Geophysical Research: Atmospheres*, *113*(D23), n/a–n/a. doi:10.1029/2007JD009662

Vogelmann, J. E., Howard, S. M., Yang, L., Larson, C. R., Wylie, B. K., & Van Driel, N. (2001). Completion of the 1990s National Land Cover Data Set for the conterminous United States from Landsat Thematic Mapper data and ancillary data sources. *Photogrammetric Engineering and Remote Sensing*, *67*(6). Retrieved from http://trid.trb.org/view.aspx?id=686441

Wardlow, B. D., & Egbert, S. L. (2008). Large-area crop mapping using time-series MODIS 250 m NDVI data: An assessment for the U.S. Central Great Plains. *Remote Sensing of Environment*, *112*(3), 1096–1116. doi:10.1016/j.rse.2007.07.019

Wardlow, B. D., Egbert, S. L., & Kastens, J. H. (2007). Analysis of time-series MODIS 250 m vegetation index data for crop classification in the US Central Great Plains. *Remote Sensing of Environment*, *108*(3), 290–310.

Wardlow, B. D., Kastens, J. H., & Egbert, S. L. (2006). Using USDA crop progress data for the evaluation of greenup onset date calculated from MODIS 250-meter data. *Photogrammetric Engineering and Remote Sensing*, *72*(11), 1225–1234.

Weng, Q., Fu, P., & Gao, F. (2014). Generating daily land surface temperature at Landsat resolution by fusing Landsat and MODIS data. *Remote Sensing of Environment*, *145*, 55–67.

White, M. A., Thornton, P. E., & Running, S. W. (1997). A continental phenology model for monitoring vegetation responses to interannual climatic variability. *Global Biogeochemical Cycles*, *11*(2), 217–234.

Wiegand, C. L., Maas, S. J., Aase, J. K., Hatfield, J. L., Pinter Jr, P. J., Jackson, R. D., … Lapitan, R. L. (1992). Multisite analyses of spectral-biophysical data for wheat. *Remote Sensing of Environment*, *42*(1), 1–21.

Wiegand, C. L., & Richardson, A. J. (1990). Use of spectral vegetation indices to infer leaf area, evapotranspiration and yield: I. Rationale. *Agronomy Journal*, *82*(3), 623–629.

Wu, B., Meng, J., Li, Q., Yan, N., Du, X., & Zhang, M. (2013a). Remote sensing-based global crop monitoring: experiences with China's CropWatch system. *International Journal of Digital Earth*, (ahead-of-print), 1–25.

Wu, B., Meng, J., Li, Q., Yan, N., Du, X., & Zhang, M. (2013b). Remote sensing-based global crop monitoring: experiences with China's CropWatch system. *International Journal of Digital Earth*, (ahead-of-print), 1–25.

Wulder, M. A., Masek, J. G., Cohen, W. B., Loveland, T. R., & Woodcock, C. E. (2012). Opening the archive: How free data has enabled the science and monitoring promise of Landsat. *Remote Sensing of Environment*, *122*, 2–10.

Wulder, M. A., White, J. C., Goward, S. N., Masek, J. G., Irons, J. R., Herold, M., … Woodcock, C. E. (2008). Landsat continuity: Issues and opportunities for land cover monitoring. *Remote Sensing of Environment*, *112*(3), 955–969.

Wulder, M. A., White, J. C., Masek, J. G., Dwyer, J., & Roy, D. P. (2011). Continuity of Landsat observations: Short term considerations. *Remote Sensing of Environment*, *115*(2), 747–751.

Wylie, D., Jackson, D. L., Menzel, W. P., & Bates, J. J. (2005). Trends in global cloud cover in two decades of HIRS observations. *Journal of Climate*, *18*(15), 3021–3031.

Wylie, D. P., & Menzel, W. P. (1999). Eight years of high cloud statistics using HIRS. *Journal of Climate*, *12*(1), 170–184.

Xiao, X., Boles, S., Liu, J., Zhuang, D., Frolking, S., Li, C., … Moore III, B. (2005). Mapping paddy rice agriculture in southern China using multi-temporal MODIS images. *Remote Sensing of Environment*, *95*(4), 480–492.

Yu, L., Wang, J., Clinton, N., Xin, Q., Zhong, L., Chen, Y., & Gong, P. (2013). FROM-GC: 30 m global cropland extent derived through multisource data integration. *International Journal of Digital Earth*, *6*(6), 521–533. doi:10.1080/17538947.2013.822574

Zhang, X., Friedl, M. A., Schaaf, C. B., Strahler, A. H., Hodges, J. C., Gao, F., … Huete, A. (2003). Monitoring vegetation phenology using MODIS. *Remote Sensing of Environment*, *84*(3), 471–475.